VARIAN associates
611 HANSEN WAY - PALO ALTO, CALIF.

HIGH PERVEANCE BEAM STUDY PROGRAM

Final Report
Second Edition
April, 1963

DIC

Prepared for: M.I.T. Lincoln Laboratory
Publications Office
Lexington 73, Massachusetts

On: M.I.T. Subcontract No. 225

Engineering Report
No. 306-1F

Copy No. 149

HIGH PERVEANCE BEAM STUDY PROGRAM

Final Report
Second Edition
April, 1963

Prepared for: M. I. T. Lincoln Laboratory
Publications Office
Lexington 73, Massachusetts

On: M. I. T. Subcontract No. 225
Purchase Order No. A-08230

Plc

By: W. L. Beaver
E. Demmel

Approved: R. B. Nelson

R. B. Nelson, Manager
Tube Research and Development

FOREWORD

The first edition of this report was issued in February, 1962, and contained a number of factual errors and misprints which have been corrected in this second edition. In addition, the first edition contained a number of interpretive and speculative statements regarding probable errors in the data and their effect on the results. Subsequent careful recalibration and examination of the experiment revealed that these interpretations were in the main correct. These statements have thus been removed and numerous corrections made in the data presented. These revisions contribute to the continuity of the presentation and add validation, but have little effect on the general conclusions which remain substantially the same as those presented in the first edition.

TABLE OF CONTENTS

LIST OF ILLUSTRATIONS

LIST OF ILLUSTRATIONS (Cont.)

LIST OF ILLUSTRATIONS (Cont.)

LIST OF ILLUSTRATIONS (Cont.)

LIST OF TABLES

I. ABSTRACT

The feasibility of using high perveance hollow beams in high power amplifiers was investigated in this program. Accumulated data of three experimental tubes justify the conclusion that performance at high perveance can be predicted on the basis of generally known design parameters. However, certain considerations which are not usually emphasized at low perveance become more important and must be given special attention.

II. PURPOSE

The purpose of this program, conducted under MIT Subcontract No. 225, was to explore the use of hollow beams with perveances of the order of microperveance 10 in high-power pulsed amplifiers. Klystron interaction is investigated because localized interaction is more readily investigated.

III. FACTUAL DATA

A. INTRODUCTION

The experimental program for which this constitutes the final report was directed toward the investigation of the use of high perveance hollow beams in high power amplifiers. The fundamental aim was to determine whether any phenomena, not usually encountered at lower perveance, would arise to disturb the performance. In addition, the possibilities of increased bandwidth were to be considered.

In previous reports, the design and test of several experimental devices were discussed. These consisted of six-gap amplifier klystrons for investigating interaction, and beam testers to examine magnetron injection gun designs. This final report covers the period from 1 January 1961 to 1 September 1961. Test results on the final six-gap klystron are discussed. In addition, the entire program is summarized and conclusions given.

As with most experimental programs involving complicated systems, the results are not always understandable in detail. A great deal of interpretation is necessary in order to detect the important effects. In spite of the profusion of data, retrospect shows that some matters should have been explored in more detail. However, the conclusions drawn are believed to represent the most important factors, certainly the most important that can be detected at this time. In brief, it appears that performance at high perveance can be predicted on the basis of known design information. However, certain considerations which are not usually emphasized become more important. These are discussed in detail in the summarizing statements in Section IV.

B. STATUS OF THE EXPERIMENT

In Quarterly Report No. 4[1] a new six-gap experiment was described. At the time of that report, the tube had been processed, but several difficulties interferred with the testing. The major problem was attributed to a loose internal connection to the anode of the magnetron injection gun. This produced intermittent operation and also a low frequency oscillation involving the gun space. Efforts to achieve a solid connection led to a fracture of the feedthrough insulator in the gun container can. The insulator was replaced, the cathode recoated, and the tube reprocessed.

When tests were resumed, the low frequency oscillations were no longer observed, which seems to justify the assumption as to their origin. However, another oscillation problem was observed. Unless the beam was greatly compressed in the vicinity of the fifth and sixth gaps, a self-excited output at about 2.5 kMc was observed.

- - - - - - -

[1] Varian Engineering Report No. 273-4Q, 1 October - 1 December 1960.

The origin of this was traced to higher order modes in the fifth and sixth cavities. The resonant mode, the same in both cavities, was the perturbed TM_{110} pillbox mode. This has a predominantly axial field and is 1 wavelength in the azimuthal direction. A mode of this type couples very well to the lowest order waveguide (cutoff) mode in the drift tube (TE_{11}). Thus, the two cavities are strongly coupled together. In a perfectly symmetrical cavity, such a mode is degenerate; i.e., its orientation is arbitrary. The pair of cavities in the tube were, however, strongly unsymmetrical. The resonant mode in the output cavity could have an orientation such that it does not couple to the waveguide. Thus, the coupled cavity combination was substantially unloaded, and oscillations could start even though the coupling to the beam and characteristic impedance of the mode were rather low. The existance at the same frequency of modes of the same field configuration in two cavities having highly different shapes is very unusual. Their existence was not observed in cold test because the frequency was so far above the operating band.

By compressing the beam near the output gap, satisfactory experiments could have been made on early cavities and significant data obtained. However, difficulty in driving the tube was observed and this was traced to a poor connection at the input loop. The poor connection was external to the tube, but in correcting it, the coaxial insulator leading into the vacuum was broken and the tube went down to air with a heated cathode.

Repair of the tube necessitated replacement of the heater and cleaning of the cathode. It was also necessary to construct a new input cavity. This could be easily fitted into the tube, assembled as it is with copper gasket connections between earlier repair cavities. Cavity No. 5 was also assembled with a copper gasket seal in its wall so that it could be disassembled and steps taken to eliminate the self-oscillation involving it and Cavity No. 6. Longitudinal slots were cut in the drift tube to move the resonant frequency away from the similar mode in Cavity No. 6. In addition, an insert was made to lengthen the drift tube between these cavities to a point where calculations indicated that oscillation should no longer start. For safety, this latter measure was deemed necessary, even though a very short drift space was the original intent.

When the foregoing repairs were carried out, the tube was again reprocessed and was in operation for several months, with interruptions by less than catastrophic vacuum leaks. Serious oscillation problems were no longer observed. It appeared that the improved collector design noticeably reduced, but did not eliminate, feedback effects. In particular, feedback effects were observed at large signal levels when successive cavities were synchronously tuned. Beam noise was still observed, but its presence had a less severe effect on small signal measurements than with previous experiments. Qualitatively, however, many of the phenomena previously observed were still seen. For example, noise observed at an early gap was still enhanced by

synchronously tuning downstream cavities.

D-c transmission was very nearly 100 per cent for the standard 1200 gauss magnetic field. Also, as with the previous experiment, the cathode deteriorated slightly for a time, but appeared to have then stabilized. Whether this represented an emission exhaustion from the cathode itself, a decrease in spurious emission from some other surface, or a change in the magnetron space-charge cloud is not known.

The method of measuring r-f voltage at the various interaction gaps was re-examined. The problem is that the cavities are very often detuned considerably from the driving frequency. The measurements of external Q and R/Q, however, are made at the resonant frequency of the cavity. Both of these quantities are affected by tuning. Also, they are both functions of frequency. Thus, when measurements are made off resonance, the calculation of voltage from the sampling power is not entirely accurate. While it was felt that this was not of major significance, measurements were made to produce a more accurate calibration. This involved tuning the cavity by means of a plunger in the drift tube and measuring coupled impedance at frequencies far removed from the resonance established by the tuner setting. Because of the effort involved, this was done on only one cavity (Cavity No. 3). Calibration of Cavity No. 2 was performed in a hot test. The beam was modulated at a fixed frequency by driving Cavity No. 1. while Cavity No. 2 was tuned over its tuning range. The test loop power was recorded and the r-f current deduced by means of the known cavity and loop parameters at the resonant frequency of the cavity. Discrepancies between the calculated r-f current and the known constant injected r-f current yielded a correction factor to the loop coupling off resonance. This correction exhibited the same trend as the correction at Cavity No. 3, which was obtained by a completely different method. However, the magnitude of the correction differed slightly. Because of the similarity of geometry, the correction of Cavity No. 2 was also used for Cavity No. 4.

As was mentioned in Quarterly Report No. 4, the output circuit of this tube was modified, resulting in a single tuned resonant circuit with a resistance at resonance of about 700 ohms. The output window is the same coaxial structure used previously. The impedance at the gap can be adjusted by varying a tuner located where this window is inserted into the waveguide, and also by providing an adjustable iris beyond the transition toward the load. A set of measurements was made of the output circuit impedance as a function of these tuning elements for use in establishing various operating conditions.

Cavity No. 5 in this tube is fixed tuned because the original design would not allow space for a tuner. Its resonant frequency is 1450 Mc, which is well above the operating band. It was felt that the effect of tuning this cavity could be achieved by simply adjusting the driving frequency, but the expected results have not always been

observed. It is a question whether valid assumptions can be made as to the variation in other quantities with frequency adjustment. This cavity is singly re-entrant as contrasted with all others which have the doubly re-entrant shape.

In previous experiments, the beam perveance was adjusted over a restricted range by varying the shape of the magnetic field at the cathode. Later, it was found that perveance could be adjusted over a wider range by applying a separate bias voltage to the gun anode. Because of the power supplies available, it was not possible to make the anode positive with respect to the drift tube because interpulse current drawn to the anode was in excess of what can be supplied by the power supply. The voltage is, of course, dc so that considerable power can be involved. By applying a negative voltage, however, the perveance can be adjusted from about 10.3 down to 6.5, over ranges which differ slightly depending on the pulse voltage and magnetic field value. It is believed that this voltage can have only a minor effect on the beam shape at the values of magnetic field used. The bias voltage which can be applied is restricted by the fact that the anode was not intended for this purpose. A high voltage insulator was not provided.

In many of the experiments, a magnetic field which is essentially uniform over most of the tube was used. This is similar to the standard magnetic field of previous reports, except near the output gap, where some adjustment has been allowed in the interest of stability. With the flexibility of magnetic field adjustment restricted by the size and placement of the magnet coils, some variation of field near Gap No. 6 is inevitable when the field in the collector is arranged for minimum return of secondaries. This is a function of the design of the collector and pole piece configurations. Careful design could undoubtedly lead to even less secondary return with nearly any desired magnetic field shape at the output gap. Figure 1 shows the variation of magnetic field on the axis. Curve A is the standard flat field, and Curves B and C are similar to the actual field used. Since adjustment for stability was not very critical, this adjustment often corresponds to maximum induced current in Gap No. 6. The remainder of the field is constant at a value of about 1100 gauss, and it is this value and a shape like Curve B that will be meant by the term "standard field."

As will be seen from the data presented, considerable variation of induced current with magnetic field can be observed in certain ranges of operation. Because of this, power line fluctuations produced a good deal of difficulty in making repeatable measurements. A differential voltmeter was built so that these fluctuations could be monitored and measurements made only when the deviation falls within some predetermined value. This resulted in considerable smoothing of the recorded data.

As with many tube experiments, measurement discrepancies were apparent from time to time. Difficulty was experienced in establishing and maintaining pulse voltage calibration. Duty factors were also subject to some fluctuation. The large

number of quantities subject to measurement necessitated the maintenance of many individual calibrations of attenuators and measuring instruments. We could not always be certain that these were not subject to fluctuation. Therefore, various sets of measurements were not always entirely consistent, although those within a given set appeared to yield very good comparisons. These factors must be considered, particularly when the results obtained on various tubes are compared. It is believed, however, that the accuracy was quite adequate for an over-all evaluation and to establish the effects of various parameters.

Table I shows the physical dimensions of the tube which are important to the interaction process. The early cavities are identical with those previously used, but later cavities and drift tubes have been modified slightly. The beam has the same outside diameter as that of the last six-gap experiment, but is believed to be somewhat thicker. The gun has a design similar to that of the beam tester described in the previous report, but with a slightly larger cathode.

TABLE I

BEAM, DRIFT TUBE AND GAP DIMENSIONS

Drift Tube Diameter	1.50 inches
Beam Outside Diameter	1.25 inches
Beam Inside Diameter	1.09 inches
Gaps 1, 2, 3, 4	0.875 inch
Gap 5	0.640 inch
Gap 6	0.538 inch

DRIFT LENGTHS

(Gap Center-to-Center)

Gap 1 to 2	6.065 inches
Gap 2 to 3	6.065 inches
Gap 3 to 4	6.065 inches
Gap 4 to 5	3.290 inches
Gap 5 to 6	2.651 inches

A large quantity of experimental data were gathered. Some of this requires extensive calculation in order to reduce it to usable form and provide correlation with theoretical expectations. This has not all been accomplished, but enough is available, it is believed, to permit valid conclusions to be drawn.

C. EXPERIMENTAL RESULTS

Preliminary measurements on the entire tube showed that the number of variables was too great for consistent and comparable results to be obtained without an initial examination of certain important parameters involving only two or three cavities. Thus, experiments involving successively larger numbers of cavities were performed, concluding with the entire tube being involved. A larger sampling of the variable parameters could naturally be made with a smaller number of cavities, and these were used to some extent to guide the selection of experiments with many cavities. Also, it was often necessary to return to explore some subsequently observed effects.

1. Small-Signal Gain

The small-signal transadmittance between Gaps Nos. 1 and 2 was measured under a variety of conditions. Figure 2 illustrates some of these results. The transadmittance expression used is

$$y_{12} = \frac{G_o \left(1 + \frac{\Delta V}{V_o}\right) \overline{M}^2}{R\,(1 + R)} \left(\frac{\omega}{\omega_q}\right) \sin \beta_q \ell \qquad (1)$$

$$R = \frac{1}{\sqrt{1 - \left(\frac{u_o}{c}\right)^2}}$$

and

V_o is the drift tube potential

u_o is the beam velocity

G_o is the beam conductance

M is the coupling coefficient

ω is the operating radian frequency

ω_q is the reduced plasma frequency of the first mode

$$\beta_q = \frac{\omega_q}{u_o}$$

ℓ is the intergap drift distance

$V_o\left(1 - \frac{\Delta V}{V_o}\right)$ is the depressed beam potential

In applying this, potential depression in the drift tube and gaps is considered. The r-f voltage level at Gap No. 1 is 600 to 800 volts peak. Low level measurements of beam loading resistance were used in converting observed voltage gain to the experimental values of transconductance shown in Figure 2.

The results given in Figure 2 are transadmittance as a function of perveance at several values of magnetic field. Frequency and voltage were constant. The magnetic field was uniform and its values are given as fractions of standard field. No interception was observed with the 1.0 and 1.2 field values, but the transmission deteriorated increasingly with perveance at the 0.8 magnetic field. Where the interception occurs is a matter for conjecture. Assuming that it all takes place prior to Gap No. 2 and that only G_o and not ω_q is affected, we can correct the observed transadmittance to the value it would have with the full current. The resulting curve is shown in Figure 2. Probably the true value based on the actual beam current passing Gap No. 2 is between the observed and corrected curves. This would still represent a significant deterioration below the 1.0 standard magnetic field curve.

Figure 2 suggests that there is a field for maximum gain, above and below which it deteriorates. Decrease at higher fields can, perhaps, be explained on the basis that the beam is more closely confined away from the wall. Thus, ω_q is slightly larger and the gap coupling coefficient slightly smaller.

The deterioration at lower fields, however, does not fit this picture. The shape of the 0.8 field curves suggests the possibility that reduction in magnetic field somehow corresponds to a change in effective plasma frequency. It can be shown that when perveance is adjusted at constant voltage, maximum transadmittance occurs at a fixed value of drift angle given by

$$\beta_q \ell = -\tan \beta_q \ell$$

$$\cong 2.03 \text{ rad } (116.5^\circ)$$

Thus, from Equation (1) the maximum transadmittance should be proportional to the beam conductance, G_o, at the perveance at which it occurs. This is approximately true in Figure 2, suggesting that the main influence of reduced magnetic field is to affect the relation between perveance and reduced plasma frequency. A variation in plasma reduction factor would do this. This cannot be explained on the basis of the simple theory of an ideal beam, but it might indicate a deteriorating beam. Subsequent observations bear out that the magnetic field has a significant effect on most observable quantities.

In spite of detailed disparities, Figure 2 shows that the transadmittance can be predicted quite closely for transit angles commonly used in klystron design using the simple theoretical expression of Equation (1). The major discrepancy is observed where the focusing field is too low to be of practical use. We can conclude that for practical purposes the errors of calculation are apt to be within the uncertainty as to the actual beam geometry and current distribution.

2. Beam Loading

The beam loading resistance was measured under various conditions with particular emphasis on its variation with signal level. By emphasizing the level sensitivity first, a set of measurements was arrived at which appears to be true at genuinely small signal.

a. Small Signal Results

The beam loading was measured at Cavity No. 2 by exciting the beam at Gap No. 1 to a constant r-f drive level, then tuning Cavity No. 2 and measuring the width of its response curve. The Q curves were wide enough to be asymmetrical due to variations in cavity characteristic impedance and loop coupling. When these effects were accounted for, the curves were symmetrical. For accurate measurements, the drive level at Cavity No. 1 was in the 600 to 800-volt peak range, producing a maximum of approximately 6-kilovolt peak at Cavity No. 2.

Figure 3 shows the observed beam loading at constant perveance as a function of drift tube voltage. The theoretical curve was computed for the infinite magnetic field case taking into account an average potential depression in the gap and relativistic effects. R-f space charge forces in the gap are not included in the ballistic loading model.

We see in Figure 3 that the correspondence between theoretical and experimental beam loading is quite good. Considering the number of calibrations which were necessary to reduce the experimental data to beam loading resistances, not too much significance should be attached to the discrepancy. However, a reduction in beam loading from the purely ballistic model because of r-f space charge forces in the gap is to be expected.

Figures 4 and 5 show beam loading resistance at constant voltage as a function of perveance with magnetic field as a parameter. Theoretical calculations over the entire range of parameters shown were not made, but there is no reason to believe that the deviation at the larger magnetic field values would be any greater than that shown in Figure 3.

In Figures 4 and 5, the reduction in magnetic field was again accompanied by a decrease in transmission. If this were an important factor, however, it would cause an increase rather than the observed reduction in beam loading resistance. Some of the added loading may be due to transverse motion of the electrons in the r-f electric fields of the gap. This causes cyclotron motion in the following drift tube, and always amounts to a gain in energy, i.e., a loading on the gap. Variation in loading with magnetic field enters by the change in cyclotron wavelength relative to the gap length, and the greater transverse motion allowed by a smaller magnetic field.

The foregoing cannot be the entire explanation, for it appears in Figure 4 that a field is reached beyond which further decrease in loading is not observed. Perhaps secondary electrons due to interception cause some of the loading. Some additional loading might also be related to magnetic field effects which are observed also in other ways (small signal transadmittance, for example). The possibility of a general deterioration of the beam cannot be discounted. We can conclude that the ballistic beam loading formulation will predict beam loading to reasonable accuracy, but that some uncertainty may exist due to magnetic field effects.

b. Nonlinear Effects

At large signal level, the Q curves are unsymmetrical even when corrected for variations in R/Q and loop coupling. Thus, the calculation of a beam

loaded Q using the width of the response curve is not strictly justified for use in determining a beam loading resistance at center frequency. Nevertheless, a Q calculated in this way is useful in observing the onset of nonlinear effects. Figure 6 shows a typical curve corrected for loop coupling only. Evidently, a more complicated model is required if this is to be used to specify a beam loading impedance at the drive frequency.

Figures 7 and 8 show the measured response width "Q_L" as a function of voltage level at the catcher and driving cavities. We note how low the voltage must be on the drive gap in order to escape saturation effects in this measurement. It is also interesting to note that two points in Figure 7 which were measured on Gap No. 3 coincide closely with the measurements made on Gap No. 2. This supports the contention that beam loading is the same at each gap if the conditions are maintained uniformly.

It seems reasonable to assume that the major deviation from linearity in these beam loading measurements is due to voltage saturation at the catching gap. It may also be that the condition of the beam, i.e., details of the bunch, also influence the amount of nonlinearity.

We recall that in previous measurements it was found that beam loading resistance tended to decrease for later cavities in the tube. It is now suggested that these are simply the result of the phenomena shown in Figures 7 and 8. These measurements were made by driving the tube upstream by two or three cavities. Even for small drive signals and allowing for a small gain per stage, the voltage at the catching cavity could be well up into the saturated range. A survey of the previous data indicates this to be true.

It is evident from the tuning at maximum response in Figure 6 that a measurable reactive effect is present. This has been observed on previous tubes, but now it is interesting to measure the large signal dependence of this effect. Figure 9 shows a measurement of frequency shift in the cavity response as a function of maximum gap voltage at resonance. Both the value at the peak and the shape of the Q curve were considered in determining the frequency shift. Here we see the effective driving current varying from inductive to capacitive as the signal level increases. This is primarily a function of the motion of the electrons in the gap under the influence of the gap voltage. The details would thus be a function of the phase angle of the voltage with respect to the current. The effect is interesting mainly from a theoretical viewpoint rather than having an effect on the design of the tube.

3. Large Signal Behavior

Questions regarding the use of high perveance which have emerged in this study mostly involve saturation effects. Consequently, considerable effort was

expended in the examination of large signal behavior. As a result of early attempts to investigate the behavior of the tube as a whole, it was apparent that a systematic investigation stage by stage should be made. Figures 10 through 29 illustrate some of the results of this investigation.

The cavity under observation is detuned to the maximum extent, and the current is saturated by adjusting the input power to Cavity No. 1. Measurements are made for various magnetic field values, drift tube voltages and perveance values. For gaps beyond No. 2, observations are made as a function of the tunings of previous cavities. For the early gaps a considerable range of voltage and magnetic field is investigated, while for later gaps the number of variables increases so that any one parameter must necessarily receive less attention. Measurements which can be compared for successive stages involve at least one drift tube voltage and two perveance values; one near the low end and one near the high end of the attainable range.

a. Two-Cavity Saturated Current

Figures 10 through 12 show saturated current at Gap No. 2 as a function of perveance with the magnetic field as a parameter. Again we see an apparent degradation in performance with the reduction in magnetic field below some threshold. At 30 kilovolts (Figure 10), no significant interception is observed. For the 35-kilovolt case (Figure 11), enough interception is seen to cloud the reliability of a magnetic field effect. At 45 kilovolts (Figure 12), observed interception at a low magnetic field value is larger and a corrected curve is shown which is based on collector current rather than cathode current. All other curves are based on cathode currents. We see that even if all interception were prior to Gap No. 2, the change in effective current would not be enough to account for the degradation in r-f gap current.

Figure 13 is a plot of saturated current with variation in tube voltage at one perveance value. We see that the effect of reducing magnetic field, or the threshold of this effect, becomes less with decreasing voltage. Here also, a corrected curve based on collector current is shown. Some effect other than interception is again observed. We will see that this interpretation cannot always be made, and will discuss the matter more fully in a subsequent section.

In making the measurements represented in Figures 10 through 12, sufficient driving power into the input cavity could not always be obtained to allow full saturation of the beam at Gap No. 2. Only the results at 30 kilovolts in Figure 10 were obtained by actually achieving saturation. With the other data, the portions of the saturation curve which could be obtained were extrapolated to estimate the saturated current. The observations extended to a point where the process of extrapolation could yield reasonably accurate peak current. Because of the shape of the

curve, however, the accuracy of determining the necessary driving voltage would be very low. Thus, the bunching parameters can only be calculated for the 30-kilovolt case. No significant difference in driving voltage with magnetic field was observed.

Table II shows the small signal, space-charge, and bunching parameters calculated for the two-gap case of Figure 10 and for subsequent three, four and five-gap cases. We notice that the intergap spacing is greater than a quarter plasma-wavelength for most cases. The decrease in current which is always observed with increasing perveance seems to be associated mainly with increasing plasma transit angle.

b. Three-Cavity Saturated Current

Figures 14 through 20 show the results of saturating the current at Gap No. 3 by adjusting the drive level at Gap No. 1. Figure 14, made with Cavity No. 2 tuned to synchronism shows affects similar to those observed in the two-gap case. Here, however, interception was such that correcting by the transmission factor causes all the points to be distributed around the dashed corrected curve. Therefore, we have a case where decreased performance appears to be correlated with interception.

In Figures 15 through 18, the frequency of the second cavity was adjusted and the beam saturated at the third gap. In each case two perveance values are shown, one high and one low but not the same in each case, although all the highs and all the lows can be compared qualitatively. In Figures 15 and 17 the normalized gap voltage is also shown. This is the gap voltage relative to d-c drift tube voltage reduced by the small-signal beam coupling coefficient. In most cases, magnetic field was held constant at a value high enough so that interception and performance degradation would not be a factor.

As with all tests of this series, the currents are calculated on the basis of the actual cavity impedance shunted by the small signal beam loading conductance. Nonlinearities in this loading will produce errors when Cavity No. 2 is tuned near the driving frequency for then beam loading is an important component of impedance. Effective r-f impedance is undoubtedly somewhat lower than the value used and hence the entering current is actually higher. This effect is operative to a considerable extent in the vicinity of the tunings for maximum currents at Gap No. 3, thus there is no real basis for calculating the phase of the r-f voltage relative to the entering current. Also, the effect on loading of an already bunched beam is not known, particularly where the phase angle between current and voltage is large. Beam loading is not a significant factor at Cavity No. 3 which is greatly detuned and presents an impedance considerably lower than the beam loading resistance, even in the presence of large signal effects.

TABLE II

COMPOSITE LARGE-SIGNAL DATA

Case	Voltage (kv)	Perveance	ℓ/λ_q	Penultimate α	Excitation Parameter $\omega_q/\omega\alpha$	Bunching Parameter X	Rel Current I_b/I_o
Two Gap	30	7	0.28	0.45	0.31	2.9	0.92
	30	10	0.31	0.55	0.31	3.5	0.88
	35	7					1.00
	35	10					0.91
Three Gap							
Synch Tuning	35	7.14	0.26	0.375	0.36	2.3	0.85
	35	9.22	0.30	0.45	0.42	2.75	0.80
Max Current	35	7.14	0.26	0.4	0.33	2.45	0.89
	35	9.22	0.30	0.49	0.32	3.0	0.81
Synch Tuning	45	7.85	0.24	0.43	0.32	2.43	0.91
	45	9.88	0.28	0.48	0.33	2.65	0.80
Max Current	45	7.85	0.24	0.42	0.33	2.32	0.97
	45	9.88	0.28	0.47	0.34	2.60	0.82
Four Gap							
Synch Tuning	35	7.18	0.26	0.45	0.30	2.75	0.83
	35	9.51	0.31	0.51	0.31	3.12	0.81
Max Current	35	7.18	0.26	0.41	0.32	2.54	0.92
	35	9.51	0.31	0.51	0.31	3.12	0.86
Synch Tuning	45	7.71	0.24	0.47	0.29	2.60	0.94
	45	9.64	0.27	0.51	0.31	2.82	0.85
Max Current	45	7.71	0.24	0.44	0.31	2.43	1.00
	45	9.64	0.27	0.51	0.31	2.82	0.89
Five Gap							
Synch Tuning	45	7.71	0.13	0.64	0.21	1.88	1.03
	45	9.67	0.15	0.63	0.24	1.88	1.03
Max Current	45	7.71	0.13	0.67	0.20	2.00	1.46
	45	9.67	0.15	0.69	0.22	2.05	1.30

The r-f currents obtained at Gap No. 3 when Cavity No. 2 is synchronously tuned are nearest to being comparable with two-cavity performance. The current entering Gap No. 2 is small and, here where the drift angle is near 90 degrees, residual velocity modulation is negligible. For comparison with other two-gap cases, the parameters for the 35 and 45-kilovolt cases are entered in Table II.

In determining the drive level for saturation, the accuracy is rather low and the points are widely distributed. This is because of the flatness of the curve of output vs drive in the vicinity of saturation. The saturated current itself can be determined quite accurately, however, and the points lie along a smooth curve.

In Figure 19, the effect of the reduction in a uniform magnetic field is again investigated. Significant degradation is noted at 0.9 standard field. Interception was seen, however. If we again correct by the transmission factor ("corrected" curve, Figure 19), we see rather good agreement with the higher field. Here we have an additional example of degradation with reduced magnetic field which, superficially at any rate, might be explained on the basis of interception.

Figure 20 shows the effect of adjusting the shape of the magnetic field while keeping the field at the cathode constant. An attempt was made to approximate the shape of field near the output which was found to produce maximum efficiency at the output gap. The field was increased in the vicinity of Gap No. 2 and allowed to fall rapidly in the vicinity of Gap No. 3. Nearly 100 per cent transmission was maintained throughout. The main effect here may be a nonuniform magnetic field in the drift space between Gaps Nos. 2 and 3. It is probably true that the average value of the field is changed as well. Thus, the plasma drift angle is also affected. We notice here that with this nonuniform field a smaller current and voltage of Gap No. 2 is required to saturate the current at Gap No. 3 but a significantly larger saturated current is produced. Superficially, the curves look very much like the result of increasing the beam voltage (for example, compare Figure 16 with Figure 18). The actual shape of the magnetic field used here could not be determined until the tube was extracted from the focusing magnet structure.

c. Four-Cavity Saturated Current

The next group of experiments consisted of measuring the saturated current at Gap No. 4 as a function of Cavity No. 3 tuning. In these experiments, the tuning of Cavity No. 2 was found to have a significant influence and increased the number of parameters to be considered. Measurements were made only at 35 and 45 kilovolts.

Figures 21 and 22 show two examples of the currents at all three gaps, and Figure 23 shows the Gap No. 3 voltage for these two cases. Figures 24 and 25 show the Gap No. 4 saturated current for all the cases considered - low and high perveance at each of two beam voltages. The parameter is the tuning adjustment of Cavity No. 2.

We see that Cavity No. 2 produces very little effect when Cavity No. 3 is tuned near synchronism. Off synchronism, however, the effect can be considerable, particularly at low voltage and high perveance. In all cases, the bunching is enhanced by tuning Cavity No. 2 lower than the drive frequency. This effect appears to be associated with long plasma drift angles. In Figure 24, we see that it can be large enough that maximum saturated current is obtained when the penultimate cavity is tuned low rather than high in frequency. In cases where Gap No. 2 is rather widely detuned, as for example in Figure 21, the currents at Gap No. 2 are comparable with those at Gap No. 3. Thus, the beam is driven to a high level along much of its interaction space. Evidently, with Cavity No. 2 tuned low (capacitive reactance), the beam entering Gap No. 3 is in a more favorable condition for producing bunching with the long 3 to 4 plasma drift angle.

In broadbanding a klystron amplifier, a distribution of cavity resonances is necessary to produce the required passband. The fact that bunching is enhanced and detuning curves flattened by tuning an early cavity to a lower frequency can thus be useful. At any rate, these results show that high level performance is apt to be optimized with saturation conditions extending over a number of drift spaces and with the level of current sensitive to the tuning of more than one penultimate cavity.

The operating parameters for synchronous tuning and maximum current conditions in Figures 24 and 25 are entered in Table II for comparison with other cases.

d. Five-Cavity Saturated Current

The next set of experiments consisted of measuring the saturated current at Gap No. 5 as a function of the tuning of Cavity No. 4. The results were found to be sensitive to the tunings of all previous cavities, adding still another parameter to be adjusted. Measurements were made only at 45 kilovolts beam voltage and two perveance values. Figures 26 through 29 show representative members of this set.

Figures 26 and 28 show the conditions for near optimum current at Gap No. 5. Figures 27 and 29 are corresponding examples with Cavity No. 3 tuned below the operating frequency. The tuning of Cavity No. 2 varies in these cases, but it has a relatively small effect on the maximum gap current and no significant effect on the shape of the curves.

Besides more driving cavities, the main difference between this and previous examples is that the penultimate drift space is only a little more than one half as long. Tuning Cavity No. 3 below the signal frequency has only a deleterious effect. This is in contrast to the four-gap experiment where tuning Cavity No. 2 low produced a marked improvement. Thus, we conclude that the latter result was associated with the long penultimate plasma drift angle. Another contrast is that the effect

of tuning the penultimate cavity is greater and more rapidly varying for the shorter drift angle. The conditions for maximum current begin to be more like those commonly observed in high power klystron amplifiers with short drift angles.

e. Comparison of Saturation Observations on Driver Gaps

In the preceding sections we have presented observations made by saturating the current at successive gaps along the tube as a function of the tuning of preceding cavities and in some cases magnetic field adjustments. It is desirable at this point to compare this information before proceeding with observations at the output gap.

(1) Effect of Magnetic Field

In the two-gap and three-gap saturation experiments, the magnetic field was adjusted in value, but kept uniform along the tube. Deterioration in saturated current was observed at fields below the standard of 1100 gauss. This was sometimes accompanied by interception, but in one case (two-cavity at 30 kilovolts, Figure 10) severe deterioration was encountered with no interception. In cases where interception was observed, the relative r-f beam current calculated from the observations was corrected by the transmission ratio. In the two-cavity cases shown in Figures 12 and 13, deterioration was still observed after correction, while in the three-cavity cases, Figures 14 and 19, the corrected curves corresponded well with the higher magnetic field observations.

When the magnetic field was varied over a considerable range, there appeared to be a threshold below which deterioration occurred and above which a small decrease might also be observed. The latter could not always be distinguished because of the experimental accuracy. That the magnetic field for deterioration moves upward with increasing beam voltage is shown most clearly in Figure 13, but can be seen by comparing Figures 10, 11 and 12.

One immediate thought is that all the measurements are referred to the same standard magnetic field level, even though the d-c beam voltage is adjusted. Electron trajectories are preserved, however, if the magnetic field is scaled as the square root of the voltage. Thus, the lower the voltage, the stiffer the beam. This certainly shows in the fact that interception occurs earlier in higher voltage beams. It is perhaps significant that this additional stiffness appears to be accompanied by less degradation in current with decreasing relative magnetic field.

In the low-level measurements, interception was also observed. More would be expected in the saturation measurements because of the larger r-f gap voltages and radial space-charge forces in the bunch. However, interception will also depend on downstream gap voltages, magnetic field shapes, etc. Efforts to

minimize these influences were made, but were limited by factors such as the necessity for stability. Tube alignment is a possible factor, which could, in fact, vary with time. Correlation of collector current with effective current at any point in the beam cannot really be justified.

Although interception may play a part in some of the measurements, it is clear that something else is also involved. Secondary electrons which result from interception could be quite variable in effect and perhaps play a part. Another factor which cannot be entirely discounted is the character of the beam itself.

The design of the gun was based on a laminar flow model which predicts the perveance quite accurately. Thus, it might be inferred that the flow in the actual gun was quite similar to the laminar model. However, it was observed that the beam was noisy, and it is known that back bombardment of the cathode occured which is not predicted by the laminar model. To this extent, the flow in the gun and beam was not ideal. If the flow in the gun was pathological in some respect, it would certainly be sensitive to both magnetic field and anode voltage. If such a condition existed, it would probably influence the beam characteristics which would in turn, be sensitive to the magnetic field variations. However, the beam was quite stiff at the values of magnetic field used, and had most of the characteristics of confined-flow focusing. It is difficult to imagine a disturbance arising in the gun which would be violent enough to produce the observed effects on saturated current, although effects on low-level measurements were another matter. Beam tester measurements, including observation with a target, were made on very similar beams. While azimuthal instability was observed, it was not excessive and the beam appeared to be well behaved in other respects.

Whatever the source of the observed magnetic field effects, the significant result is that a sort of threshold of magnetic field exists, below which performance deteriorates measurably. This threshold may be higher than if deterioration were due to interception alone, but not much higher. At the higher voltages, in fact, deterioration in current was always accompanied by interception. It seems likely that avoiding interception will continue to be sufficient to avoid degradation in performance. Similar observations will be made when high efficiency operation at the output gap is discussed. Detailed design changes may be found which will lower the required focusing marginally, but unusually large magnetic fields are likely to be necessary with designs employing high density beams passing near metallic circuits.

(2) Saturated Currents Involving Two Cavities

In Table II, comparable results for the various saturation experiments are given. In the three, four and five-gap cases, the synchronously tuned penultimate cavity condition is expected to represent nearly pure two-cavity klystron interaction. These can then be compared with the two-gap case and with

the calculations in Webber's first paper.[2] (We will refer often to the ballistic calculations made by Webber.)[2,3] The data to be compared were taken at a uniform magnetic field of 1.1 of a standard field. This is sufficiently near the field for best results in all cases so that magnetic field effects can be discounted.

We recall that all the intergap spacings, with the exception of 4 to 5, are identical, the geometries of all gaps are the same and the dimensions of the first four cavities are the same. The parameters computed are those which, from Webber's results, are believed to be important:

ℓ/λ_q = the penultimate drift length as a fraction of reduced plasma wavelength

α = normalized r-f voltage at the punultimate gap

$\omega_q/\omega\alpha$ = the excitation parameter, and

X = the ballistic bunching parameter

The parameter ω_q/ω for this tube with the assumed beam geometry is shown in Figure 30 as a function of perveance. The plasma drift angle for the early intergap spacings is shown in Figure 31.

Unfortunately, as we previously noted, Gap No. 1 could be driven only hard enough to saturate the beam at Gap No. 2 for 30 kilovolts beam voltage. However, this should serve well enough as a comparison.

In comparing with Webber's results, we need a way of distinguishing a quantity equivalent to his normalized radius, γb. This comparison is provided by choosing a γb giving the plasma reduction factor calculated for our tube. Over the range of operation this is found to vary from about 0.3 to 0.4 so that his curves for $\gamma b = 0.4$ should provide the best comparison. Webber finds the effect of this radius factor to be small for drift lengths which are usual in klystron design. For long plasma drift angles such as we have here, however, a considerable variation with this parameter is seen in his Figures 6, 7, and 8. Smaller γb, with enhanced short range forces, suffers decidedly in the region near and beyond a quarter wavelength.

Referring to the relative currents shown in Table II, Page 15 we see a small discrepancy in saturated current between Gap No. 3 and Gap No. 4

---

[2] S. E. Webber, "Ballistic Analysis of a Two-Cavity Finite Beam Klystron," IRE PGED Transactions, Vol. ED-5, No. 2, April, 1958, p. 98.

[3] S. E. Webber, "Large Signal Analysis of the Multicavity Klystron," IRE PGED Transactions, Vol. ED-5, No. 4, October, 1958, p. 306.

which is well within the range of accuracy of the measurements and the various calibrations. A large discrepancy of about 10 per cent, however, is observed between the quasi-two-gap interaction with a synchronously tuned penultimate cavity and data obtained at Gap No. 2. It is unlikely that a difference of this magnitude can be accounted for by lack of accuracy. Rather, it may reflect the effect of the feedthrough terms from modulation in previous stages. Miscalculations, however, might exaggerate the apparent effect.

Data obtained at Gaps Nos. 2, 3, and 4 cover the range of $\beta_q \ell$ around 90 degrees. Cavity No. 5 is, however, separated from its penultimate cavity by only 45 to 55 degrees of reduced plasma angle. As expected, an increase of saturated r-f current for shorter drift spaces is observed. Currents are again smaller than an extrapolation of the genuine two-gap result. The results of these experiments are summarized in Figure 32. Currents at Cavity No. 2 are comparable with Webber's[4] computed data for $\gamma b = 0.8$. The speculative extrapolation of these two-gap results yields relative r-f currents of 1.15 to 1.20 d-c beam current for short drift angles. Currents in the quasi-two-gap (synchronously tuned penultimate cavity) experiments follow the same trend with reduced plasma angle. They are, however, smaller by an amount less than, but similar in magnitude to, the current at the penultimate gap. This is significant in indicating the serious effects associated with signal conditions at the penultimate gap.

Also listed in Table II are the modulation indices α and Webber's bunching parameter $\omega_q/\omega\alpha$. As previously noted, the accuracy of measuring α is rather low, but still there is a remarkable consistency in the data. The agreement with Webber's computed bunching parameters is quite good over the entire range of these experiments.

It is interesting to note in the three and four-gap cases that the bunching parameter for maximum saturated current occurs quite near the value of the argument which gives a maximum of $J_1(X)$. It would be possible to match the saturation curves reasonably well to the Bessel function, although space charge undoubtedly plays a very significant role. In the five-gap case the bunching parameter is significantly less, as Webber's results indicate it should be.

We can now conclude that, for two-gap interaction, the performance of the high perveance beam is consistent with the results of Webber. Experience has previously indicated that these computed results represent the performance of lower perveance devices with reasonable accuracy.

- - - - - - -

[4] S. E. Webber, "Ballistis Analysis of a Two-Cavity Finite Beam Klystron," IRE PGED Transactions, Vol. ED-5, No. 2, April, 1958, p. 98.

(3) Multicavity Saturation Current

Figures 15 through 20 show most clearly the effect of detuning the penultimate cavity. Except very near resonance, the gap presents a nearly pure reactance whose magnitude is adjusted. The voltage is the product of this reactance with the induced current in the gap. The current in the beam is inferred by assuming a small signal beam loading conductance shunting the gap which reduces the net induced current. This loading conductance is due to bunching while the electrons are in the gap under the influence of the gap voltage. When the gap voltage and entering current are large, however, the induced current will undoubtedly not be affected in the same way. Moreover, the loading effect will be a function of the phase angle. It seems reasonable to believe, in fact, that the effective beam loading conductance may diminish when the entering current is larger and when the phase angle increases. Then the gap voltage would have a phase of more nearly 90 degrees with respect to the actual current in the beam than would be indicated by small signal beam loading. Ninety degrees is the value of phase found by Webber to be the most effective in bunch enhancement and used in his calculation.[5]

In spite of ambiguities regarding the actual phase and magnitude of the induced current, we know that, except near resonance, the gap impedance substantially controls the ratio of voltage to r-f current in the beam. Some particular ratio will produce optimum bunching. Thus, we see the saturated current rising as the penultimate cavity is tuned higher than resonance. Then, after the maximum is passed it falls again. As higher beam voltage is applied, the Gap No. 2 detuning for maximum Gap No. 3 current increases. This is because the beam conductance increases so that a lower gap impedance produces the same relative bunching conditions.

Figure 33 shows the relative beam current with optimum penultimate tuning as a function of reduced plasma angle for several multicavity experiments. Comparing with the quasi-two-cavity data (Figure 32), we see that the enhancement with detuning increases steadily with decreasing plasma angle. In the five-gap case, this improvement has reached 45 per cent. This sort of result is also shown qualitatively in Figures 3 and 5 of Webber's second paper. It is significant that the variation in both voltage and perveance can be expressed in this single parameter. This consistency suggests that the respective penultimate gap impedances can indeed be varied over a sufficient range to achieve a true optimum.

In Figures 24 and 25, we see examples of the sensitivity of the bunching to the tuning of cavities prior to the penultimate. This will almost certainly be the case when the beam is driven to large signal in these prior drift spaces. The surprising thing about the four-gap experiments is the effect of tuning Cavity No. 2

- - - - - - -

[5] S. E. Webber, "Large Signal Analysis of the Multicavity Klystron," IRE PGED Transactions, Vol. ED-5, No. 4, October, 1958, p. 306.

low. We have shown that this is associated with the unusually long penultimate drift space (> 90 degrees). With shorter drift spaces, the best tuning for earlier cavities is high. This long drift space effect might be used to enhance the bandwidth in a practical tube design.

We turn now to the qualitative comparison of our results given in Table II, with the computations given in Webber's second paper.[6] The maximum current cases in Table II are to be considered. None of the sets of results presented by Webber fit the case of our tube with any accuracy. Also, his range of drift angle does not cover all of our cases. In our case, the first tunnel length is about a quarter space-charge wavelength, ω_q/ω ranges from 0.13 to 0.16 and the γb is about 0.4. Webber's Figures 7 and 12 come nearest to these values, although he does find variation in details with first tunnel drift length and also with γb. In fact, the variation with γb appears to be larger than was found with the two-cavity case. The major effect of this parameter is in the relative importance of harmonic, or short range space charge forces. A smaller γb (smaller space-charge reduction factor) produces a relative enhancement of these forces. It is in the close bunches produced by three-cavity interaction where this would be the most strongly felt.

Examining the cases given in Webber's Figures 7 and 12 we see that maximum bunching is obtained with a relative current entering the penultimate gap decreasing with increasing last drift angle. This is observed in our cases where this current ranges from about 0.4 to 0.6 for the three and four-gap experiments and is 0.8 to 0.9 in the five-gap case. Within a given set, the general tendency is to decrease with increasing drift angle. These values are seen to be in reasonable agreement with what one would expect from an extrapolation of Webber's results.

The values of $\omega_q/\omega\alpha$ at which maximum bunching occurs increase with increasing drift distance, but remain about the same for a given drift distance over a wide range of parameters. In Webber's Figure 10, the effect of the first drift distance is explored. The regions of constant $\omega_q/\omega\alpha$ appear to move to larger second drift distances when the first drift distance is increased. Thus, a diagram equivalent to Webber's Figures 7 and 12 but for one-quarter wave first drift distances, might have the regions of constant $\omega_q/\omega\alpha$ moved out slightly. Nevertheless, for our cases with drift distances of 0.25 to 0.3 plasma wavelengths, observed values of $\omega_q/\omega\alpha$ of about 0.3 appear to be definitely smaller than Webber's theory would predict. The five-gap case, having a last drift space of 0.13 to 0.15 plasma wavelength is within the range of Webber's curves. The observed $\omega_q/\omega\alpha$ of about 0.2 is again significantly smaller than theory predicts. This means that a bunching voltage which is larger by perhaps 30 to 40 per cent is required. This was not found in the two-cavity case and appears to be peculiar to bunch enhancement by a penultimate gap. This conclusion requires a good deal of extrapolation and perhaps should not be taken too seriously. It will evidently be sensitive to the condition of the entering beam. It can also be

---

[6] S. E. Webber, "Large Signal Analysis of the Multicavity Klystron," IRE PGED Transactions, Vol. ED-5, No. 4, October, 1958, p. 306.

interpreted as reflecting the nonideal interaction in the actual gaps (effects of field shape, space charge forces, etc.). It does, however, point up the necessity for adequate flexibility in penultimate cavity impedance.

(4) Conclusions

The conclusions to be reached in these experiments are that the large signal results are in general agreement with the ballistic theory of Webber. This might be expected since the disk model should represent the thin hollow beam with reasonable accuracy. The trends in observed current and also improvement with penultimate cavity detuning have been correlated with plasma drift angle as the major parameter.

f. Measurements at the Output Gap

Measurements made involving the entire tube consisted mainly of observing power output from Cavity No. 6 under various operating conditions. The power was measured using a directional coupler and thermistor, with frequent calibrations using the water load. When the tube was tuned up for maximum output power, the water load was always used as the final measurement of efficiency. Thus, the efficiencies quoted are based on water load power and cathode current. A strong degree of interdependence between tuning adjustment and magnetic field shape was observed. To avoid undue complications, however, an entire set of measurements were made with a single set of cavity tunings. While this did not produce completely optimized power output it was near enough so that any results will surely be valid when the power is optimized.

As previously noted, the so-called standard magnetic field was not uniform in the region of the output gap. The shape was selected for stability reasons, and it was necessary to maintain this, or a similar one, during measurements on the output circuit. It was even necessary at times to vary the shape in order to achieve stability in all desired ranges of operation.

Unquestionably, the beam moves out closer to the drift tube in the region of Gap No. 6. Therefore, an assured value of beam coupling coefficient cannot be assigned. Hence most of the results are evaluated in terms of gap driving current rather than a calculated beam current. This also makes sense, because the output circuit is most often operated with a predominantly resistive impedance. Voltage saturation effects make the evaluation of a current entering the gap unrealistic. For some purposes, however, it is useful to assign limits to the gap coupling coefficient. Table III shows these coefficients for two commonly used beam voltages. V_o is the drift tube voltage. V_b is the assumed gap voltage used in the computation. M_6 is the gap coupling coefficient for the queiscent beam calculated in the same way as the coefficients for the entire tube. $M_{6\ max}$ is a gap coefficient calculated for the

TABLE III

OUTPUT GAP COUPLING COEFFICIENTS

V_o	V_b	M_6	$M_{6\ max}$	$\frac{M_{6\ max}}{M_6}$
45	40	0.82	0.91	1.11
35	31	0.77	0.88	1.13

beam displaced until it just grazes the drift tube. Under large signal conditions with severe radial electron motion, this geometry could never be achieved if, indeed, it could at all with attainable magnetic field shapes. Thus, this maximum coefficient is to be taken as a sort of upper bound. The actual coupling coefficient will lie somewhere in between the two values given.

The bulk of the output measurements were made with a fixed set of tuning adjustments for previous cavities. This was done in order to avoid the excessive number of parameters which would have been necessary had the cavity tunings been subject to adjustment. At one point, the power output was optimized with respect to both cavity tuning and magnetic field. Table IV shows the drive frequencies and cavity tunings both for the standard test and optimized cases.

TABLE IV

OPTIMIZED TUNING OF TUBE AT 50 KILOVOLTS

	Resonant Frequency	
	Saturation Tests	Optimized at 50 Kilovolts
Drive Frequency	1300 Mc	1292
Cavity No. 2	1250 Mc	1262
Cavity No. 3	1330 Mc	1339
Cavity No. 4	1372 Mc	1362
Cavity No. 5	1450 Mc	1450

There is very little difference, and it can be assumed that cavity tunings will not significantly alter the conclusions drawn from the test results.

The conditions and results of the high efficiency test are shown in Table V.

TABLE V

OPTIMIZED OUTPUT

Voltage = 50 kilovolts
Current = 93 amps
Microperveance = 8.3
Power Output = 2.0 Megawatts
Efficiency = 43 per cent

An efficiency of 43 per cent at microperveance 8.3 is the best performance observed in this program. Considerable care was taken to insure calibration accuracy; the power output being based on a water load measurement and efficiency on total cathode current.

The extensive testing consisted of measuring saturated power output with several output circuit impedance values and over a range of beam voltages and perveances. It was also found that one of the important parameters is magnetic field value and shape. This is less subject to quantitative evaluation, because the actual shape of the field was arrived at empirically, and cannot be measured until the tube is extracted from the focusing magnet. This is not an easy process, and has a high likelihood of rendering the tube inoperative. Thus, the magnetic field shapes will not be measured until the useful life of the tube is over. We can, however, make qualitative inferrences as to the shape in some cases from previous field measurements which have been made.

For various reasons, not the least of which is measurement consistency and computational convenience, most of the measurements were made at a single frequency. For a number of reasons this was chosen to be 1300 Mc. The output circuit resonance was, however, centered somewhat off this frequency, and the full resistive impedance (about 700 ohms) could not be reached with the adjustments available. Thus, most of the measurements were made at a maximum resistance of 550 ohms. Considerable previous exploration of the effect of output circuit impedance has shown that the output is not very sensitive to impedance adjustment in this range. A very small percentage increase in efficiency might be realized, but nothing significant would be gained by this adjustment and the major conclusions would not be affected. This relatively low impedance does, however, probably accentuate the observed variation in efficiency with beam voltage.

The actual value of the output circuit impedance is one of the least reliable quantities used in computing voltages and currents. There is, for example, often an inconsistency between power output computed from the observed output gap voltage and that actually observed in the output waveguide. This is only a minor annoyance, however, and in no way influences the trends which develop.

Figures 34 and 35 show the saturated output expressed as efficiency for 35 and 45 kilovolts, for three different output circuit impedances, and over a range of perveance values. Here we see the degradation in performance with increasing perveance which has been previously observed. The currents driving Gap No. 6 for these cases are shown in Figures 36 and 37.

These results were obtained at 1.1 times standard magnetic field, but with a shape at the output gap similar to Curve C of Figure 1. We have seen that this value of field appears to be large enough so that serious variations with field level are not to be expected. This is borne out by the measurements shown in Figure 36. As can be seen, the difference between the 1.1 and 1.2 times uniform magnetic field is relatively small. However, it is found that as the voltage increases the performance can be enhanced to an increasing extent by adjusting the magnetic field shape. The shape is similar to the optimum field shown in previous reports,[7] although it differs in detail. The important thing seems to be that the field increase in the vicinity of Gaps Nos. 4 and 5 and decrease rapidly toward Gap No. 6. The equilibrium radius of the beam is first compressed, then allowed to expand at Gap No. 6, even beyond the original radius in the gun. This is believed to be roughly the same field shape that was used to enhance the saturated current in the three-cavity experiment.

The amount of adjustment to optimize the power decreases with beam voltage until at 35 kilovolts very little adjustment from the standard flat field is required to optimize the power. In fact, for this lower voltage, adjustments further back along the tube seem to produce more effect than field adjustments near the output. We see also in Figure 38 that at the lower voltages, (35 kilovolts, for example) increasing the flat field beyond 1.1 times the standard value has produced a decrease in power output. This is the peaking of saturated current for attainable magnetic field values which was also observed in the experiments on previous cavities. Decreasing saturated current with increasing field may be an effect of gain variation in previous stages.

The fact that the enhancement in performance with magnetic field shape is also true at a lower level of r-f voltage at the output gap is shown in Figure 39. The results in Figure 38 were obtained with an output impedance of 555 ohms, while the impedance for Figure 39 was 167 ohms. The effect of magnetic field adjustment

- - - - - - -

[7] Varian Engineering Report No. 273-4Q, 1 October - 31 December 1960.

is even greater for the lower impedance, perhaps as a result of voltage saturation effects for the higher impedance. These observations will be discussed in more detail when further information is presented.

Figure 39 does not give the entire picture because when perveance is held constant, we would expect observed efficiency to increase with beam voltage. The efficiency can be expressed in the following way:

$$\eta = \frac{1}{2} \frac{R_g}{R_o} \left(\frac{I_G}{I_o} \right)^2 = \frac{1}{2} R_g K_o V_o^{1/2} \left(\frac{I_G}{I_o} \right)^2 \qquad (2)$$

The gap resistance, R_g, is constant throughout the experiment so that if the relative gap current did not change, the efficiency would be proportional to the square root of the voltage. Using this expression for efficiency, the relative gap currents for the case of Figure 39 can be computed with the result shown in Figure 40. An increase in gap current with increasing voltage can be expected on the basis of prior results, because of the reduction in plasma wavelength and improved gap coupling coefficient. It is the divergence of the two curves shown in Figure 40 that is the interesting result. This is the basis for the field adjustment affect which is noted in Figures 38 and 39. This has been observed in all previous experiments but enough data have not been available to evaluate it. The relation of this to interception and coupling coefficient will be discussed later when additional information has been presented.

In Figures 34 through 37 we have seen the decrease in efficiency and gap driving current with increasing perveance. In Figure 41, the results of these and other experiments are plotted as gap driving current vs the plasma angle of the penultimate drift space. The results are for both low and high impedance of the output circuit. At each voltage, perveance increases downward along the curve. Although the magnetic fields are slightly different, the major difference between the two sets is the result of voltage saturation in the output gap. The affect of adjusting the magnetic field shape for optimum output is shown in the lower set of curves as the difference between the solid and dash lines.

A feature of Figure 41 not seen before is the distinct separation with operating voltage. Evidently, some parameter besides the plasma drift angle is important. Coupling coefficient cannot play a part because it would produce a discrepancy in the opposite direction. This separation with voltage still exists with optimized magnetic field as is shown in the lower set of curves in Figure 41. However, the spread is reduced by field optimization. This effect will be discussed in more detail later.

Another interesting observation in Figure 41 is the slope of the constant voltage curves. The experiments with previous stages indicate a degradation with drift angle, but the slope here is much too steep to be consistent with the magnitudes of currents observed for the drift angles of the previous stages. The three-cavity results shown in Figure 33 cannot be compared directly because a coupling coefficient was used to calculate beam current rather than gap current. For comparison, the three-cavity data are plotted in terms of relative gap current in Figure 42. The spread with voltage is now due to coupling coefficient. One difference in the three-gap and output gap experiments is that, for three gaps, the tuning of the penultimate cavity was optimized at each point. However, when current was measured at Gap No. 6, the impedance of the penultimate cavity was only about one-half of the optimum penultimate cavity impedance of previous experiments. This cannot explain the effect of varying the voltage, for the tuning of the penultimate cavity would be more nearly optimized for the 45-kilovolt case where the beam impedance is lower. However, it might explain an exaggerated effect of increasing perveance for this will move the penultimate cavity tuning further from optimum. In addition, saturation is important over two drift spaces preceding the output gap. Thus, we might expect an exaggerated effect of increasing the perveance as the cumulative result extending over several stages.

Figures 43 through 46 show additional information regarding the operating parameters for various cases already considered. Figure 43 shows the Gap No. 6 voltage for some of the cases considered in Figure 38. The voltages are, of course, directly proportional to the driving currents. From Figure 43, one would think that the output circuit impedance is simply much too low for the lower voltages and perhaps for all voltages when standard field shape is used. However, it has been found that attempts to raise the power at any voltage by increasing the output circuit impedance have not produced significantly greater efficiency. This is related in part to voltage saturation conditions at the output gap.

Figure 44 shows the relative gap current as a function of gap voltage. This was taken from the preceding data in which the drive was optimized at each point. For the 45-kilovolt case, the Gap No. 5 voltages are shown in Figure 45. Here we see that the Gap No. 5 voltage increases with increasing output impedance and hence Gap No. 6 voltage. No significant amount of this increase was detected at 35 kilovolts.

Figure 44 represents the best current available at each gap voltage. The 35-kilovolt case is a true voltage saturation curve, but the 45-kilovolt case is not. By raising the Gap No. 5 voltage, we increase the velocity spread and also the degree of bunching. It may be that with a large r-f voltage on Gap No. 6 overbunching can be tolerated. The gap voltage might produce a type of phase focusing with a larger net energy transfer. Such a mode of operation might simply not be accessable at 35 kilovolts because of the reduced gain. That this might be true is suggested by the fact that the relative Gap No. 5 voltage is significantly lower at 35 kilovolts. If Cavity No. 5 were tunable, improved results at 35 kilovolts might be obtained.

Whatever the cause, Figure 44 indicates that operation at 35 kilovolts is susceptable to early voltage saturation. The shape suggests that maximum power would be obtained for a relative gap voltage of only a little more than 0.7. Figure 46 shows that enhanced output with magnetic field adjustment is obtained at 35 kilovolts with an increase in Gap No. 5 voltage as opposed to a decrease at higher beam voltages. This further suggests that the gain is marginal at 35 kilovolts and improvements are obtained by improving this. Still, Figure 41 shows that the best current obtained at 35 kilovolts does not suffer greatly, compared with the current at other voltages.

The general increase in Gap No. 5 voltage with perveance shown in Figure 45 fits with our general picture of the interaction. Space charge debunching becomes more important and larger driving voltages are required. It should be remembered however that the Gap No. 5 impedance is fixed and the actual operating conditions become a balance between the input current, which is near saturation, and the voltage required to accomplish further bunching. If the impedance could be changed, we might find that the Gap No. 5 voltage would rise even more rapidly with perveance.

Figure 46 shows how the Gap No. 5 voltage varies with beam voltage and also the effect of magnetic field adjustment. The shape of the adjusted field varied considerably with beam voltage, as was previously mentioned. The shapes were arrived at empirically in order to optimize power output. Although shape cannot yet be determined, it can be inferred from coil currents that the shape for the higher voltages corresponds closely to that found for the previous tube. The magnetic field increases to a peak in the vicinity of Gaps Nos. 4 and 5 and then falls rapidly near Gap No. 6. The amount of required adjustment decreases with beam voltage until, at 35 kilovolts, the magnetic field is nearly linear or is actually reduced in the vicinity of Gaps Nos. 4 and 5. In Figure 46 it is seen that for the higher beam voltages, the Gap No. 5 r-f voltage decreases when the optimizing adjustment is made and the drive again adjusted for saturation. The fact that Gap No. 5 voltage decreases suggests that the coupling coefficient is a factor. The r-f beam current at Gap No. 5 may be as large as in the linear field case.

Figures 47 through 55 show examples of saturation curves made at various operating conditions already discussed. These all show a definite saturation at the output followed by a drooping characteristic for higher drive. This is different from observations with the previous tube where the output was observed to increase to a steady level, which was maintained over a wide range of drive. It has been established that this latter behavior is associated with low gain in the tube. Similar characteristics were observed with the present tube when the cavities were more widely detuned than with the present experiment. Most of the observations on the previous tube were made with Cavity No. 2 disabled so that the gain was inherently low. Moreover, observations were nearly always made with the tube tuned for

maximum attainable output consistent with stability. Thus, a rather unusual tuning scheme was determined. The gain for the tuning used in the present experiment was in the vicinity of 40 db at saturated power output.

Figures 47 and 48 show the saturation characteristics for 35 and 45 kilovolts, each at about the same perveance value. Besides detailed differences due to the plasma wavelength, we have suggested that operation at 35 kilovolts suffers from smaller coupling coefficient and larger beam impedance. The coupling coefficient measures the effectiveness of the given gap voltage in producing velocity modulation in the beam. The beam impedance affects the amount of voltage induced by a given relative current on the beam.

$$\frac{V}{V_o} = \left(\frac{I_G}{I_o}\right)\frac{Z_G}{R_o} = \left(\frac{I_G}{I_o}\right) K_o V_o^{1/2} Z_G \qquad (3)$$

Z_G = Gap impedance

R_o = Beam impedance

K_o = Perveance

The effect of lower gain shows up in the later stages where saturation at a particular gap occurs when the current at the preceding gap is near saturation. Moreover, less relative driving voltage is available because of the higher beam impedance. Thus, the voltage at Gap No. 6 in the 35-kilovolt case saturates later and over a wider range of input voltage than with the 45-kilovolt case. The bunching conditions are farther from optimum, and the resulting current is lower. Still, as shown in Figure 41 the currents in the 35-kilovolt case are better for a given plasma drift angle than for the higher voltages. It is simply suggested here that the impedances are marginal, and currents would be somewhat better with improvement in impedance. This can be inferred from the slope of the 35-kilovolt curves in Figure 41 relative to those at other voltages.

Figures 48 and 49 show operation at the same beam voltage but different perveance values. Here we see the effect of increased space charge only. The beam impedance is more favorable for the higher perveance case as shown in Equation (3). The increased gain is seen at the earlier stages, but the saturated currents improve to a lesser extent. In addition, the saturated current at Gap No. 5 improves less than that at Gap No. 4, and at Gap No. 6 to a lesser extent yet. This shows the cumulative effect of increased plasma drift angle. The result is a substantial decrease in relative current at the output. This would show to a smaller extent if the cavity tuning (particularly penultimate) were optimized at each perveance value.

Figure 50 represents a set of measurements made at approximately the same conditions as in Figure 49 but with a higher output circuit impedance. It was previously found, as shown in Figure 45, that a greater penultimate cavity voltage was required at a higher output impedance. In Figure 50 we see that this occurs because the current at Gap No. 6 saturates when Gap No. 5 is significantly nearer saturation. This undoubtedly produces a rather large effect on the structure of the bunch at Gap No. 6. This further strengthens our previous suggestion that a larger voltage (higher impedance) at Gap No. 6 allows the acceptance of an overbunched beam, even with a larger velocity spread.

Figures 50, 51 and 53 show the effect of adjusting the value and shape of the magnetic field. Figures 52 and 54 are the corresponding relative beam currents computed from the gap impedances and coupling coefficients. It should be noted that coupling coefficients appropriate to the quiescent beam were used. Thus, the currents shown are more usefully related to gap driving currents insofar as comparing data at different voltages is concerned.

Adjusting the shape of the field at this voltage, we recall, consists of a substantial increase in the region of Gaps Nos. 4 and 5, and a rapid decrease with distance toward Gap No. 6. The coupling coefficients at Gaps Nos. 4 and 5 are reduced, and the Gap No. 4 to 5 plasma drift angle is increased because the beam is farther from the wall. The average position of the beam in the 3 to 4 and 5 to 6 drift spaces and at Gap No. 6 cannot really be determined. Comparing Figures 51 and 53, we see that the gains up to Gap No. 3 are not significantly affected. The 3 to 4 low-level gain appears to be slightly lower, but the saturated current at Gap No. 4 is reduced significantly. The 4 to 5 low-level gain is reduced measurably, and saturated current is also lower. The 5 to 6 low-level gain is increased, but the net gain to Gap No. 6 is reduced. The Gap No. 6 saturated current, which is maximized by the adjustment, is greater.

The behavior at Gaps Nos. 4 and 5 suggest that the major factor is the increased plasma drift angle, although coupling coefficient is undoubtedly a factor. The low-level gain increase between Gaps Nos. 5 and 6 suggests that the plasma drift angle there is reduced significantly. Subsequent experiments, not covered by this report, revealed a strong interdependence between changes in reduced plasma angle due to the shaping of the magnetic field and the tuning of Cavity No. 4. From these tests it was concluded that an expansion of the beam, associated with a decreased plasma angle immediately preceding the output gap, generally improved the saturated current as long as beam interception was kept sufficiently low. The impedance level on Gap No. 4, however, dictated the degree of compression or expansion of the beam in the region between Cavities Nos. 3 and 5. A high impedance at Gap No. 4 required a compression associated with a larger $\beta_q \ell$. A low impedance required an expansion with a smaller $\beta_q \ell$. The main effect of the shaping of the magnetic field may therefore be seen as an adjustment of the $\beta_q \ell$ of the large signal stages related to the tuning

scheme of the tube. The level of the current at Gap No. 6 is also influenced by the position of the beam in other ways. These effects, to be discussed next, will help explain the necessity for the shape of the magnetic field.

An important operational factor in any high power tube is the fraction of the total cathode current which reaches the collector. In some designs it is necessary to minimize this and we need to evaluate the cost in performance. Also, in an experimental tube, interception may be important in its effect on the results. Unfortunately, in most of the experiments on high-level effects at the output gap, the collector was disabled due to arcing so that beam transmission could not be measured. The cause was finally found and some transmission measurements made, perhaps enough for a sensible evaluation.

Figure 55 shows the per cent transmission to the collector vs r-f drive level for one of the higher efficiency experiments. The field was adjusted for optimum power output. We see that with this magnetic field shape the no-drive transmission is only 82 per cent, falling to about 74 per cent at maximum power output. This interception is no worse than with many high power pulsed tubes, but for many newer applications it could not be tolerated. It could not be tolerated at all in a high power c-w tube.

Figure 56 shows transmission as a function of beam voltage for two different magnetic field configurations. The standard field shape is similar to Curve B in Figure 1, while the lower curves were made with a field shape similar to that of Curve C in Figure 1.

It should be noted here that the correspondence of field shapes cannot be taken entirely literally. The measurements shown in Figure 1 were made before the tube was inserted into the magnet structure and with a particular pole piece configuration. However, upon insertion of the tube, some adjustment in pole piece configuration was necessary. In operating the tube it was necessary to adjust the magnetic field for various reasons. Quite often stability was the main motivation. Since the field shape in the collector is not independent of that in the latter part of the interaction region, an arbitrary field shape could not always be used. Thus, the coil currents in experiments such as the lower curves in Figure 56 do not correspond exactly to those in Figure 1. The correspondence is, however, believed to be considerably closer than 10 per cent.

Figure 57 shows the results of a more comprehensive evaluation of transmission. To better understand this, the positions of the magnet coils relative to the cavities is shown in Figure 58. The entire magnet stack was surrounded by an iron shield which decreased the field variation obtained by adjusting the coil currents. Figure 57 shows both transmission and efficiency in an experiment similar to those previously described. The output circuit impedance was 555 ohms. A Coil No. 7 current of 7.5 amps and Coil No. 8 current of 4.4 amps corresponds to a standard field with a shape similar to Curve B in Figure 1. The dashed curve is the transmission at zero drive with Coil No. 7 at 7.5 amps.

We see in Figure 57 that maximum efficiency is obtained with Coil No. 7 current at about 12 amps and very small, or zero, current in Coil No. 8. This is a very radical field, perhaps more peaked near Cavity No. 5 than the optimum field for the previous tube shown in Quarterly Report No. 4. Judging from prior experience, a small improvement in efficiency could probably have been obtained by adjusting magnets prior to Coil No. 7. We see that for this maximum power condition a transmission of 72 per cent is obtained. It is interesting that for any other Coil No. 7 current the transmission for optimum power output was very near this value.

Figure 59 shows a schematic diagram of the output gap and the portion of the collector in its vicinity. We see that the drift tube beyond the gap has a 20 degree flare. Interception along this flare is not likely for any of the standard field configurations, which have a far shallower spread in this region. Interception is not even likely with the radical fields in which Coil No. 8 is reduced to zero. The most likely spots for interception are in the drift tube entering Gap No. 6 and at the drift tube tip nearest the collector.

We see in Figures 56 and 57 that significant interception takes place even with zero drive, i.e., with no perturbation due to r-f fields. This interception increases with beam voltage and with perveance. If the beam were ideally located, uniform over its thickness and zero elsewhere, this interception could not be accounted for on the basis of the field shapes which were believed to exist. For example, in Curve C of Figure 1 the axial magnetic field is down to 84 per cent of its uniform value at the collector end of the gap. The outer diameter of the beam would thus increase about 10 per cent to 1.37 inches. This is still adequate clearance with perfect alignment of the beam in the drift tube.

The interception can be explained on the basis of imperfect alignment or a fuzziness on the outside of the beam; probably both. Absolutely perfect alignment is too much to expect, particularly when we remember that the beam is about 30 inches long and a displacement of less than 0.1 inch would be important. In addition, we know that electronic interaction in the gun and azimuthal instability in the beam are present. These can have a significant effect on the current distribution near the edge of the beam. These become more severe as perveance is increased, and will also be restrained by increasing the stiffness of the beam. Lowering the beam voltage at constant magnetic field increases the stiffness and we see that the zero drive curves in Figure 56 tend to agree with the idea of beam edge fuzziness.

Since interception is observed to take place with no r-f fields present, it is not surprising that it increases in the presence of the large r-f fields associated with high level interaction. Both deflection due to radial gap fields and outward motion due to space-charge fields can be important. It is not possible to make a quantitative calculation of these, but it is clear that significant boundary perturbation

exists. Individual electrons will move approximately in a helical motion at the cyclotron frequency. The axial distance traveled in one cyclotron period varies from about 1.2 to 1.4 inches, so each drift space contains several cycles. Because of the longitudinal bunching, electrons in various phases of this motion are mixed, producing a bunch which can be considerably thicker than the unperturbed beam.

The position where interception takes place will, of course, be important because of its effect on interaction and for thermal reasons in a practical tube design. Interception before entrance to the output gap is important in evaluating the effect on efficiency. Since interception takes place with zero drive, it seems likely that at least a fraction of the interception will take place before the output gap when the perturbing r-f fields are large.

The cases shown in Figure 56 were measured with an output circuit impedance of 167 ohms, while the impedance in Figure 57 is 600 ohms. The major difference is then the amount of r-f voltage at the output gap. A comparison using a field shape in Figure 57 equivalent to that in Figure 56 shows the transmission with low impedance to be 90 per cent, while that at high impedance is 82 per cent. Thus, fields at the output gap account for a considerable fraction of the interception in the case shown in Figure 57. This can be partly at the entrance to the gap, because the electron bunch enters the gap when the radial gap fields produce an outward force. It is interesting to note also that the constant Coil No. 7 current curves in Figure 57 flatten out with the transmission still significantly less than 100 per cent. This is in spite of the fact that the influence of Coil No. 8 extends up into the drift space prior to the output gap. This again indicates that a significant fraction of the interception takes place before the entrance to the output gap. Therefore, it is reasonable to suppose that interception is a factor in determining the current at Gap No. 6, and thus the efficiency.

The decrease in efficiency for low Coil No. 8 currents in Figure 57 seems likely to be due to interception prior to Gap No. 6. The decrease in efficiency for higher Coil No. 8 currents can be attributed at least partially to beam position. We have already discussed the fact that a contracted beam increases the plasma drift angle and vice versa. The fact that the lower Coil No. 7 current curves produce higher efficiency for larger Coil No. 8 currents indicates this influence of beam position on bunching. Another important factor is the coupling coefficient in the output gap. An expanded beam at the output gap would maximize this. The calculations shown in Table II indicate that the magnitude of the change in small-signal coupling coefficient would probably be considerably under 10 per cent, but it still might have some significance.

The foregoing results indicate that the field shape giving maximum efficiency is a compromise between improvement of bunching effectiveness, coupling

coefficients, and beam interception. Size and position of the magnet coil offers only limited flexibility and the improvement of one parameter is very often accompanied by the deterioration of another.

The effects discussed in the preceding paragraph are undoubtedly important. It was not established whether some other effect of the magnetic field and its shape is also important. For example, the improvement in Cavity No. 3 current by improving the magnetic field shown in Figure 20 was obtained with substantially no interception. Until the magnetic field shapes can be measured, a comparison of the results at the output gap cannot be made.

The effect of interception is also important to the gap current information presented in Figure 41. There the upper curves corresponding to low circuit impedance were obtained with a magnetic field shape similar to that of the lower curves in Figure 56. Interception must be a factor in the variation of r-f current with voltage and perhaps the exaggerated effect of perveance. If, for example, the relative gap current had been based on collector current rather than total beam current, the curves would be more nearly coincident and have a shallower slope. While it is not realistic to assign the entire interception to regions previous to the output gap, the effect of interception on the interpretation of the output gap results cannot be ignored.

We see now that the relative gap currents shown in Figure 41 are smaller than they might be with an optimum design. Interception prior to the output gap is undoubtedly important. It is also important to remember that the currents driving the gap rather than the beam currents are shown. The coupling coefficient is undoubtedly lower than 0.9. Thus, relative beam currents of at least 1.35 have been recorded. The drift distance between the output and penultimate cavities is about 0.12 of a plasma wavelength. Referring to Figure 7 of Webber's second paper we find that our results agree reasonably well with his ballistic theory for three cavities, particularly allowing for perhaps a 10 per cent improvement with magnetic field and penultimate cavity impedance adjustment. It can thus be stated with assurance that insofar as the measurements made with this tube are concerned, the r-f current obtainable in the beam is in reasonable agreement with the ballistic calculations of Webber. Reasons for divergence and exaggerated effect of certain parameters can be given, although these may not be the only factors involved.

IV. SUMMARY

The original aim of this program was to demonstrate the feasibility of obtaining wider bandwidth and other advantages through the use of high perveance beams. The particular emphasis was on high power amplifiers. A design at a microperveance of 10 was selected as representing a genuine improvement over existing devices. A beam power level of 5 Megawatts was selected as being reasonably high power without introducing excessive modulator difficulties. Finally, klystron interaction was chosen as the experimental vehicle because it was felt to represent a more easily calculated interaction.

At microperveance 10, a hollow beam is a necessity because of potential depression problems. At the beginning of the program the design of a convergent hollow beam gun looked too formidable as the primary aim was to study interaction. Thus, the necessity to use a nonconvergent cathode dictated that the frequency be lower than might otherwise be desirable. A center frequency of 1300 Mc was chosen and, since testing equipment was acquired, this frequency has persisted in all the experiments.

As the program progressed, observations were made which cast doubt on our knowledge of the basic interaction mechanisms. Lack of detailed stage-by-stage information on conventional klystron designs hampered the progress to some extent. Thus, we concentrated more heavily on studying various aspects of the interaction rather than simply demonstrating feasibility. In retrospect, it would have been better in the beginning to concentrate on simpler experiments aimed at investigating various aspects of the design. As it was, full tube designs were tested, giving results which were not always easy to interpret. Still, sufficient information is available so that some general conclusions can be reached.

A. EXPERIMENTS PERFORMED

The experimental program consisted of the construction of three tubes and a large program of testing these experimental devices. In addition, two beam testers were built to investigate the design of magnetron injection guns. Much of the program was spent in devising and continually refining experimental methods, both for the design of rather unusual components and for performing detailed measurements. The most important measurements are the ones which are not usually made on klystrons. To make them meaningful and capable of comparison has been a problem. To calibrate the cavities, for example, a great amount of cold test work has been necessary. However, even with this extensive cold testing, the results were not always consistent, requiring interpretation which does not contribute to evaluation of the basic problems. This is one of the reasons why simpler and more direct experiments would be desirable.

1. Experimental Tubes

The first tube was designed with a rectilinear flow cathode immersed in a magnetic field. An enlarged radius compared with conventional design was required in order to alleviate cathode loading problems. The beam was made unusually thick for the same reason. In subsequent tubes, the magnetron injection gun was available, allowing a greater range of dimensional choice, hence the drift tube was more conventional in size. Table VI compares the important features of geometry and electrical characteristics of the three tubes. All tubes contained six interaction gaps, the number of cavities that it was felt would produce sufficient stagger tuning ability to utilize the full output circuit bandwidth in a practical design.

In Tubes Nos. 1 and 2, the first five cavities were tunable, and the output circuit fixed. In Tube No. 3, both Cavities Nos. 5 and 6 were fixed tuned. In Tube No. 1, the cavities were tuned by adjusting the gap, while in Tubes Nos. 2 and 3 the tuning adjustment was a ring which could be moved in the cavities. Tube No. 2 is the only one in which the output circuit was broadbanded by means of an additional external cavity. In Tube No. 1, a commercially available output window was used, which could not be satisfactorily broadbanded. Thus, the response was inherently narrow band, but subject to adjustment by tuning the matching transformer. In Tube No. 3, the broadband window design of Tube No. 2 was used, but with a single tuned internal cavity. Here the impedance could also be adjusted over a considerable range using external impedance transformation methods.

The large drift tube in Tube No. 1, compared with the others, has some significance. The beam coupling coefficient changes more rapidly with radius. Even with the beam grazing the drift tube, the coupling coefficient is substantially lower than with the other tubes.

With the gun used in the first tube, the size of the beam could be defined with some accuracy. Also, the flow emerging from the gun was probably relatively near the ideal of uniform flow free from velocity variations. In Tube No. 2, the first model of the magnetron injection gun was used. The cathode surface was nominally parallel to the magnetic field. The dimensions of the beam emerging from the gun could only be inferred from crude luminous target observations, and small signal r-f measurements. With electronic interaction known to occur in the gun, the beam boundary could not have been very well defined, and thickness was evidently greater than would be inferred from purely energetic considerations.

In Tube No. 3, a more advanced magnetron gun was used. The cathode was tapered so that the emerging beam is more like confined flow. The dimensions can be more accurately inferred from scaled models tested at low voltage. However, known electronic interactions in the gun and aberrations at the drift tube entrance

TABLE VI

MECHANICAL AND ELECTRICAL PARAMETERS
OF THREE EXPERIMENTAL TUBES

GEOMETRY	EXPERIMENTAL TUBES		
	1	2	3
Mechanical			
Drift Tube Diameter (inches)	2.750	1.50	1.50
Beam OD (inches)	2.386	1.25 (nominal)	1.25
Beam ID (inches)	1.880	1.15	1.09
Beam Thickness (inches)	0.253	0.050	0.080
Beam-to-Drift Tube Spacing (inches)	0.182	0.125	0.125
Gap Spacing (inches):			
1 - 4	0.60	0.875	0.875
5	at 1.3 kMc	0.875	0.640
6	0.60	0.650	0.538
Intergap Spacing (inches):			
1 - 3	4.77	6.065	6.065
4 - 5	4.77	3.776	3.290
5 - 6	4.77	2.775	2.651
Gun	Rectilinear Flow	Cylindrical Magnetron	Tapered Magnetron
Electrical			
Frequency (Mc)	1300	1300	1300
Beam Voltage (kv)	50	50	50
Microperveance	10	10	10
γa (radians)	2.2	1.2	1.2
$\beta_q \ell$ (degrees):			
Driver	66°	96°	97°
Gaps 4 - 5	66°	60°	53°
Gaps 5 - 6	66°	44°	42°
ω_q/ω	0.139	0.158	0.160
f_p (Mc)	560	1700	1350

would be expected to produce a certain lack of definition of the beam edge. In addition, in all cases a certain amount of azimuthal instability is known to exist. This was observed in the magnetron gun testers and seems likely in the case of Tube No. 1. The electronic interaction in the beam which leads to this would undoubtedly further degrade the definition of the beam edge. Thus, while all theoretical calculations were made on the basis of an ideal beam, allowance must be made for uncertainty as to the actual dimensions.

Attention given to collector design in Tubes Nos. 1 and 2 proved to be inadequate. This problem is more severe than with the usual solid beam tube because of the relatively larger confining magnetic field and the concentration of current over a narrow range of radius. For the low average power used in these experiments, the area over which current is intercepted has no particular significance, but the return of secondary electrons proved to be a serious problem indeed. In the second tube in particular, instabilities inhibited many otherwise desirable measurements. It was always necessary to compromise the adjustments to achieve even reasonable stability. The large amount of noise emerging from the magnetron gun made this problem particularly troublesome. In fact, it may be that considerable noise amplification takes place within the gun itself, so that electrons returning to this region could produce feedback over a considerably larger gain path than might be thought from the measured gain of the tube. This could also be true to some extent of the observed coherent oscillations as well. In Tube No. 3, collector design was given considerable attention, particularly with respect to returned electrons. While the conditions achieved in operation were not ideal, instabilities and enhanced noise were far less troublesome. This seems to bear out the assumption that returned electrons from the collector were a major source of previous difficulties.

The perveance of the gun used in Tube No. 1 was fixed by its physical design parameters. In Tube No. 2, perveance was a rather strong function of the magnetic field. It could be varied by adjusting both the value and shape of the field in the gun. Since adjustments of the shape in the gun might involve changes in beam dimensions as well, this was avoided and the perveance was inevitably a function of the value of the focusing field. This made it impossible to effectively separate the roles of magnetic field and perveance in determining the characteristics of the tube. Best operation was obtained at a very high magnetic field value and resulting low perveance. With Tube No. 3, perveance could be adjusted to some extent by applying a separate voltage to the magnetron gun anode. The independent effect of perveance and its relation to voltage and other parameters could be determined.

2. Beam Testers

Beam testers were constructed to explore the suitability of two versions of the magnetron injection gun for use in the experimental tubes. These contained a luminescent target made from fine tungsten mesh to observe the beam cross section.

These measurements were too crude to allow an accurate determination of the beam boundaries. The general shape could be seen. Azimuthal instabilities were observed in both testers. However, the degree of current accumulation into individual filaments could not be determined accurately. The targets could be moved axially to a limited extent, and no variation in the intensity of the pattern could be observed.

These beam testers were equipped with a pair of cavities to measure the small signal operation as part of the beam evaluation method. The measured gains and other parameters agreed quite well with theory and the results obtained on the experimental tubes. Beam noise was also observed at about the same level as observed at the input end of the tubes.

B. COMPARATIVE RESULTS

As the program progressed, measuring methods were refined and experiments themselves were improved in various ways. By far the most significant results were obtained with Tube No. 3. The tubes vary a good deal in their design, however, and a wider spectrum of experience is represented by comparing results where possible. The major conclusions to be reached are those which bear on the reliability of design methods of high power amplifiers with perveance significantly higher than is conventionally used. If the most important factors affecting performance are known, the design for any particular set of specifications can be evaluated.

1. Small Signal Results

Throughout the experiments, the small signal transadmittance was always qualitatively consistent with simple theory. In Tube No. 1, agreement with theory was within the observed variation from stage-to-stage. The variation is partly attributable to cavity calibration and partly to variation with the magnetic field strength which was not understood at that time. In Tube No. 2, the experimental transadmittance was slightly lower than the theoretical value but within the accuracy of measurements and knowledge of the beam dimensions. In Tube No. 3, good agreement with theory was obtained.

In all experiments, a variation in gain with magnetic field was observed. The variation was never large except where the cumulative effect of several cavities was observed. This may be related to a deterioration in the beam itself. It was undoubtedly aggravated by the severe sensitivity of space charge parameters to beam position and current distribution characteristic of high density hollow beams.

In the first two tubes, beam loading measurements showed a considerable disparity between theory and experiment. Beam loading conductances from 1.5 to 2 times theoretical were commonly measured. In more recent experiments, this was traced to the effects of potential depression in the gaps themselves. Earlier theoretical

results had, in fact, not even taken into account potential depression in the drift tube. The theory used is the infinite magnetic field, ballistic theory neglecting space charge. The method of taking into account potential depression is admittedly crude, consisting of the assignment of an equivalent uniform velocity across the gap. It does, however, give results which correspond quite closely to experimental determinations at magnetic fields high enough for complete confinement of the beam. Observed increases in beam loading conductance with decreasing magnetic field have not yet been completely explained. This may be partly assignable to the energy involved in transverse motion induced in the gap. However, there does appear to be a threshold in the magnetic field beyond which the variation in beam loading is greatly reduced. This could be related to the variation in the cyclotron wavelength at the gap. Since interception is observed concurrently with this effect, secondary electrons may play a part in the loading. However, irrespective of the reasons, observed variations were seen at a magnetic field below that which would ordinarily be used. Hence, the ballistic beam loading theory seems to be adequate for the purpose.

2. Large Signal Effects

Most of the observations at large signal levels were directed toward investigation of factors important in determining the ultimate efficiency of the tube. In Tubes Nos. 1 and 2, the measurements were confined largely to conditions which optimize the output. With Tube No. 3, a more comprehensive program of measurements all along the tube were undertaken. The aim was to investigate divergences, if any, from common experience or from the results of Webber's ballistic calculations, which are the only large signal theoretical results available.

In all cases, efficiency was observed to increase with voltage. In addition, maximum efficiency required a special field shape in which the field was larger in the region of Cavity 4 and Cavity 5 and falling off rapidly at the output gap. This was apparent especially in Tubes Nos. 2 and 3 at the higher operating voltages.

Tube No. 1 operated at constant microperveance of 10 and produced a maximum efficiency of less than 30 per cent. This poor performance was believed to be due in part to poor beam coupling coefficient. To obtain highest efficiency, Tube No. 2 required a magnetic field including that in the gun larger than the design value. This was accompanied by a reduction in perveance. The magnetic field and perveance effects could not be separated effectively. The maximum efficiency observed in a consistent set of measurements was 38 per cent at microperveance 6.6 and 59 kilovolts. However, at one point early in the life of the tube 41.5 per cent was observed. A likely explanation of this discrepancy is deterioration in alignment, but this could not be established. The maximum efficiency observed with Tube No. 3 was 42.5 per cent at microperveance 8 and 50 kilovolts.

It is believed that one of the most important factors in determining the amount of r-f current that can be produced in a beam is the space-charge debunching effect. The importance of space charge is also borne out in the calculations of Webber. With Tube No. 3, it was found that the plasma angle of the last drift space appeared to be the most significant parameter. Figure 60 shows results from all tubes plotted as a function of this quantity. The currents at Gap No. 6 of Tubes Nos. 1 and 2 are extrapolated to low r-f voltage on the saturation curves given in previous reports. The points representing Gaps Nos. 4 and 5 of Tube No. 2 were taken from the saturation curves in Quarterly Report No. 4. These cavities were not greatly detuned, so the gap voltages were high. Undoubtedly, voltage saturation effects lower the observed gap driving current. The points representing Tube No. 3 were all taken at low voltage on the catching gap. Also, it should be realized that gap driving currents are shown. A range of coupling coefficients are represented so that the relative positions would be slightly different if r-f beam current could be plotted. However, the unknown position of the beam in some of the experiments makes a coupling coefficient calculation quite artificial.

A very definite and well defined trend toward larger currents at smaller drift angles can be seen in Figure 60. It is interesting, in view of its poor performance, that Tube No. 1 appears to be quite consistent with the Tube No. 3 results. However, the results from Tube No. 2 are inferior. In making this comparison it should also be remembered that the Gap No. 6 results of Tube No. 3 were not optimized at each point as were all the other results. Moreover, it was observed that for short drift angles, the optimizing process involves a tuning of more than just the penultimate cavity. Consequently, the Gap No. 6 currents of Tube No. 3 would unquestionably be higher if properly optimized.

In the previous section, where the Tube No. 3 results were discussed in some detail, it was found that the currents induced in the beam compare reasonably well with Webber's results. Because of its similarity to the Tube No. 3 results, we can say that Tube No. 1 also conforms insofar as maximum current is concerned. This shows that lower r-f beam current due to the long plasma drift angle was primarily responsible for its poor performance.

The Tube No. 2 design is near enough to that of Tube No. 3 so that we would expect similar results. Some speculative reasons can be assigned to its poorer performance. In Tube No. 3, even with optimized magnetic field shape, the relative induced current deteriorated with increasing voltage when plotted against the plasma drift angle. Tube No. 2 was operated at very high voltage where efficiency was greatest. However, efficiency did not fall off rapidly with decreasing voltage, indicating that the induced current at lower voltages was better. Thus, Tube No. 2 displayed the same tendency for deterioration in relative current with increasing voltage. In Tube No. 2, the greatest contributing factor to the poor performance was

believed to be interception. During most of the test periods, the collector current could not be measured in either tube and a comparison of transmission can not be made. It is suggested, however, that an aggravated interception problem in Tube No. 2 might explain the discrepancy in performance. This could, for example, be due to a misalignment of the tube in the magnetic field. The better results obtained early in the life of the tube indicate that alignment may have deteriorated subsequent to that time.

Another difference between Tubes Nos. 2 and 3 was the gun design. Any space charge interaction in the gun could be expected to be more severe in Tube No. 2, because of the higher degree of re-entrance of the beam. While the measured noise in the beam from the two magnetron guns was the same order of magnitude, the beam insofar as interaction is concerned, may have been considerably different.

Besides r-f current in the beam, efficiency is determined by the r-f gap voltage which produces maximum power. A maximum of power exists because the r-f driving current of the gap decreases with increasing gap voltage. Eventually, nonlinearities cause the driving current to drop rapidly; an effect we call voltage saturation. The induced gap current for zero gap voltage is equal to the actual current in the beam reduced by the beam coupling coefficient. One might expect serious nonlinearities when the r-f voltage seen by the beam approaches the d-c beam voltage reduced by some factor related to the r-f velocity spread. Thus, the onset of voltage saturation would be expected to occur for larger gap voltages when the coupling coefficient is smaller. It is our experience that this does not occur. Voltage saturation may occur at an even smaller gap voltage relative to beam voltage when the beam coupling coefficient is poorer. The current induced in the gap at maximum power appears to be approximately proportional to that at zero gap voltage, i.e., proportional to the small signal beam coupling coefficient.

Undoubtedly, the r-f gap voltage for maximum power depends on many aspects of the bunching process. It was found in these experiments that the relative gap voltage (V_g/V_0) generally decreases with decreasing beam voltage. This would naturally be true if the circuit impedance was constant, but it also appears to be true for the best impedance.

Experience has indicated that for the highest voltages and efficiencies, the relative output gap voltage ranges from 0.85 to 0.92. This is significantly lower than is commonly experienced with lower perveance, high-power klystrons. With a given r-f beam current at the entrance to the gap, this will have a direct influence in reducing efficiency. A factor here is undoubtedly bunch shape and velocity spread, but this is important in any klystron. However, in a high perveance klystron a feature of increased importance is potential depression. In these tubes, the average potential of the beam in the drift tube is 5 to 8 per cent below drift tube potential. For a high degree of bunching, the potential in the bunch may fall two or more times this fraction.

The instantaneous potential with the bunch centered in the gap is far lower than this, although this is not actually a measure of electron velocity. The effect of longitudinal space-charge fields in the gap was not evaluated completely, but this effect may very well be significant in the conversion process. These fields are proportional to the potential depression which is unusually large at high perveance, even with a hollow beam. In any case, the kinetic energy of the electrons entering and leaving the gap is lower because of potential depression. This obviously detracts from the energy that can be converted, reducing r-f voltage and efficiency.

We see that, ultimately, efficiency is determined by the amount of r-f current which can be induced in the beam, the coupling coefficient at the output gap, and the degree of nonlinear beam loading, or voltage saturation, which determines the r-f voltage for maximum power. The r-f current capability of the beams we have studied does not appear to be significantly poorer than is expected in any klystron. The efficiency will, however, be lower because gap effects limit the r-f voltage to a lower value than for lower perveance tubes.

3. Stagger Tuning

Tube No. 2 was the only tube in which the output circuit was broadbanded. The reasonably predictable behavior of low level operation means that the effect of staggering the cavity tunings is calculable to the same extent as for other klystrons. Calculations based on the simple, single space charge mode transadmittance expression were made for Tubes Nos. 1 and 2, using an analog computer. The calculations on Tube No. 1 involved fewer than the total number of cavities and were shown to be qualitatively correct as long as large signal saturation effects were not important.

In other, more conventional tubes, calculations have been shown to predict the overall stagger-tuned bandwidth with reasonable accuracy. Lack of knowledge of the actual beam parameters, and perhaps high level effects, result in the fact that cavity tunings cannot be predicted with sufficient accuracy for presetting. The broadbanding of an actual tube design must be an empirical process. Thus, a wideband output circuit, as was only available in Tube No. 2, is necessary for meaningful stagger tuning measurements.

The stagger tuning results on Tube No. 2, given in Quarterly Report No. 1,[8] show a 3 db bandwidth of 13.5 per cent with a peak efficiency of 28.5 per cent. This is narrower to a significant extent than the output circuit bandwidth. Consequently, the limitation must be assigned to the stagger tuning of the driver. Since the optimum-drive bandwidth was observed to be considerably wider than the actual band edges, due to an overdriven condition, the bandwidth could undoubtedly be improved by additional resistive loading on some of the cavities, notably Cavity No. 2.

- - - - - - -

[8] Varian Engineering Report No. 273-1Q, 1 January - 31 March 1960.

The extreme bandwidth of the output circuit resulted in a resistance of about 400 ohms. Subsequent efficiency measurements, reported in Quarterly Report No. 4, indicate that this low impedance may have cost about 20 per cent in power. Thus, with optimum impedance, which could be easily obtained over the bandwidth of the driver section, the efficiency might have been between 33 and 34 per cent. This compares favorably with experience on other klystron amplifiers which are stagger tuned for maximum bandwidth.

V. CONCLUSIONS

The main conclusions desired in this program are those relating to the eventual performance of high perveance tubes when measured against known theory and design methods. While certain details of operation are still not understood, it is believed that firm conclusions with respect to overall performance and design can now be stated.

The fundamental overall conclusion is that no new effects were discovered. Tentative explanations based on well known phenomena can be found for most apparent anomalies and departures from expectations. Design procedures must, however, take into account effects which are not usually considered. Emphasis on some aspects of design also becomes exaggerated. These have to do with the unusually dense beams and large space charge per unit length.

A. SMALL SIGNAL TRANSADMITTANCE

When the effects of potential depression are taken into account, the simple, single space-charge mode, small signal transadmittance is sufficiently accurate for design purposes. Effects of reduced magnetic field were observed which were not completely understood but these occur at magnetic fields which are smaller than can be tolerated for other reasons. The accuracy of this simple theory appears to be well within the knowledge of beam position and other important parameters. There seems to be little point in further refining the idealized theory.

B. SMALL SIGNAL BEAM LOADING

Small signal beam loading can be computed to sufficient accuracy using the ballistic, infinite magnetic field theory. Potential depression in the gaps is very important. This can apparently be taken into account by the simple expedient of assigning a uniform potential giving the same d-c transit time as the actual potential in the gap. A single correction factor to the potential at gap center is probably adequate over a wide range of conditions.

Effects of magnetic field on beam loading were also observed. The additional energy of transverse electron motion is believed to be the most important factor in this effect.

C. EFFICIENCY

The ultimate efficiency achievable is a function of both the nature of the r-f current induced in the beam, and of events which occur in the output gap itself. Maximum r-f currents which can be produced in the beam are consistent with the theoretical results of Webber. However, both the current and its usefulness at the output gap are sensitive

to factors involving the value and shape of the magnetic field over a substantial fraction of the tube.

The major magnetic field effect is believed to be the position of the beam in the drift tube and its effect on the plasma drift angle. The influence of small changes is much greater for the hollow beam geometry. Interception plays a significant part where improvement in bunching is brought about by moving the beam nearer the wall. Current lost through interception degrades the performance, and the best adjustment of field is a balance between improved bunching and interception.

An efficiency of 43 per cent was observed with the third experimental tube in this program. The current induced in the output gap at maximum power was approximately equal to the d-c current. This is 20 to 30 per cent below the current which would be observed at the gap with no r-f voltage, the reduction being assignable to voltage saturation (nonlinear beam loading). This r-f gap current is approximately equal to that seen in high power pulse tubes producing about 50 per cent efficiency. Power maximizes with an r-f gap voltage of approximately 0.9 beam voltage, which is lower than commonly encountered in low perveance tubes. A major factor in determining this gap voltage is believed to be potential depression, which reduces the kinetic energy of the electrons, thus the energy available for conversion.

D. BANDWIDTH

One of the original motivations for this high perveance program was to increase the bandwidth of high power klystron amplifiers. Increased bandwidth comes about through decreased beam impedance so that lower impedance circuits produce the same result. Actual bandwidth in operation was only demonstrated in one experiment. It has been demonstrated, however, that no unusual effects occur in high perveance interaction, and that the methods of calculating bandwidth commonly used are applicable. Thus, the bandwidth achievable can be estimated from common experience, which indicates that a driver section can be designed which will make use of the full bandwidth of a coupled cavity output circuit.

The bandwidth actually achieved was about 13.5 per cent, although indications of greater capability were seen. Experiments on a single frequency basis indicate that, as is common experience, bandwidth will be accompanied by decrease in efficiency. This is because optimum efficiency requires a rather careful balance of the tuning of several cavities which cannot be achieved over a wide band.

E. MAGNETRON INJECTION GUN

Design considerations of the first experimental tube are convincing evidence that a highly convergent gun is required for a practical high perveance tube in the microwave range of frequencies. Required beam current densities are just too high to draw from

a cathode which has no convergence. From a design viewpoint the most practical gun which has been proposed is the magnetron injection gun. Its outstanding feature is lack of necessity for an internal anode electrode. Also, no careful shaping of the magnetic field is required.

The first magnetron injection gun tried was empirically designed, having a cylindrical cathode immersed in a uniform magnetic field. In a beam tester this appeared to give an entirely satisfactory beam. R-f tests, however, revealed a noise level about 5 orders of magnitude above shot noise. Any accompanying velocity spread could not be determined by measuring klystron interaction. The second gun, designed according to a laminar flow model developed in our laboratories, was expected to have less noise. However, the beam from this design produced noise at about the same level.

Experimental evidence is clear that back bombardment of the cathode takes place with sufficient energy to give rise to considerable secondary emission. The noise is believed to be associated with the interaction which produces this. There must also be a corresponding velocity spread in the beam. The noise has sufficient level so that it would be a problem at the output for gains greater than 40 db. For this reason, magnetron injection guns should be subjected to further investigation before being used in a practical high power amplifier.

F. APPLICATION TO TRAVELING-WAVE TUBES

This investigation has shown that the application of a high perveance hollow beam to a klystron amplifier is reasonably well predictable using existing theory. This suggests immediately that application to high power traveling-wave tubes should be similarly predictable. In fact, application to traveling-wave tube design may be more favorable.

Besides lower operating voltage, one of the reasons for using high perveance is to achieve bandwidth improvement. As with the klystron, a traveling-wave tube profits in this respect from the increased beam conductance. With the klystron, however, the improvement is partly cancelled by the less favorable circuit design. The gaps must be made shorter due to the reduced electron velocity. Traveling-wave tubes need not suffer from this, however, because velocity and bandwidth are not similarly related. If the circuit bandwidth can be maintained, the bandwidth will improve with perveance because of an increase in the gain parameter.

We have seen that klystrons suffer in efficiency with increased perveance and that this appears to be inevitable. While the reduced beam potential as a source of efficiency degradation is also true in a traveling-wave tube, the efficiency may be improved due to the reduced beam impedance. The gain parameter, C, improves and this is believed to result directly in improved efficiency. Thus, efficiency degradation may not be observed in a traveling-wave tube. Moreover, we have found that beam interception

appears to play a role in determining the performance of a klystron. It is certain that part of this results from transverse velocities due to large gap voltages. Interception will play a similar role with traveling-wave tubes, but in this application energy is extracted over several interaction gaps. The gap voltages are generally smaller and will produce less perturbing effect on the beam.

Another appealing application of the hollow beam geometry is for traveling-wave circuits in which elements are located inside as well as outside the beam. This is hardly possible with the klystron because of feedback effects. With this geometry, the coupling between circuit and beam is a function of the annular space through which the beam passes, and thus the beam can be enlarged to a much greater extent than with a hollow aperture circuit. Where methods can be found to avoid difficulty with higher order modes, this type of circuit design may have substantial advantages.

G. SPECIAL FEATURES OF HIGH PERVEANCE

To increase perveance well beyond usual solid beam values (to perveance 10, for example) a hollow beam must, for a number of reasons, inevitably be used. In a solid beam design at high power levels, a grid can not be used in the anode aperture. However, its absence in a high perveance solid beam design will severely effect the uniformity of cathode emission, current distribution over the beam cross section, and the beam boundary. The thin hollow beam, especially one which is produced by a magnetron injection gun, is less subject to these effects. There is also the problem of potential depression. A solid beam of high perveance has a depression in potential of the inner electrons with respect to the outer electrons which is far too great for useful application. This depression is greatly reduced by concentrating the current in a thin annular ring. However, such a design has certain difficulties and special features which need to be considered before its utility in any particular application can be evaluated.

The beam current as a function of beam power and perveance is:

$$I_o = K_o^{2/5} P_o^{3/5}$$

A larger perveance implies a larger total current in the beam. Yet, for reasons we have given, this current must flow in a thin hollow geometry. Unless the diameter is much larger than for the solid beam case, the current density will be very high, being inversely proportional to the beam thickness. For circuits which do not contain an inner electrode the diameter can be enlarged only to a limited extent. With a klystron, the coupling between cavities particularly at high order resonances is a limitation. Also, in any case, the gap coupling coefficient suffers increasingly with greater radius.

There are also restrictions on the beam thickness. A thick beam has a lower current density, but greater potential depression and poorer coupling to the inner electrons. A thin beam is more susceptible to azimuthal instabilities. The final choice of thickness depends on a balance of many conflicting factors. It will, however, be quite thin and have a current density much greater than a solid beam at the same power level.

Another consequence of high perveance is that the thin, high density beam must flow as close as possible to the metallic drift tube walls. One reason for this is the depression in potential of the beam with respect to the wall. The relative potential can be written approximately:

$$\frac{\Delta V}{V_o} = \sqrt{\frac{m}{2e}} \; \frac{K_o}{2\pi\epsilon} \; \frac{\Delta r}{r_o}$$

where r_o is the outer radius of the beam, Δr is the beam-to-drift tube spacing, V_o is the applied drift tube potential, and K_o is the perveance.

We see that the relative potential drop increases linearly with increasing perveance. The effect has some importance in high perveance design, although it can usually be neglected in lower perveance tubes. There is also an additional potential depression in the interaction gaps which has a similar dependence on perveance. Moreover, in a strongly bunched beam, the equivalent perveance in the bunch is substantially greater. The loss in efficiency due to the potential depression has already been discussed. The beam should be as close as possible to the drift tube wall to produce best efficiency.

The spacing between the beam and the drift tube wall also has an important influence on the plasma wavelength. The plasma frequency in the dense beams at high perveance is unusually large, as large as the operating frequency in some cases. However, its effect is reduced by the fact that most of the r-f space charge field is radial, thus greatly reducing the longitudinal forces which influence the bunching. Therefore, it is plausible that radial dimensions will have a strong effect on the plasma reduction factor. Especially a change in the beam-to-drift tube spacing of a nearly constant thickness of the beam, caused for instance by shaping the magnetic field, will severely perturb the reduced plasma frequency. Even with the smallest reduction factors available, the ratio of reduced plasma frequency relative to operating frequency, ω_q/ω, is larger than with most low perveance designs.

With klystron amplifiers, the intergap drift distance of the large signal portion of the tube needs to be small in terms of plasma wavelengths. This affects the achievable re-entrance of the cavities. Thus, the lowest possible effective plasma frequency is desirable. This again requires that the beam pass close to the drift tube wall. Furthermore, operation will be sensitive to this distance in actual practice so that perturbations in the focusing field are observable and important.

We see from the foregoing that the beam-to-drift tube distance is an important design parameter and needs to be small. There are, however, restrictions due to the consequences of interception of current on a metallic structure. For high average power applications interception beyond some minor amount cannot be tolerated. In addition, a serious degradation in r-f performance accompanies any serious loss of current prior to the region where energy conversion takes place. With the thin high density beams useful at high perveance, serious interception involves only a very small radial motion.

Even if we start with a perfectly aligned ideal beam, its exposure to r-f gap voltages and its own space charge fields will cause boundary perturbations. These will lead to interception unless the average edge of the beam is some distance from the wall. Also, any practical beam will not have an abrupt boundary but rather will have a fuzzy edge due to thermal velocities, lens aberrations, and perhaps electronic interaction in the gun in the case of the magnetron geometry. Added to this are the azimuthal instabilities associated with the hollow beam geometry. These may vary from tube to tube, depending on the initial perturbations upon emergence from the gun. They will almost certainly contribute electrons which are displaced outward from the original beam boundary.

In addition to the foregoing beam effects and perhaps more important is the problem of misalignment. Greater than usual care can be taken, but allowance must be made for a certain tolerance. Misalignment can be due to mechanical displacement in a uniform magnetic field, or to nonaxially symmetric perturbations in the magnetic field itself. It should be noted that even in the L-band tubes tested in this program, lack of alignment of the order of 0.050 inch or less in a length of several feet would be important.

The foregoing considerations require greater attention to the quality of the beam and focusing system than would ordinarily be the case. A higher perveance beam requires a stronger focusing system than a lower perveance beam at the same power level. The necessity for excellent control of the beam edge requires additional stiffening of the beam. Thus, to achieve the best performance available with increasing perveance, a substantial increase in focusing field is required. Where a uniform magnetic field is used, the magnetic field is apt to be much greater than with low perveance designs.

VI. ACKNOWLEDGEMENT

Varian Associates wishes to express its gratitude to Dr. Lee MacKenzie of Cornell University, whose contributions have been responsible to a large extent for the advancement of the program. Dr. Lee MacKenzie was associated with this project for one year.

VII. ILLUSTRATIONS

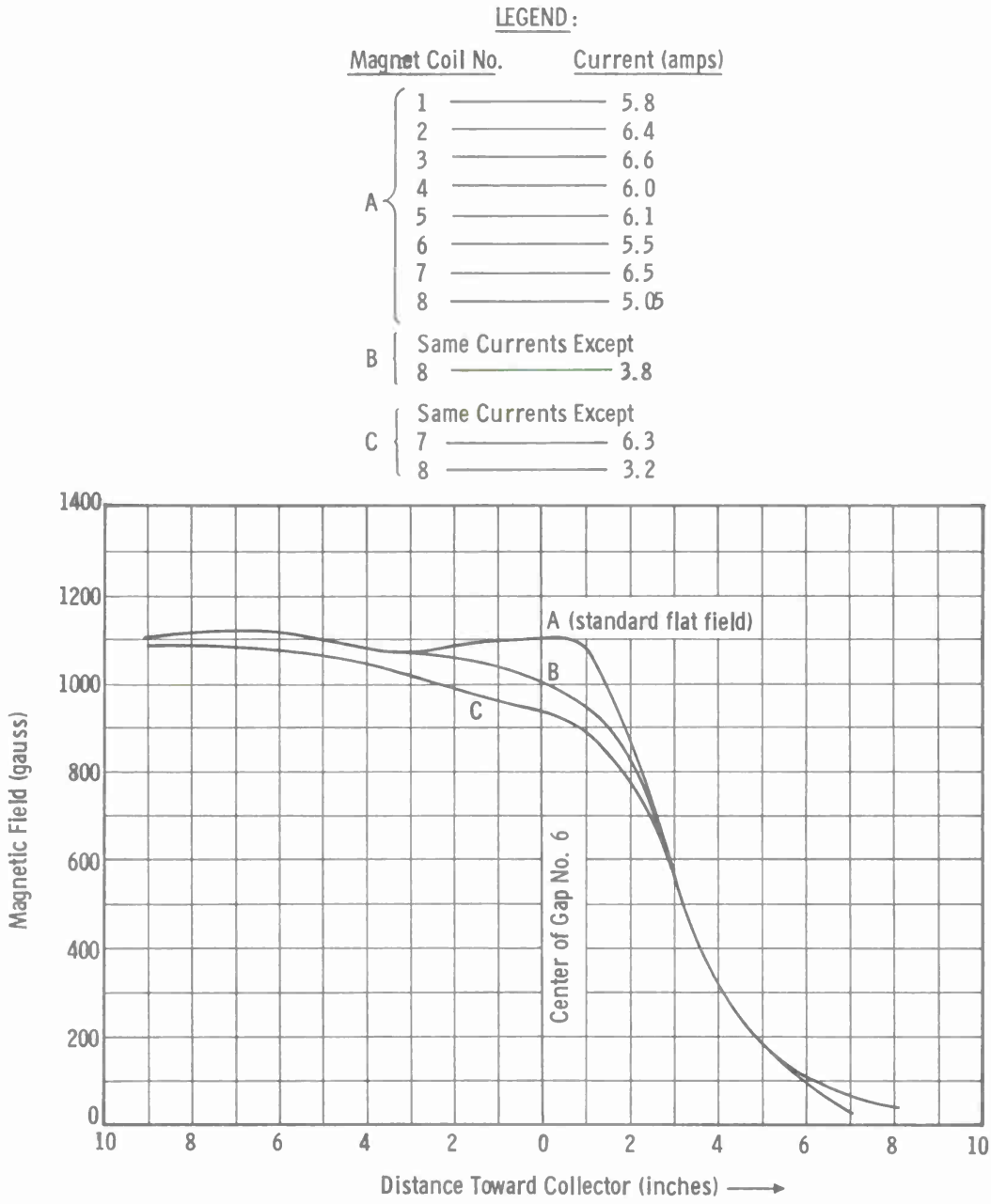

FIGURE 1
VARIATION OF AXIAL MAGNETIC FIELD NEAR THE OUTPUT GAP

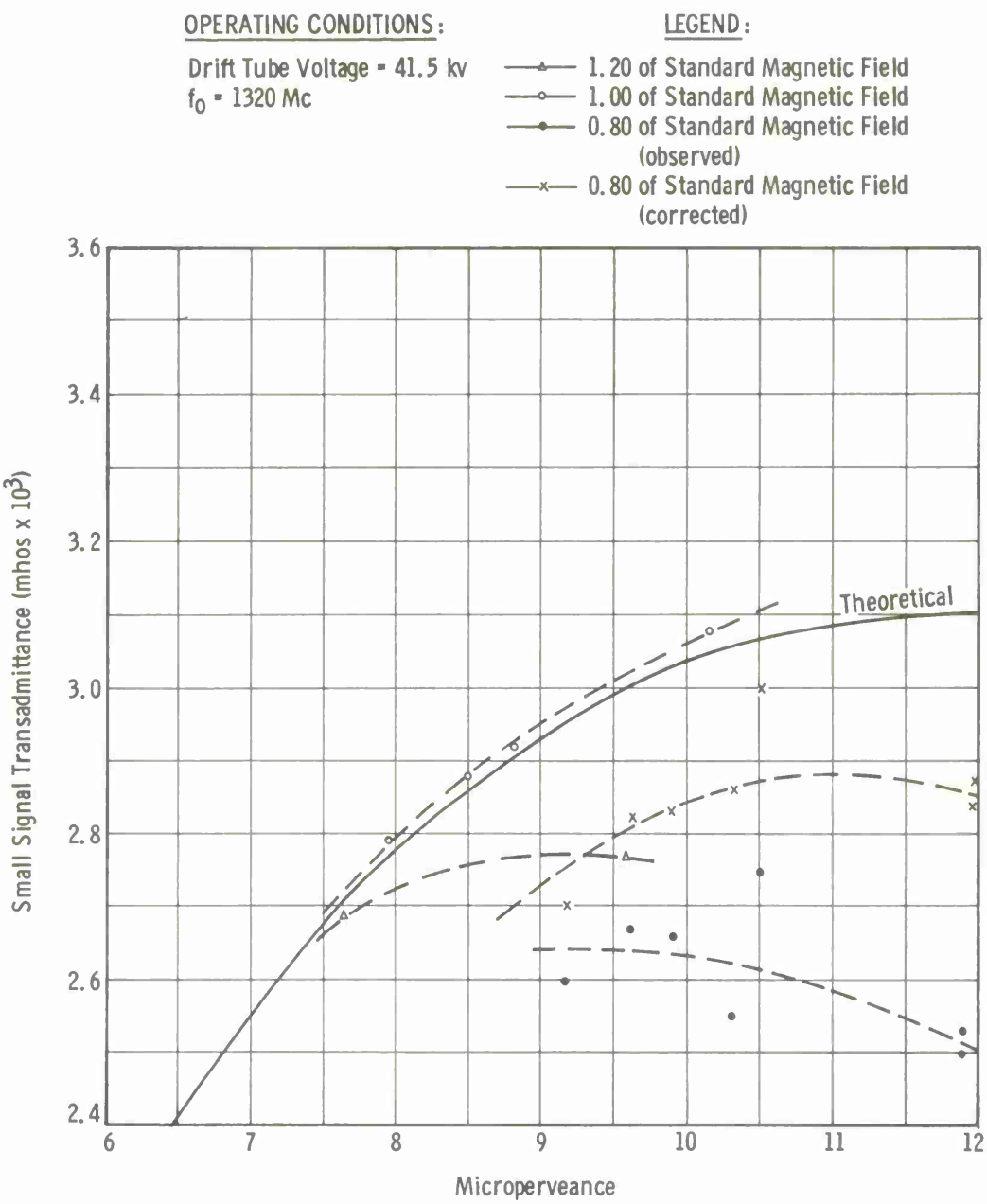

FIGURE 2
SMALL SIGNAL TRANSADMITTANCE, GAP NO. 1 TO GAP NO. 2

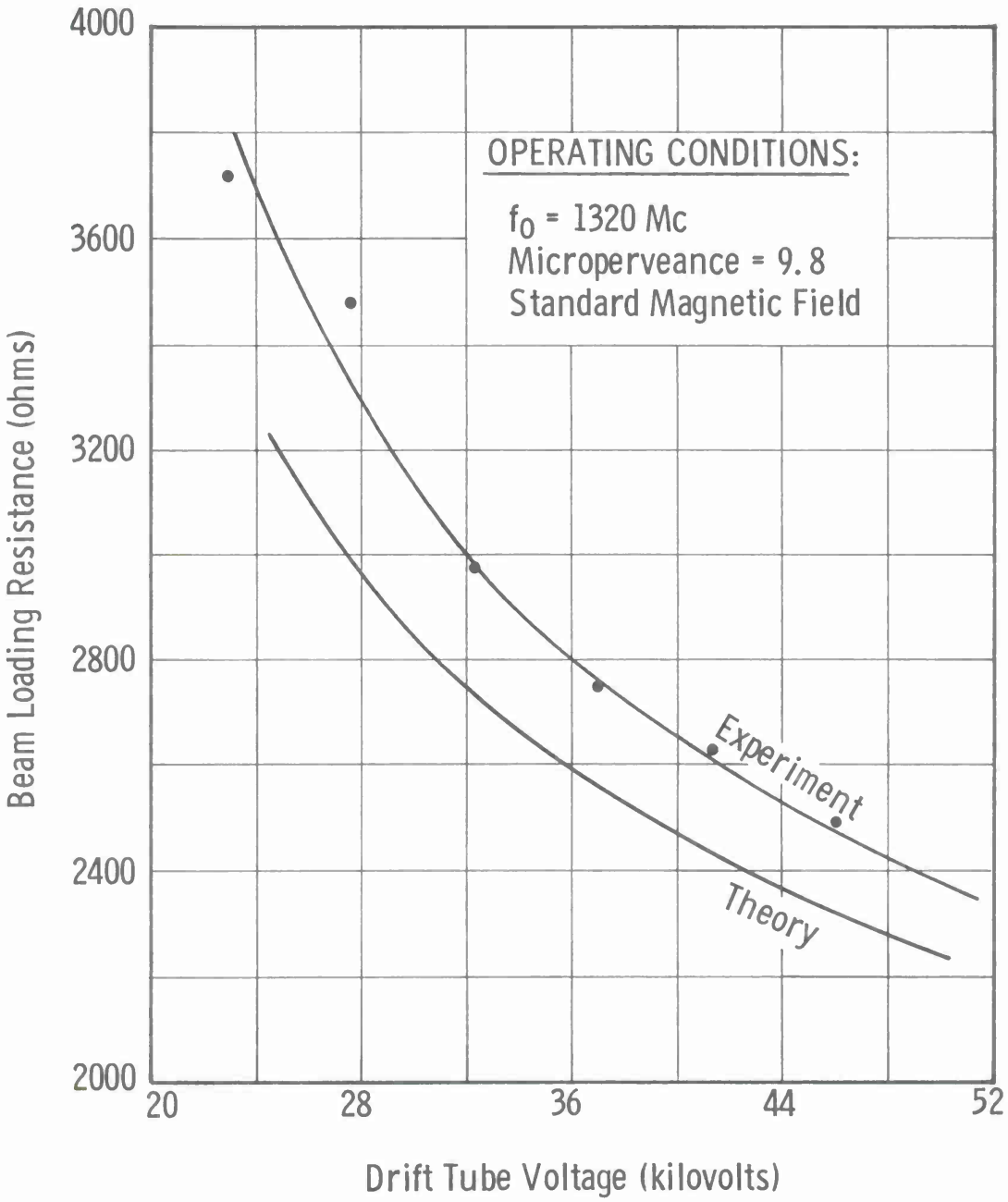

FIGURE 3
BEAM LOADING RESISTANCE VS DRIFT TUBE VOLTAGE

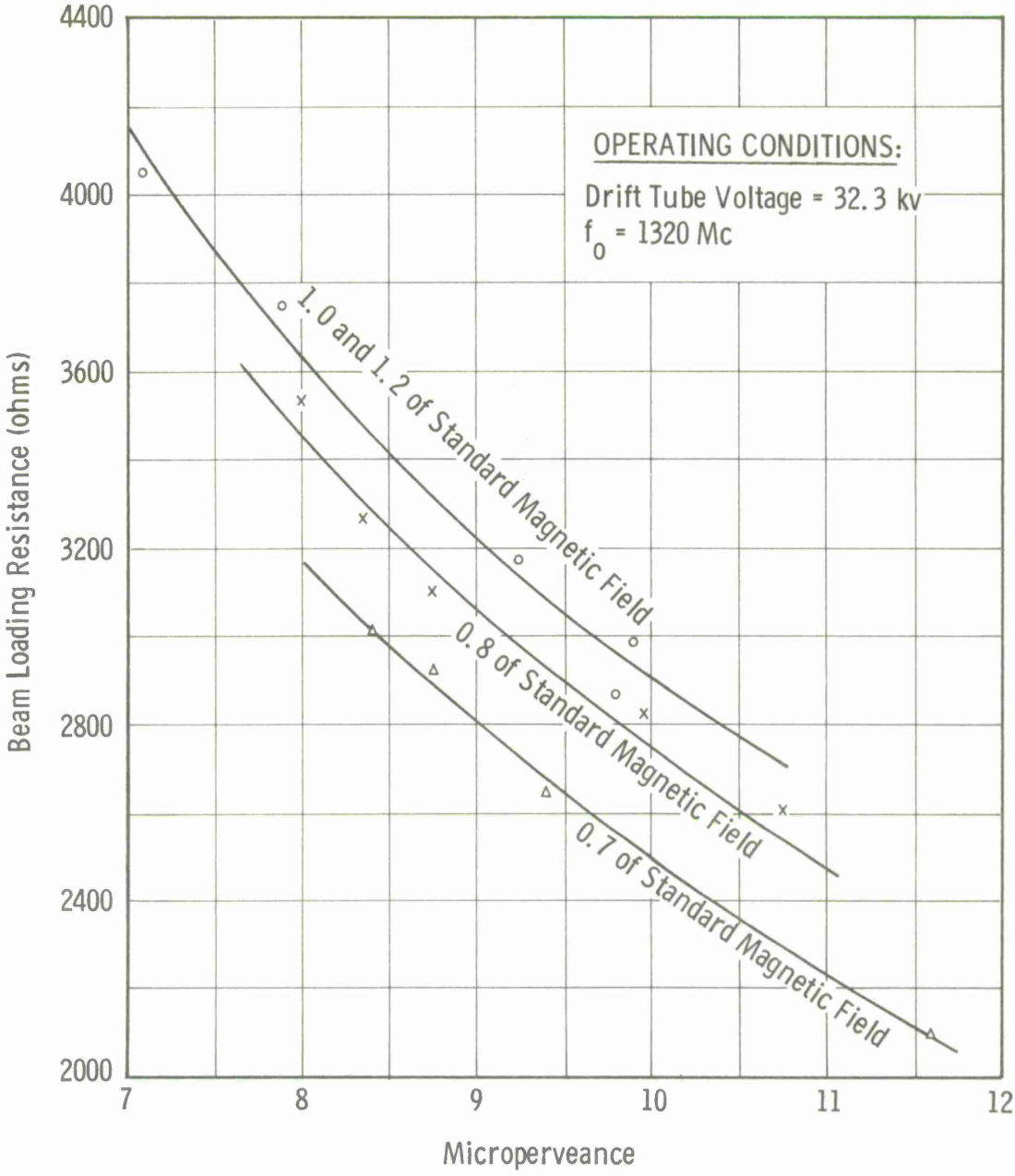

FIGURE 4
BEAM LOADING RESISTANCE VS PERVEANCE,
DRIFT TUBE VOLTAGE = 32.3 KILOVOLTS

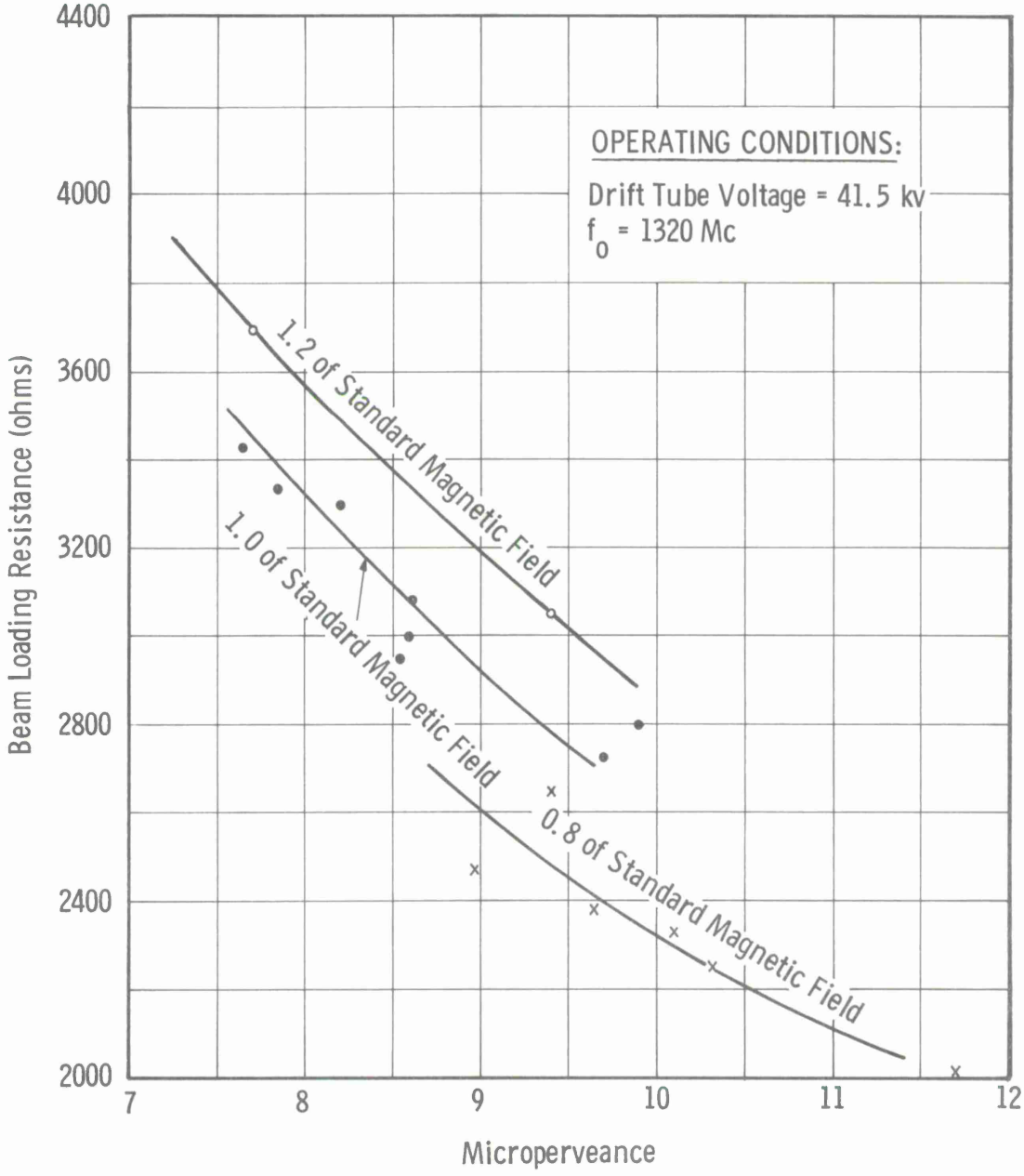

FIGURE 5
BEAM LOADING RESISTANCE VS PERVEANCE,
DRIFT TUBE VOLTAGE = 41.5 KILOVOLTS

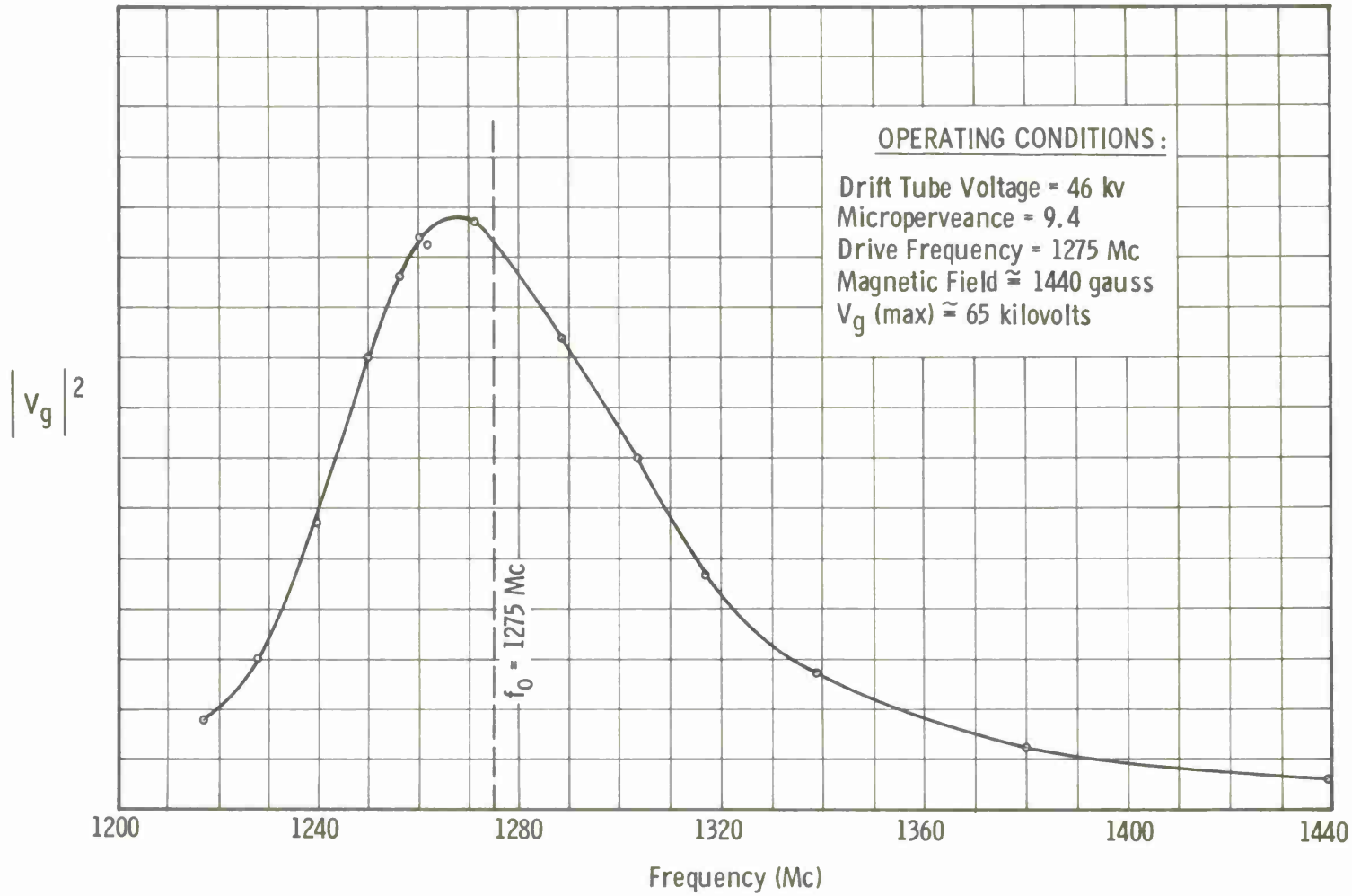

FIGURE 6
A TYPICAL RESPONSE OF CAVITY NO. 2
TO A STRONGLY MODULATED BEAM

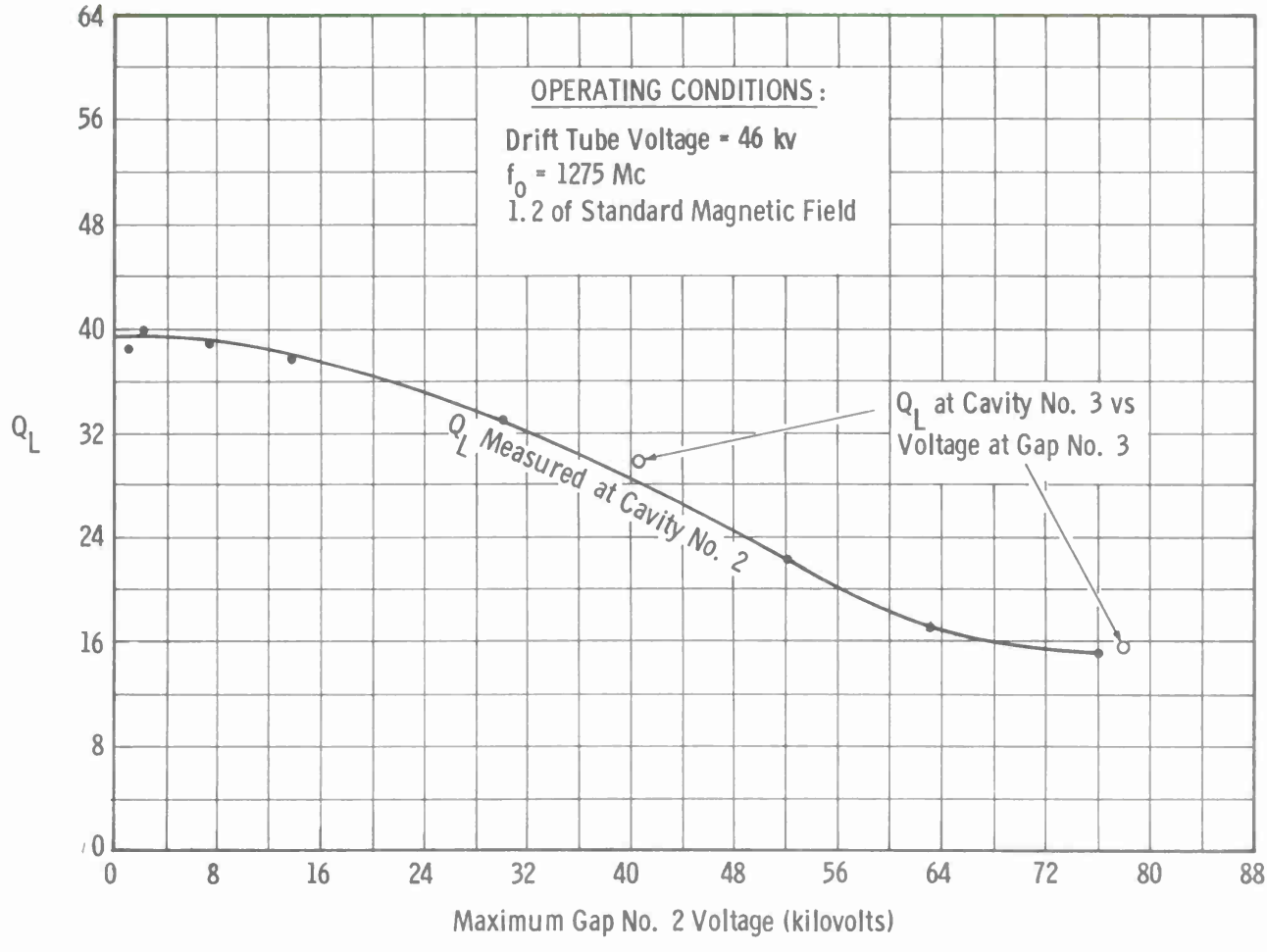

FIGURE 7
INDICATED LOADED Q OF CAVITY NO. 2
UNDER LARGE SIGNAL CONDITIONS VS VOLTAGE AT GAP NO. 2

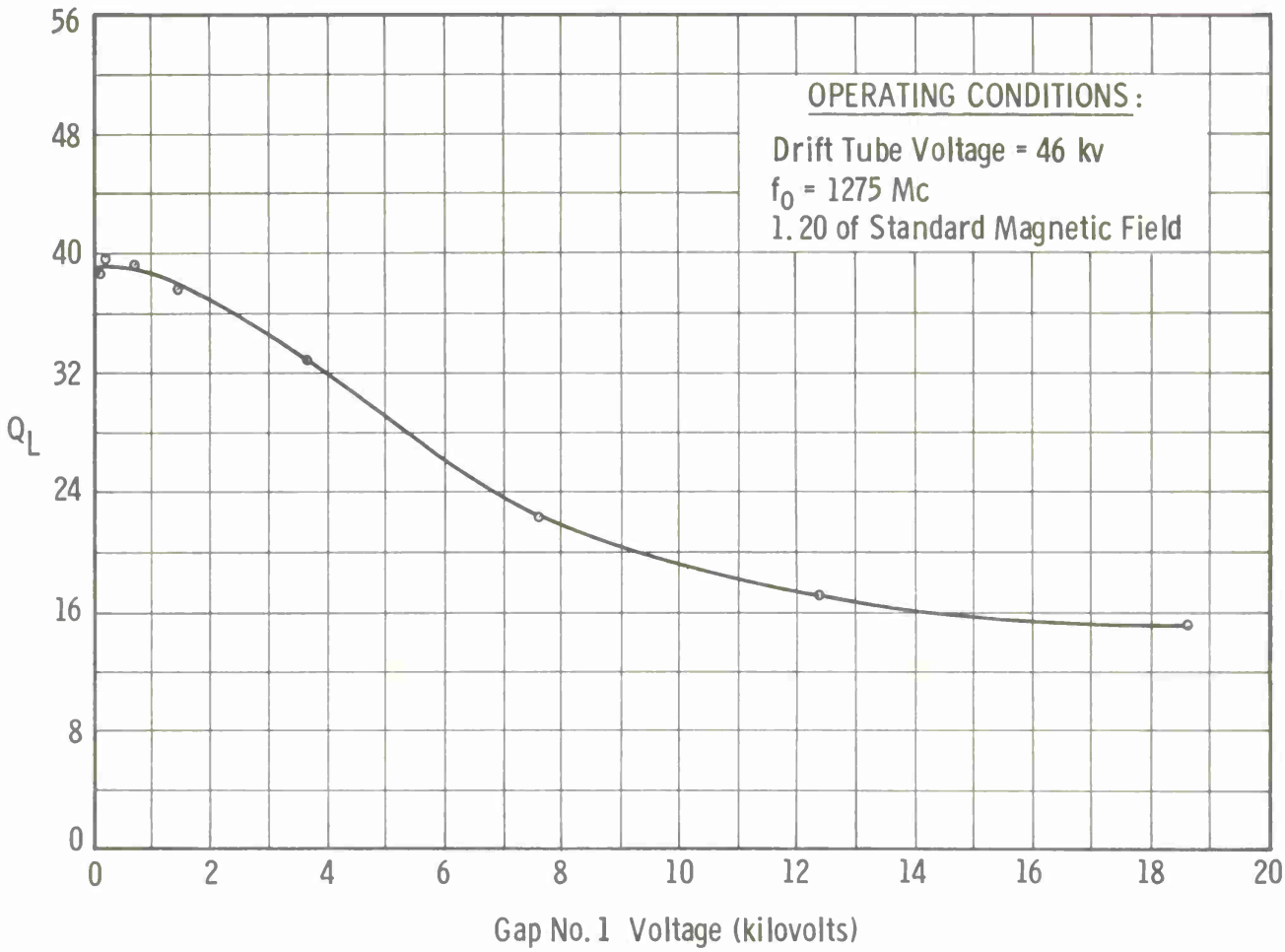

FIGURE 8
INDICATED LOADED Q OF CAVITY NO. 2
UNDER LARGE SIGNAL CONDITIONS VS VOLTAGE AT GAP NO. 1

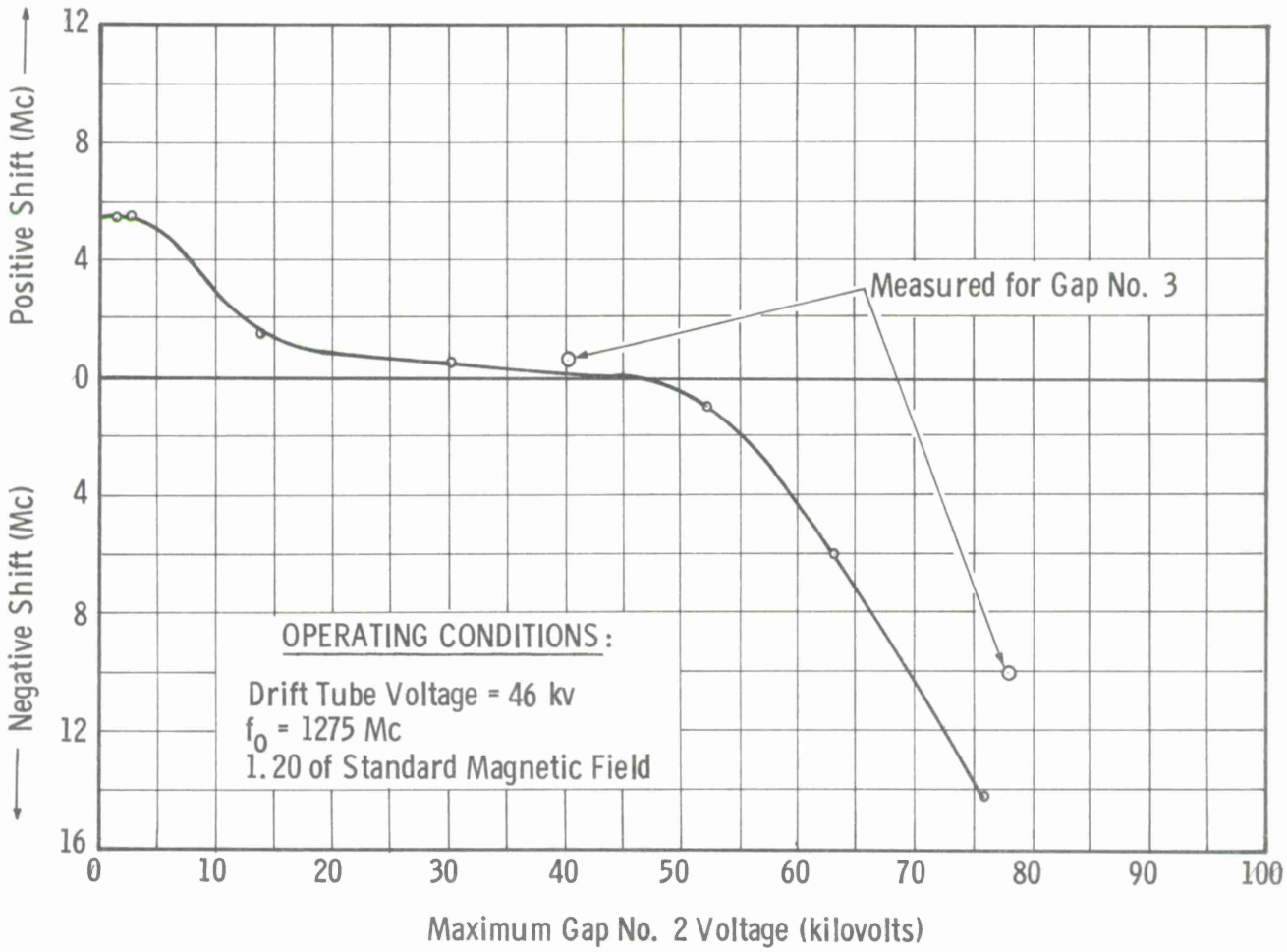

FIGURE 9
INDICATED SHIFT OF RESONANT FREQUENCY VS GAP VOLTAGE

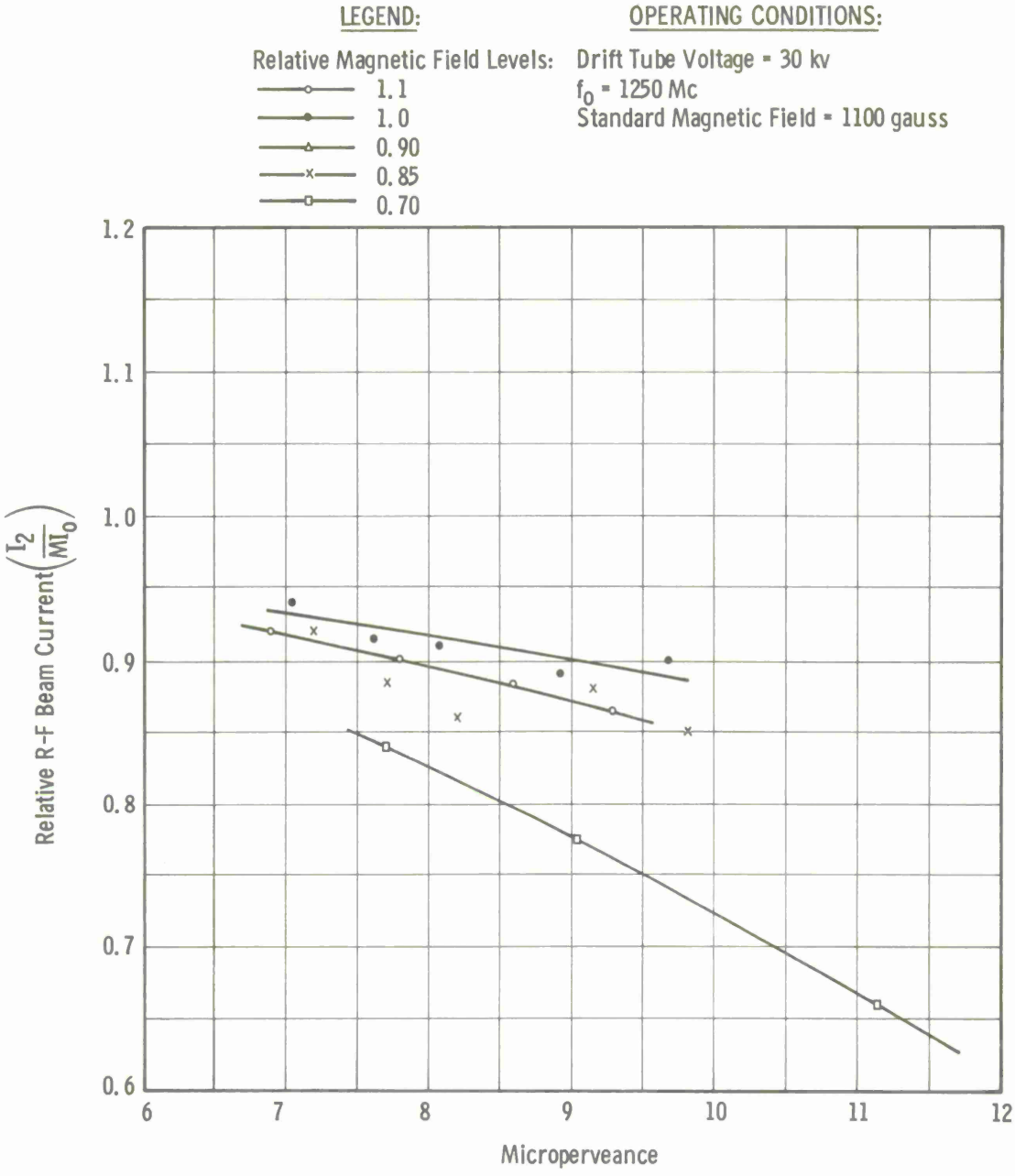

FIGURE 10
SATURATED CURRENT AT GAP NO. 2,
DRIFT TUBE VOLTAGE = 30 KILOVOLTS

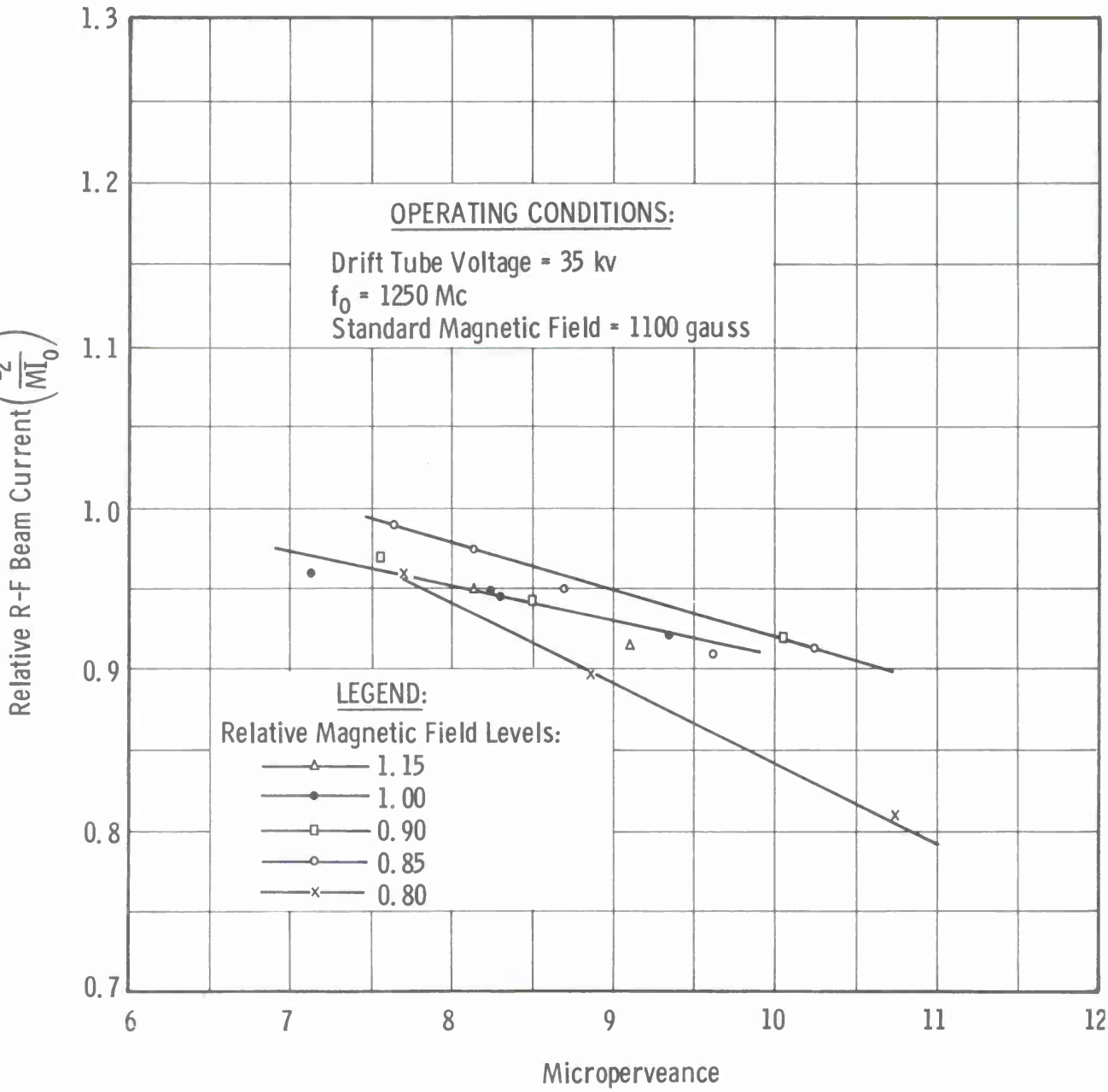

FIGURE 11
SATURATED CURRENT AT GAP NO. 2,
DRIFT TUBE VOLTAGE = 35 KILOVOLTS

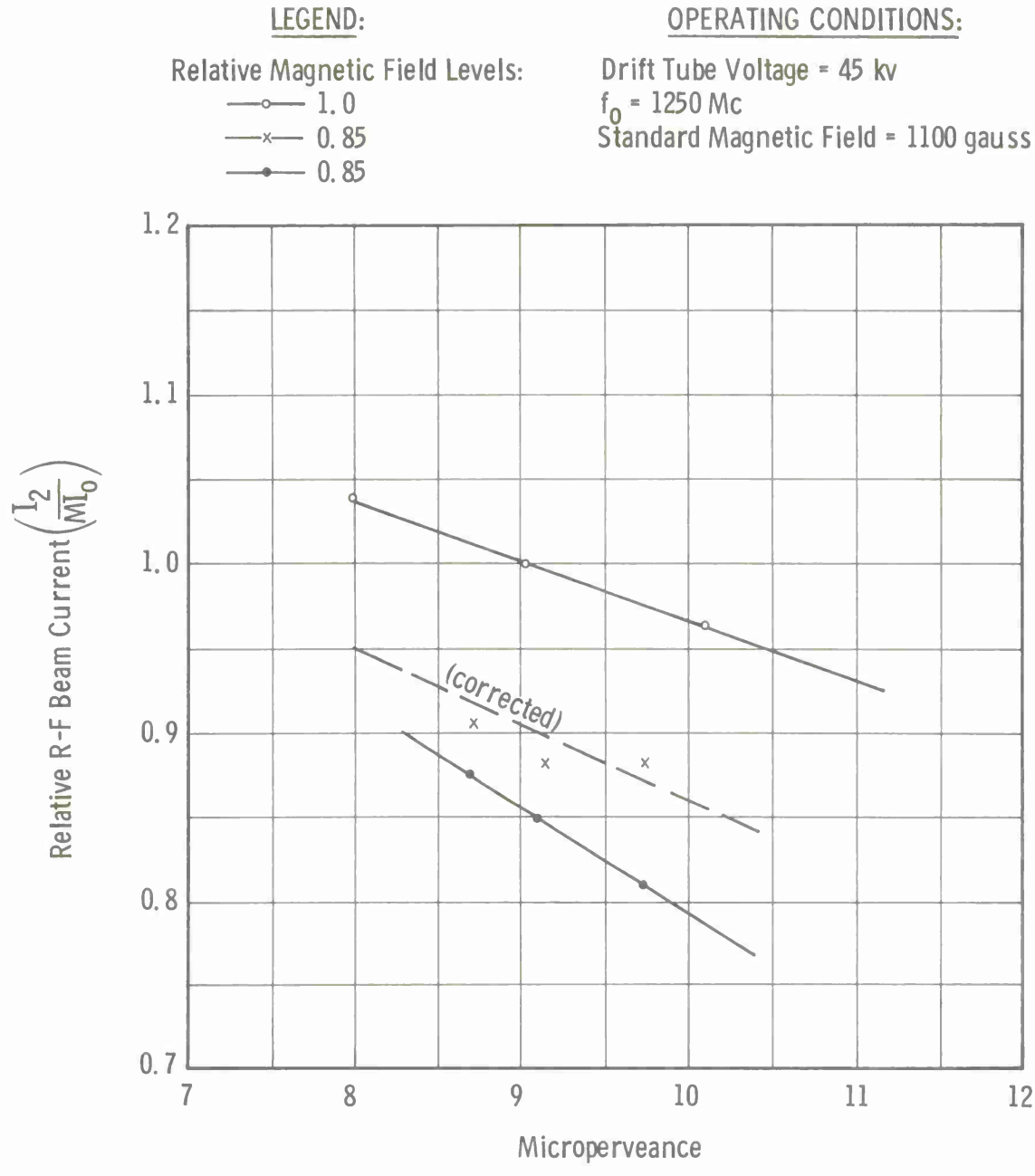

FIGURE 12
SATURATED CURRENT AT GAP NO. 2,
DRIFT TUBE VOLTAGE = 45 KILOVOLTS

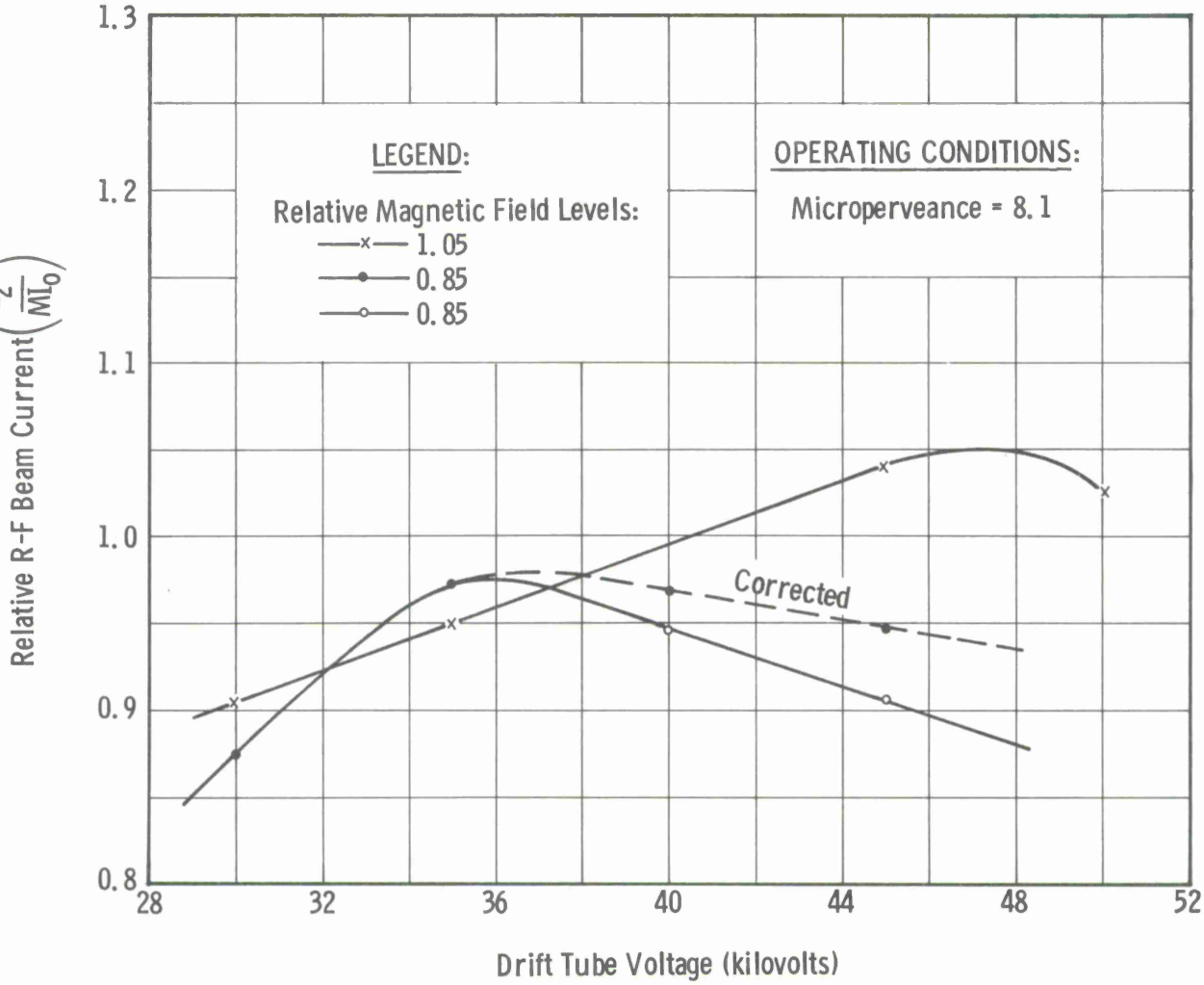

FIGURE 13
SATURATED CURRENT AT GAP NO. 2 VS DRIFT TUBE VOLTAGE

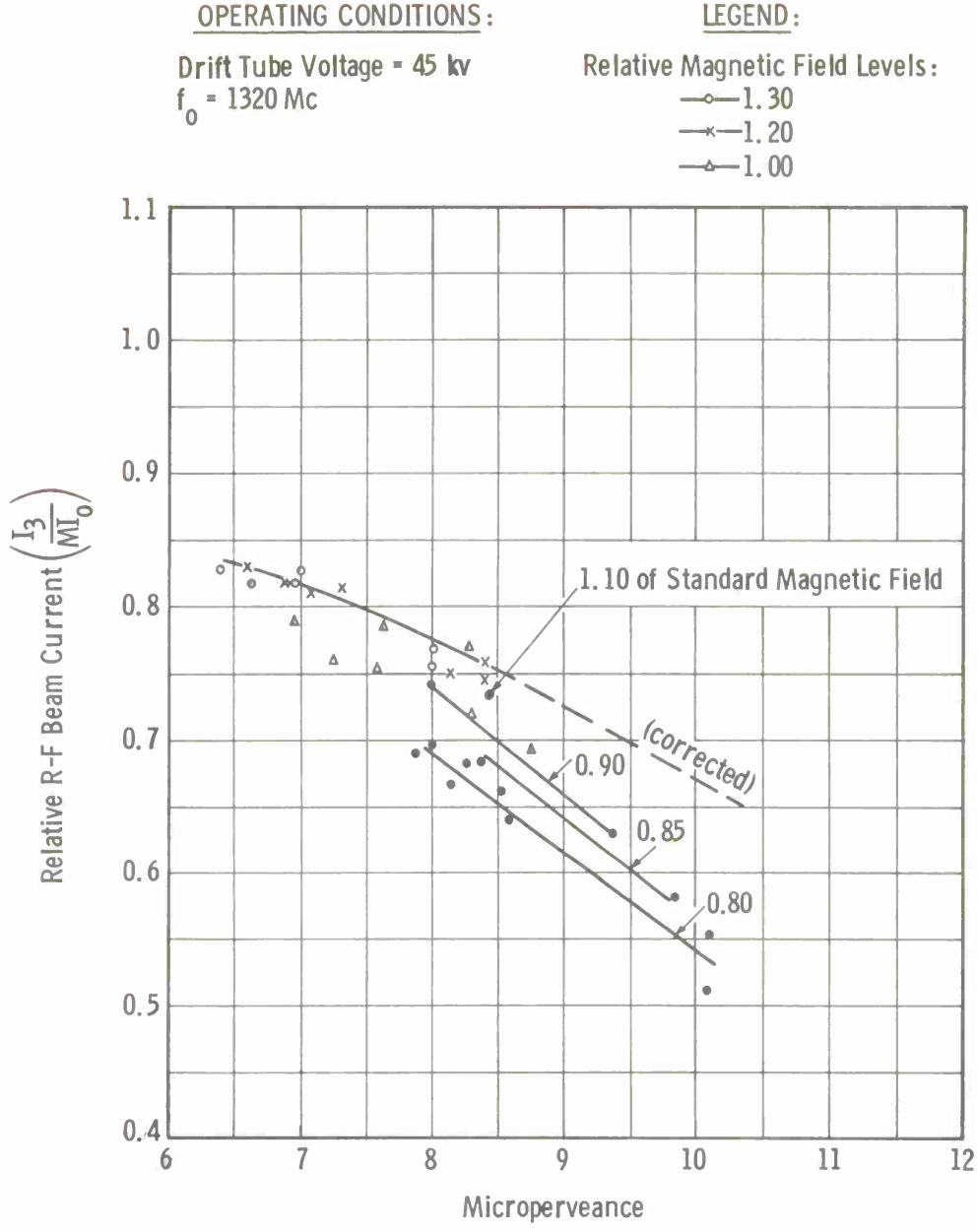

FIGURE 14
SATURATED CURRENT AT GAP NO. 3,
CAVITY NO. 2 SYNCHRONOUSLY TUNED

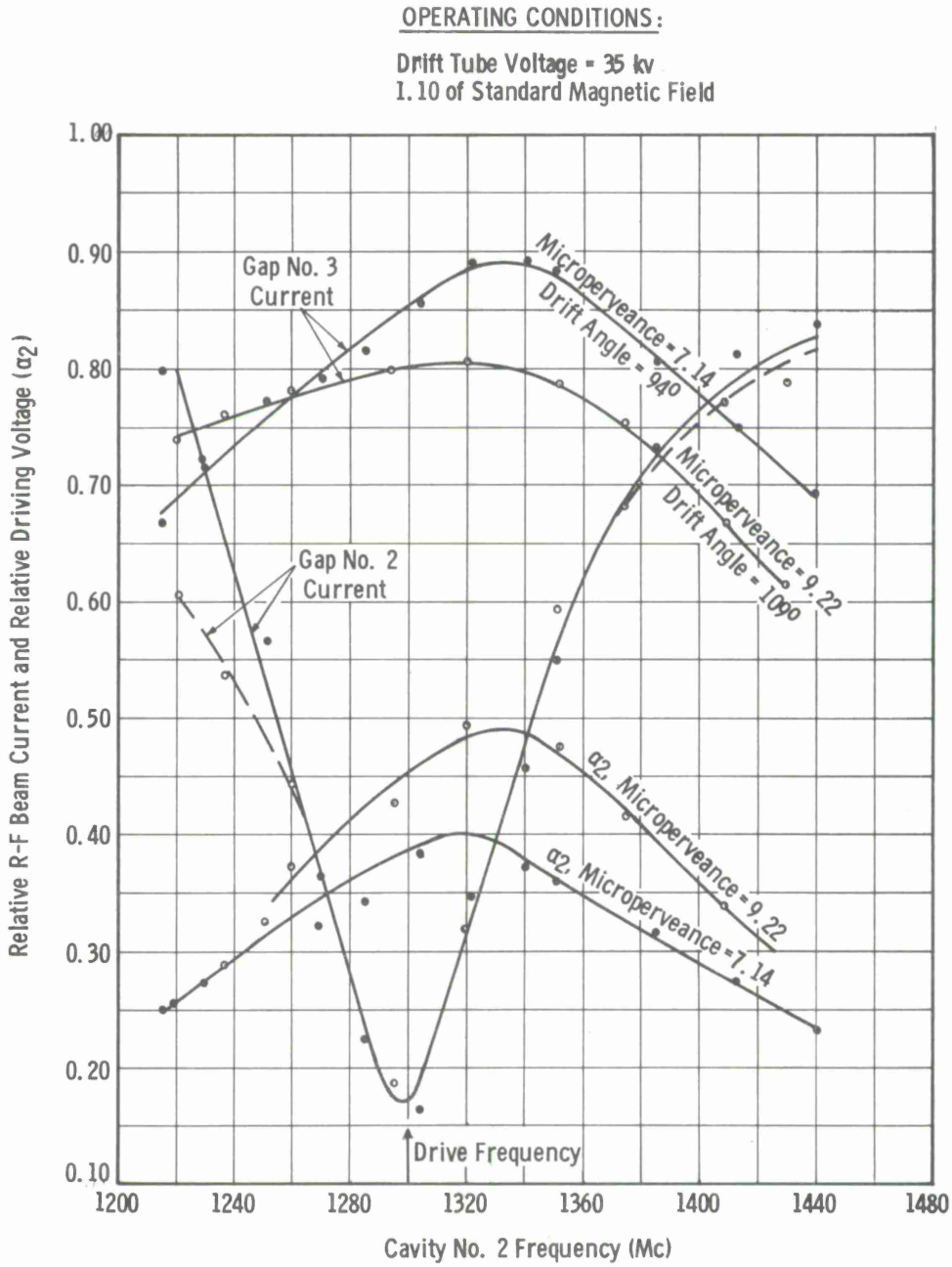

FIGURE 15
SATURATED CURRENT AT GAP NO. 3 VS TUNING OF CAVITY NO. 2, DRIFT TUBE VOLTAGE = 35 KILOVOLTS

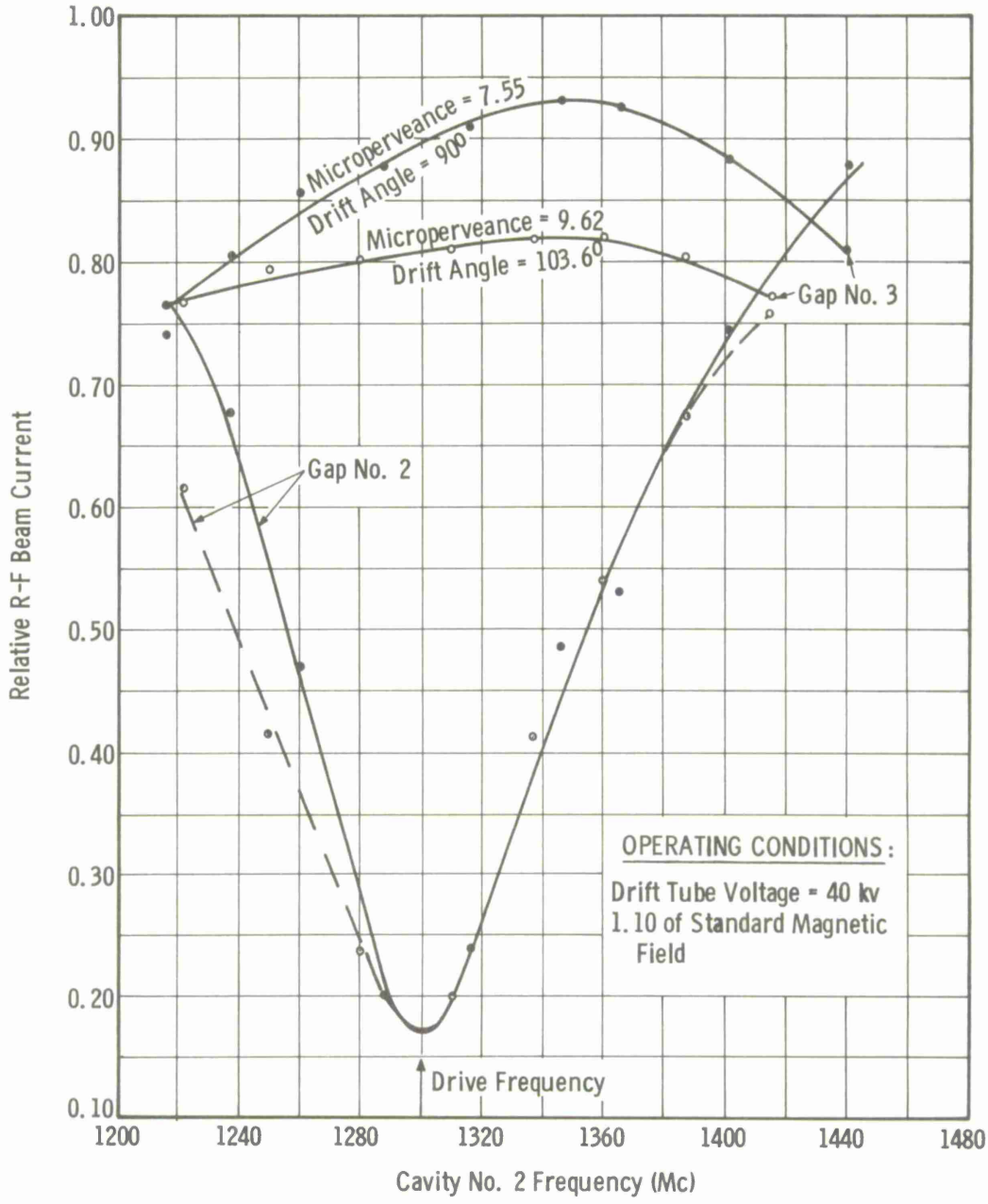

FIGURE 16
SATURATED CURRENT AT GAP NO. 3 VS TUNING OF CAVITY NO. 2, DRIFT TUBE VOLTAGE = 40 KILOVOLTS

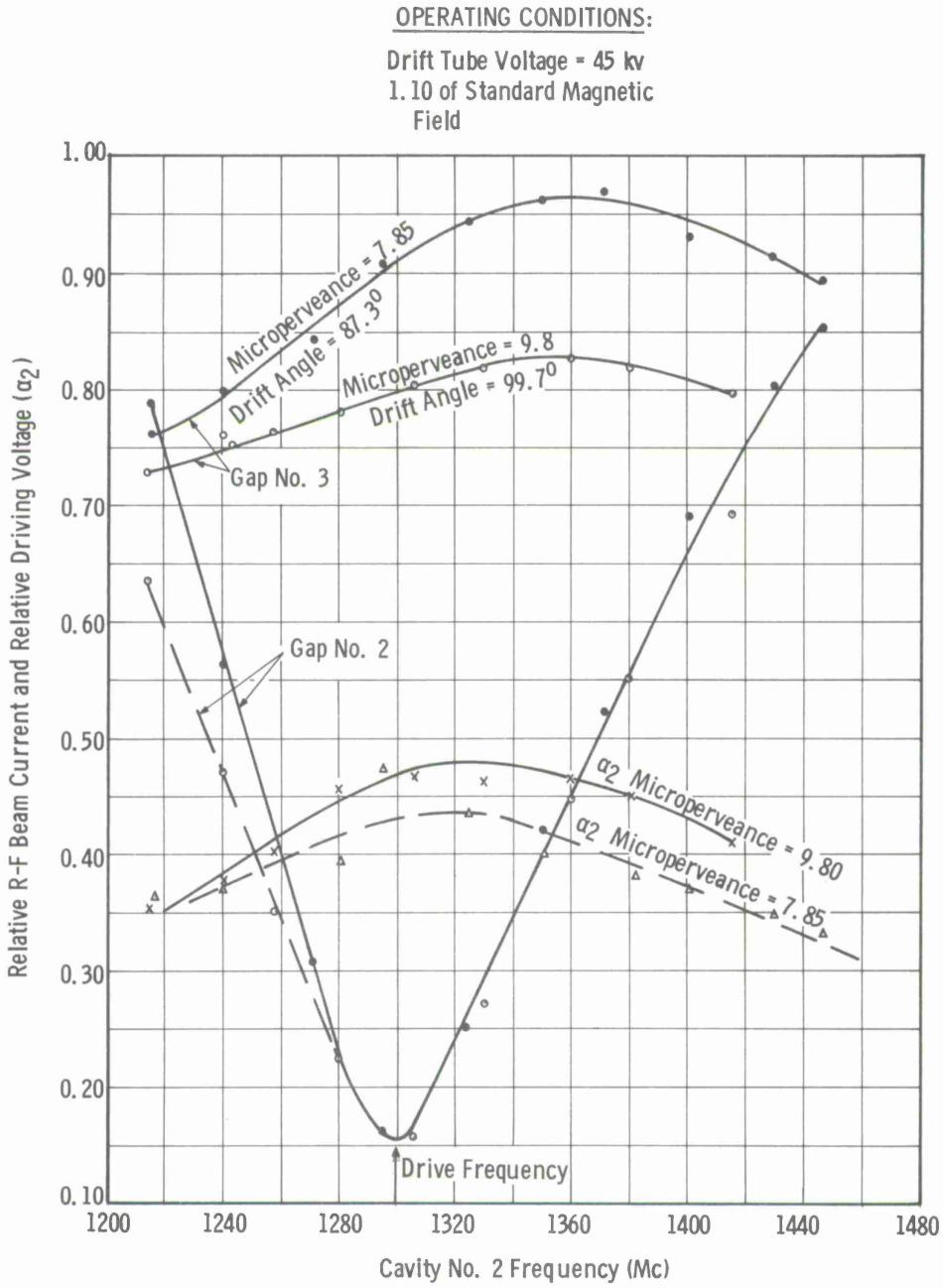

FIGURE 17
SATURATED CURRENT AT GAP NO. 3 VS TUNING OF CAVITY NO. 2, DRIFT TUBE VOLTAGE = 45 KILOVOLTS

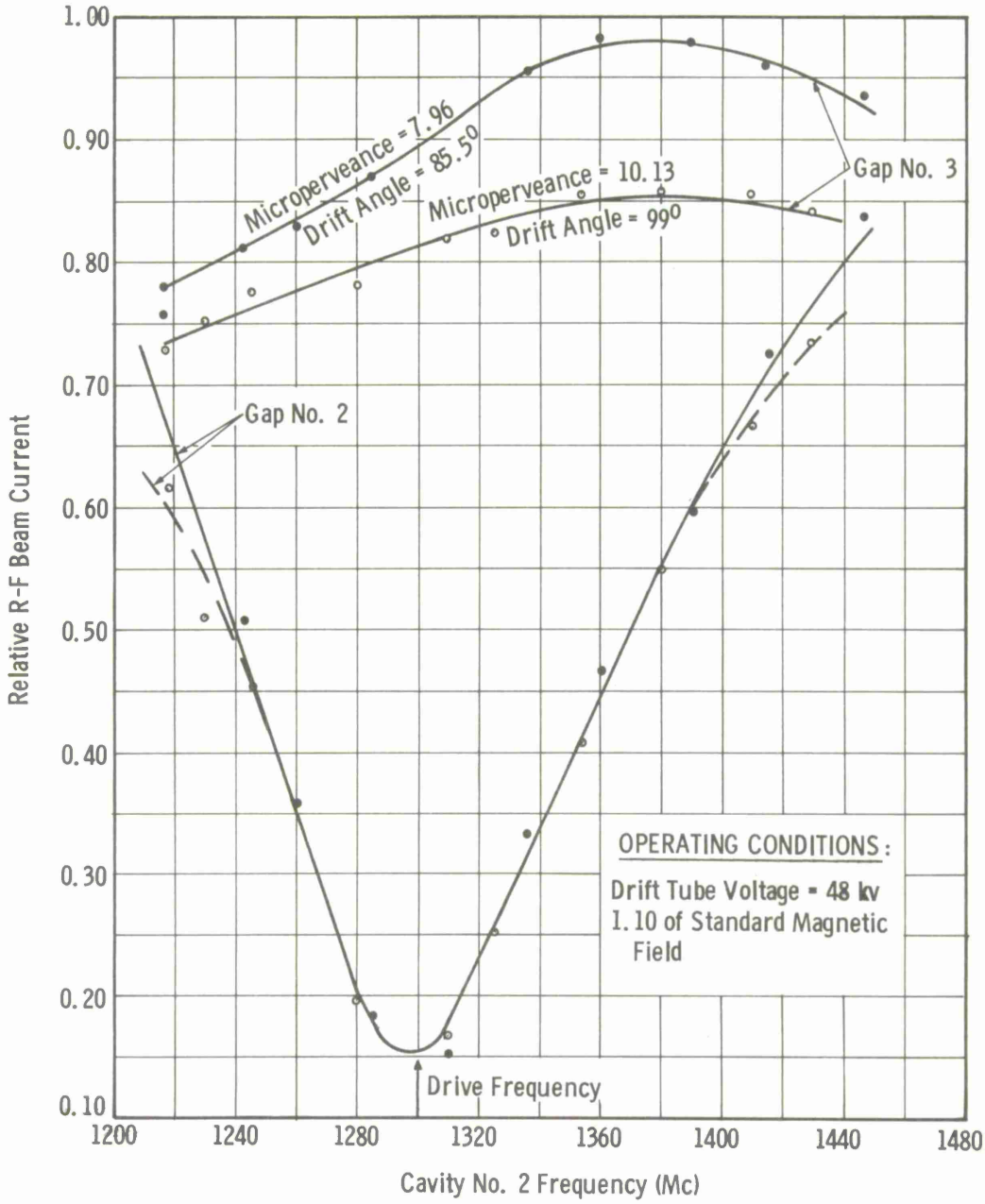

FIGURE 18
SATURATED CURRENT AT GAP NO. 3 VS TUNING OF CAVITY NO. 2, DRIFT TUBE VOLTAGE = 48 KILOVOLTS

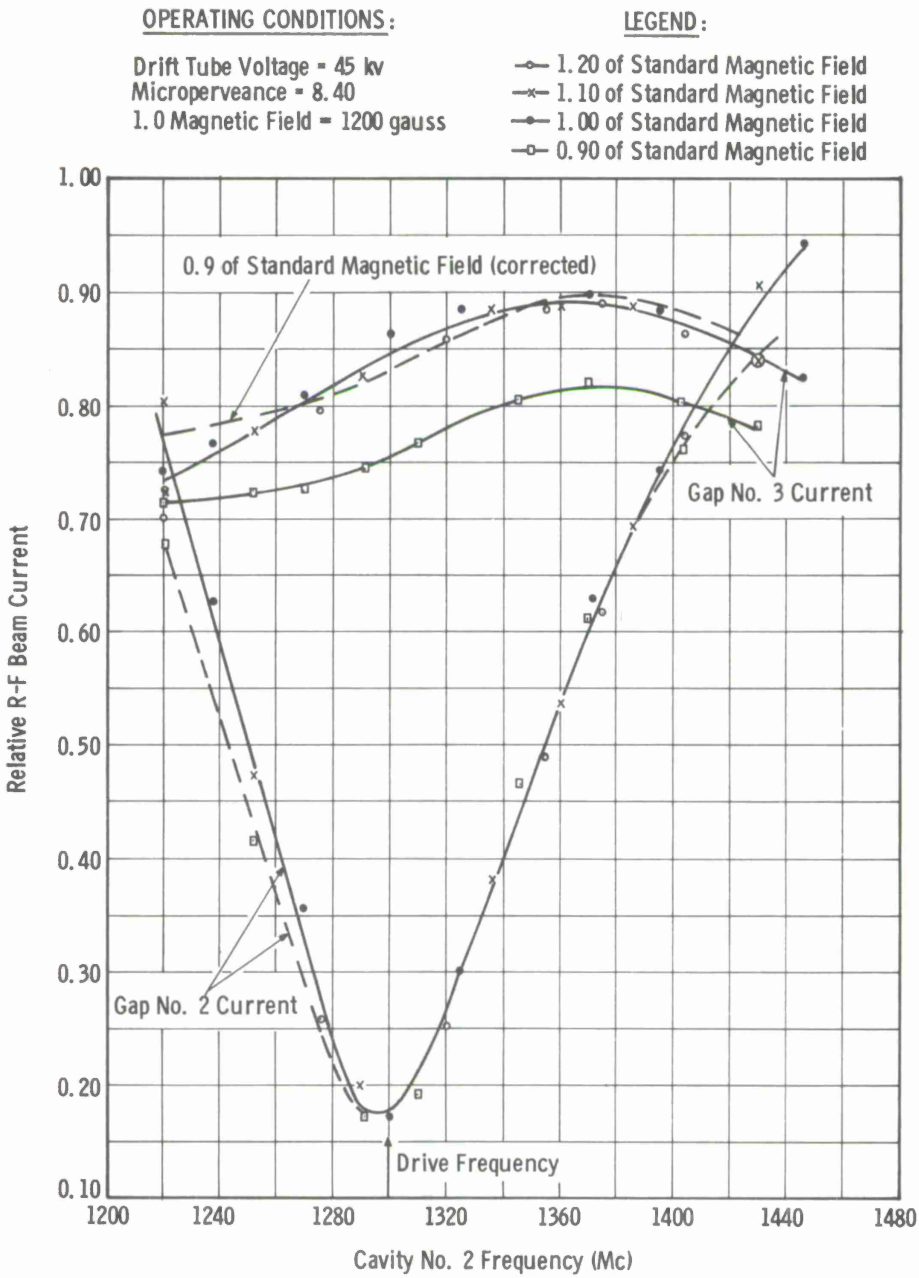

FIGURE 19
EFFECT OF MAGNETIC FIELD LEVEL
ON SATURATED CURRENT AT CAVITY NO. 3

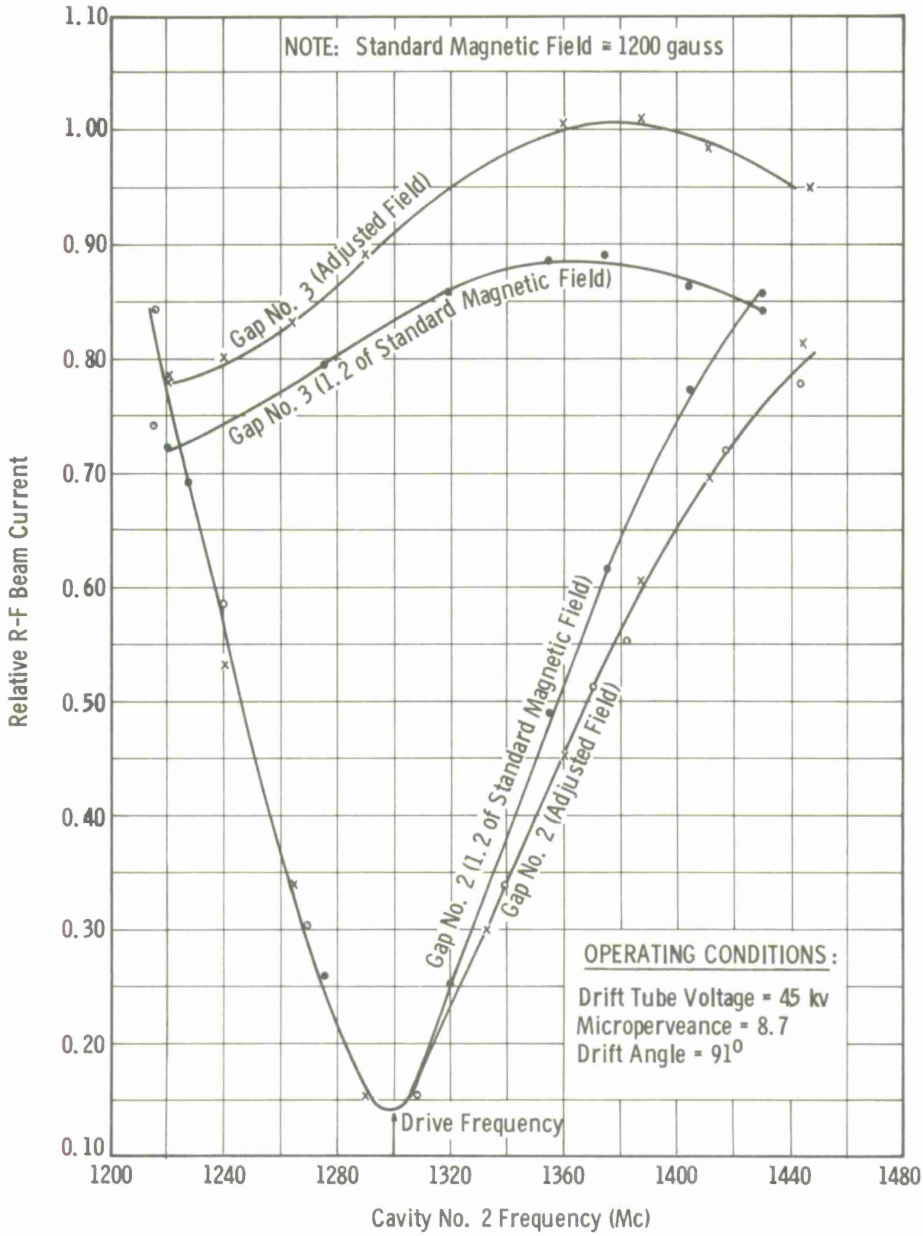

FIGURE 20
EFFECT OF MAGNETIC FIELD SHAPE
ON SATURATED CURRENT AT CAVITY NO. 3

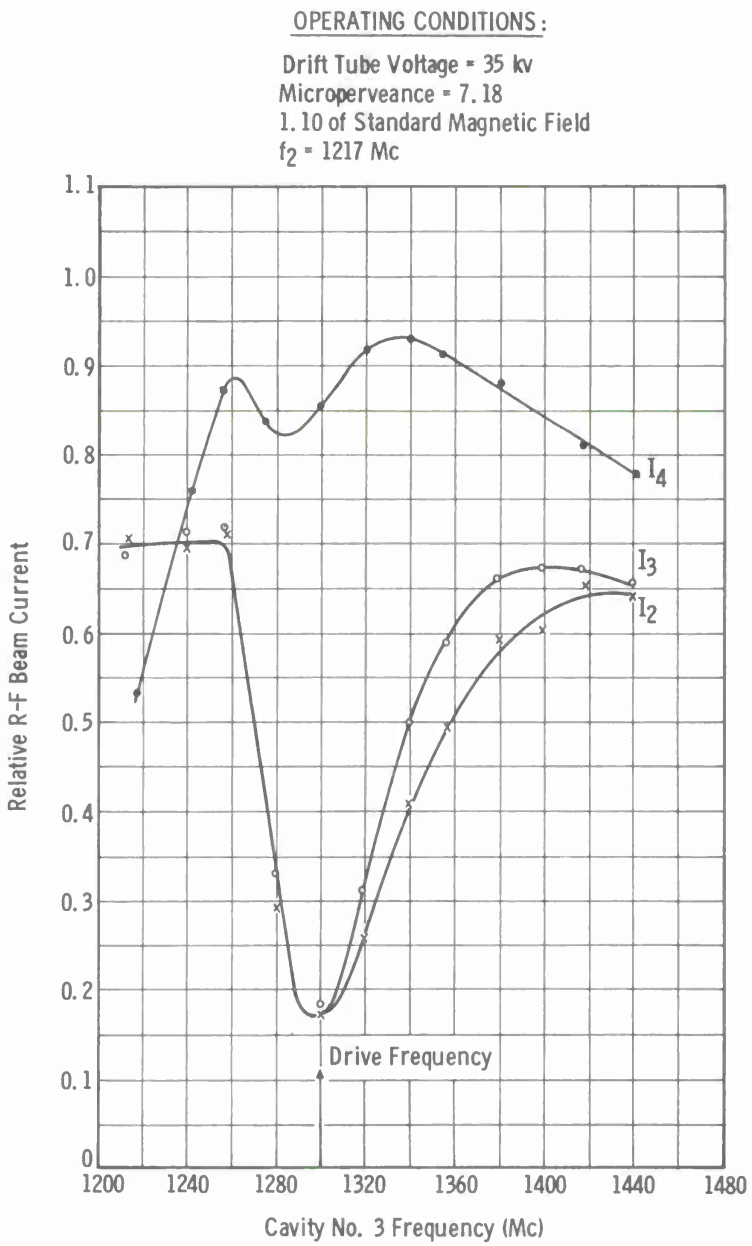

FIGURE 21
SATURATED CURRENT AT GAP NO. 4 VS TUNING OF CAVITY NO. 3 WITH CAVITY NO. 2 TUNED BELOW DRIVE FREQUENCY, DRIFT TUBE VOLTAGE = 35 KILOVOLTS

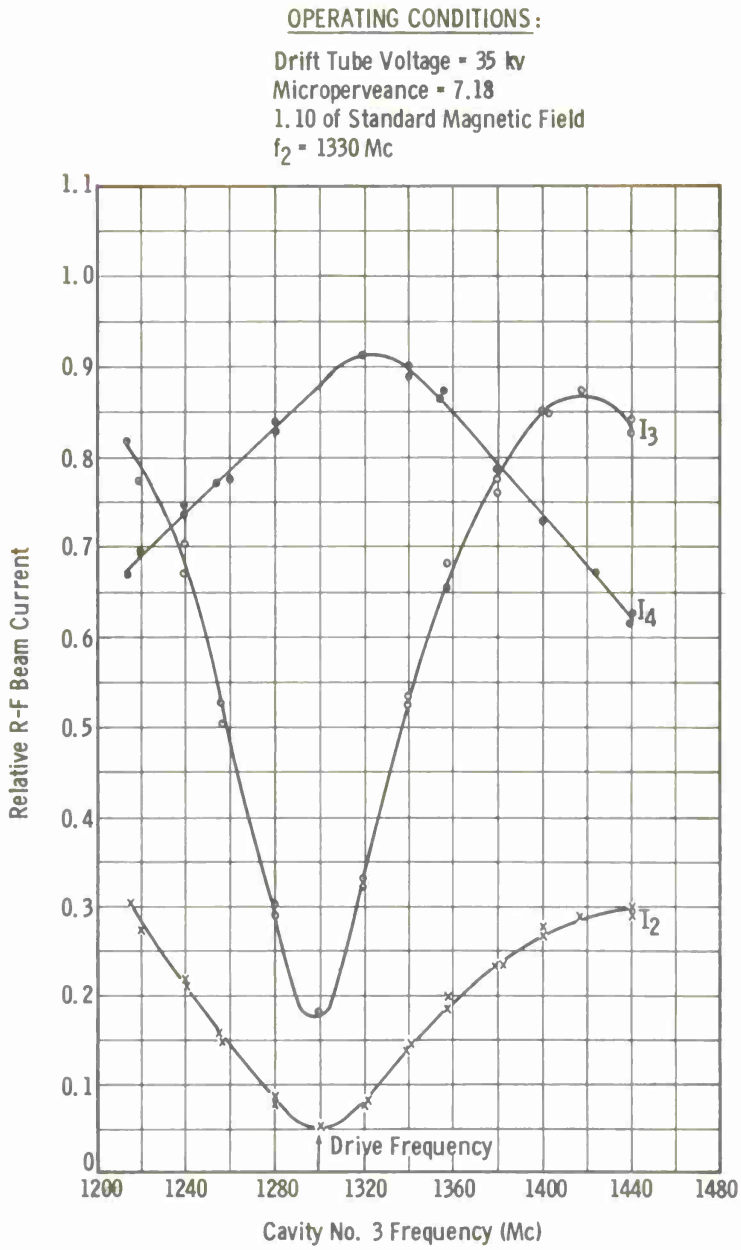

FIGURE 22
SATURATED CURRENT AT GAP NO. 4 VS TUNING OF CAVITY NO. 3 WITH CAVITY NO. 2 TUNED ABOVE DRIVE FREQUENCY, DRIFT TUBE VOLTAGE = 35 KILOVOLTS

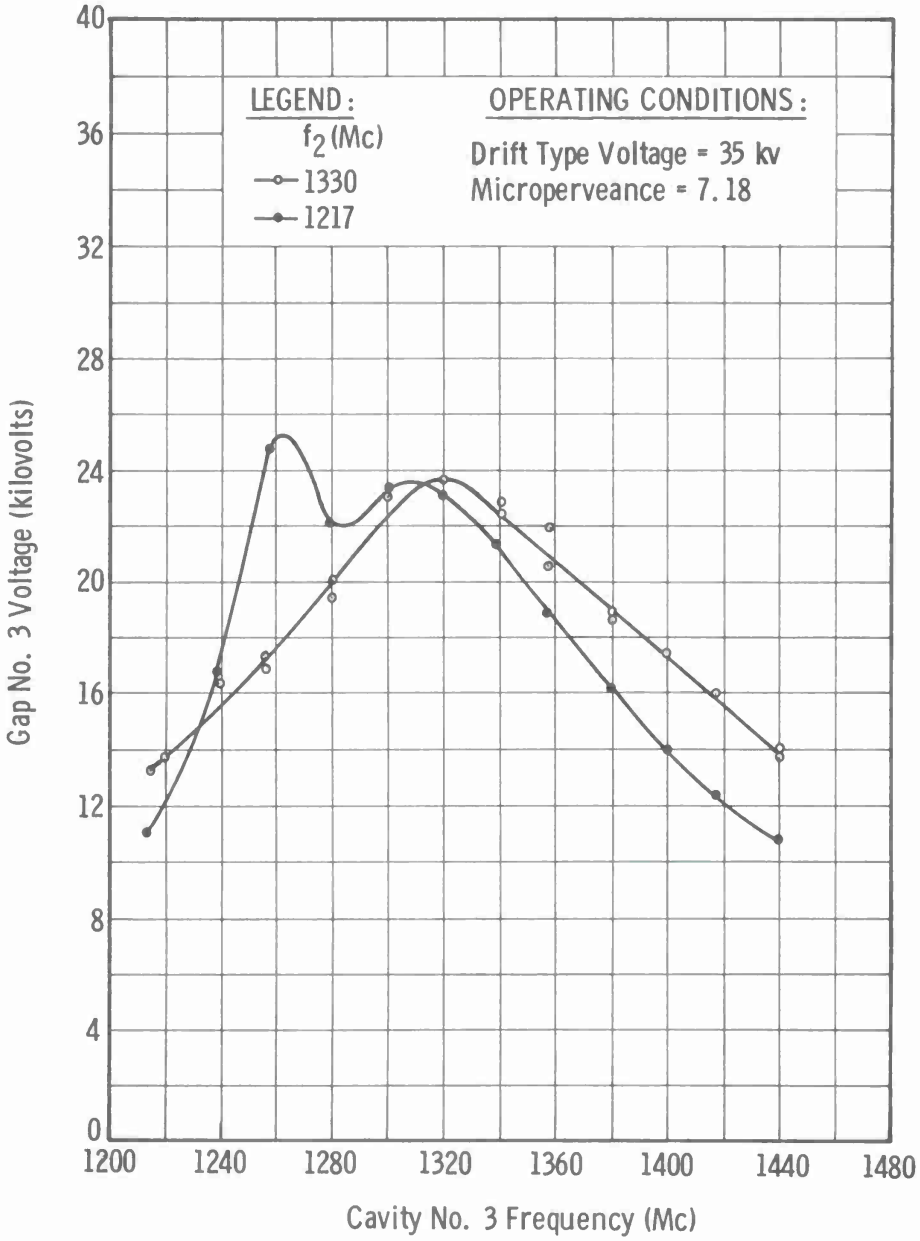

FIGURE 23
R-F VOLTAGES AT GAP NO. 3 FOR CONDITIONS OF FIGURES 21 AND 22

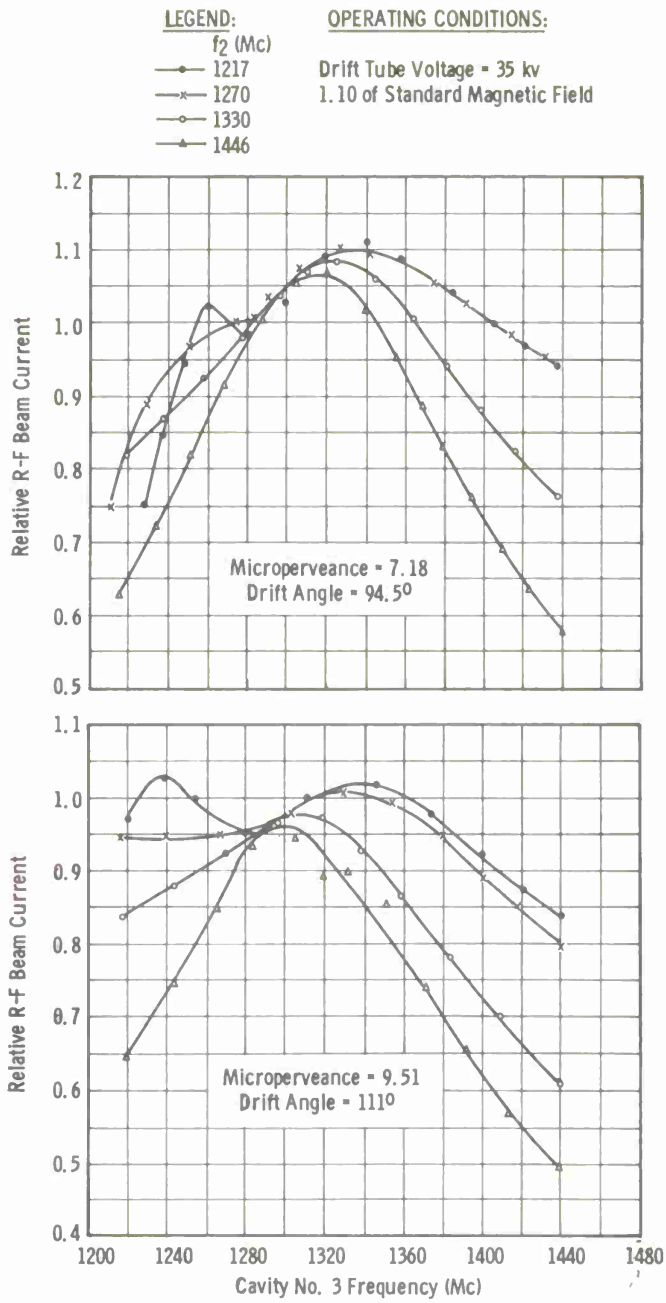

FIGURE 24
SATURATED CURRENT AT GAP NO. 4,
DRIFT TUBE VOLTAGE = 35 KILOVOLTS (COMPOSITE DATA)

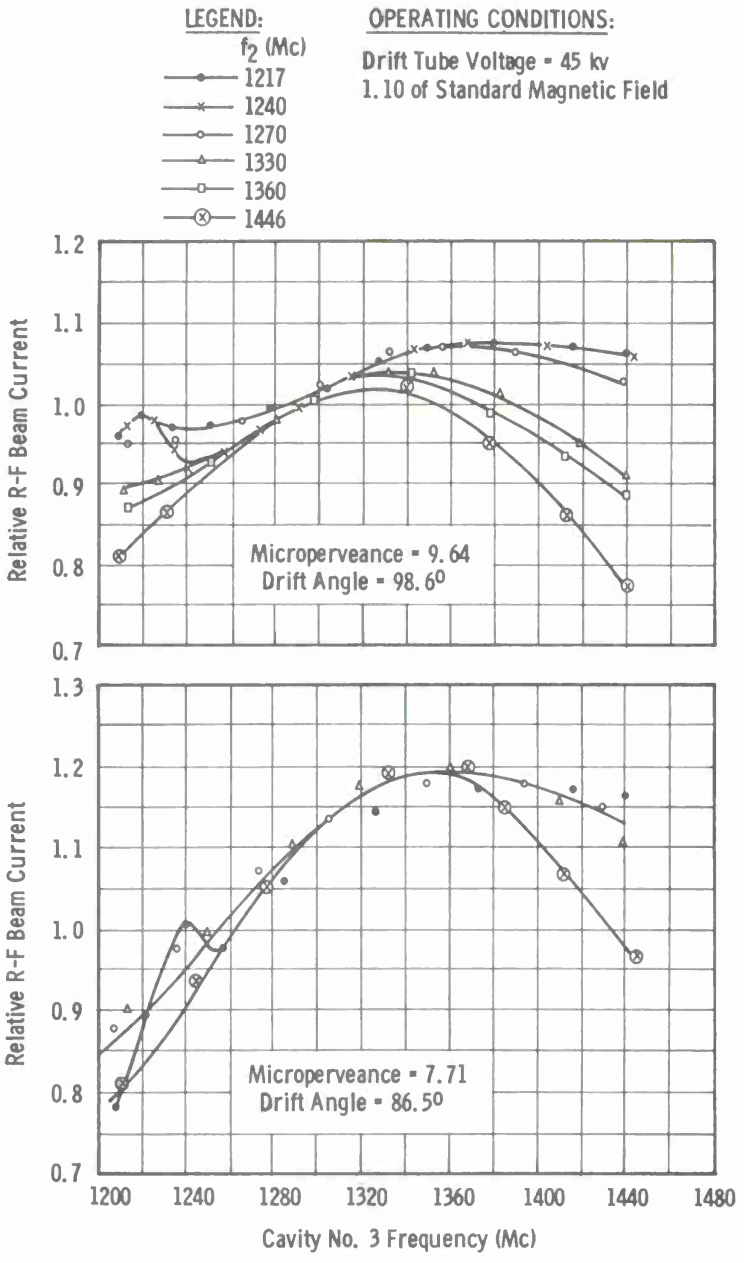

FIGURE 25
SATURATED CURRENT AT GAP NO. 4,
DRIFT TUBE VOLTAGE = 45 KILOVOLTS (COMPOSITE DATA)

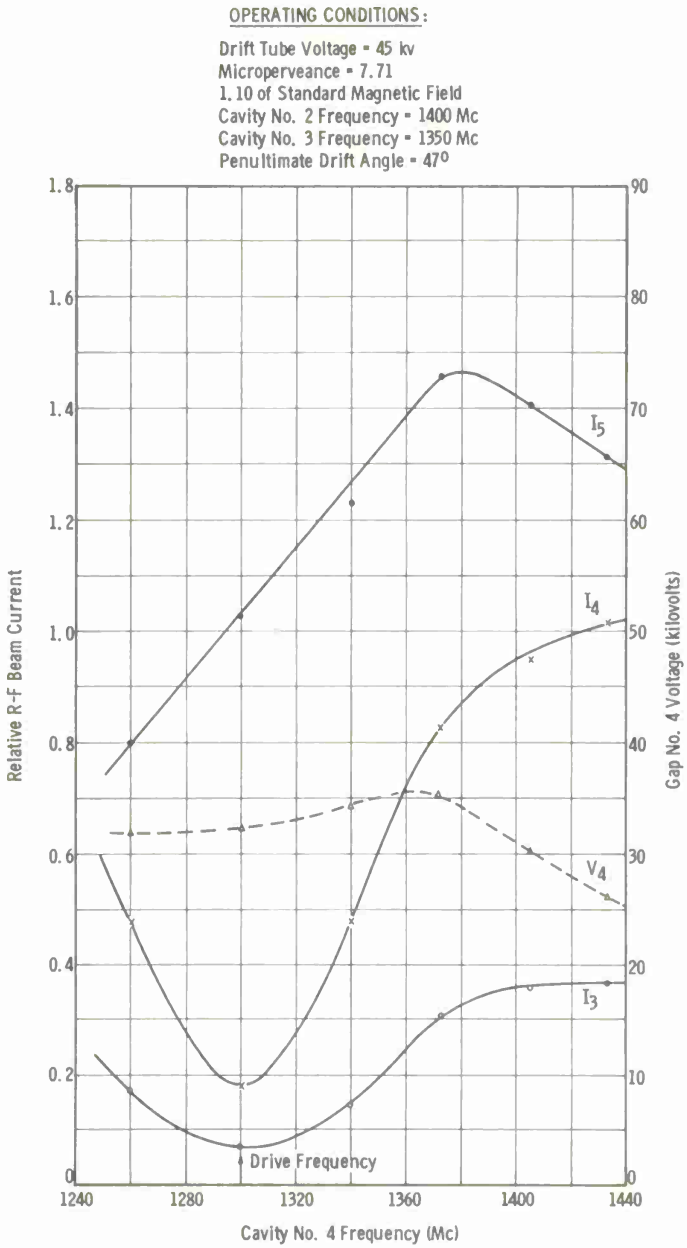

FIGURE 26
SATURATED CURRENT AT GAP NO. 5 VS TUNING OF CAVITY NO. 4 WITH CAVITIES NOS. 2 AND 3 TUNED HIGH, DRIFT TUBE VOLTAGE = 45 KILOVOLTS, MICROPERVEANCE = 7.71

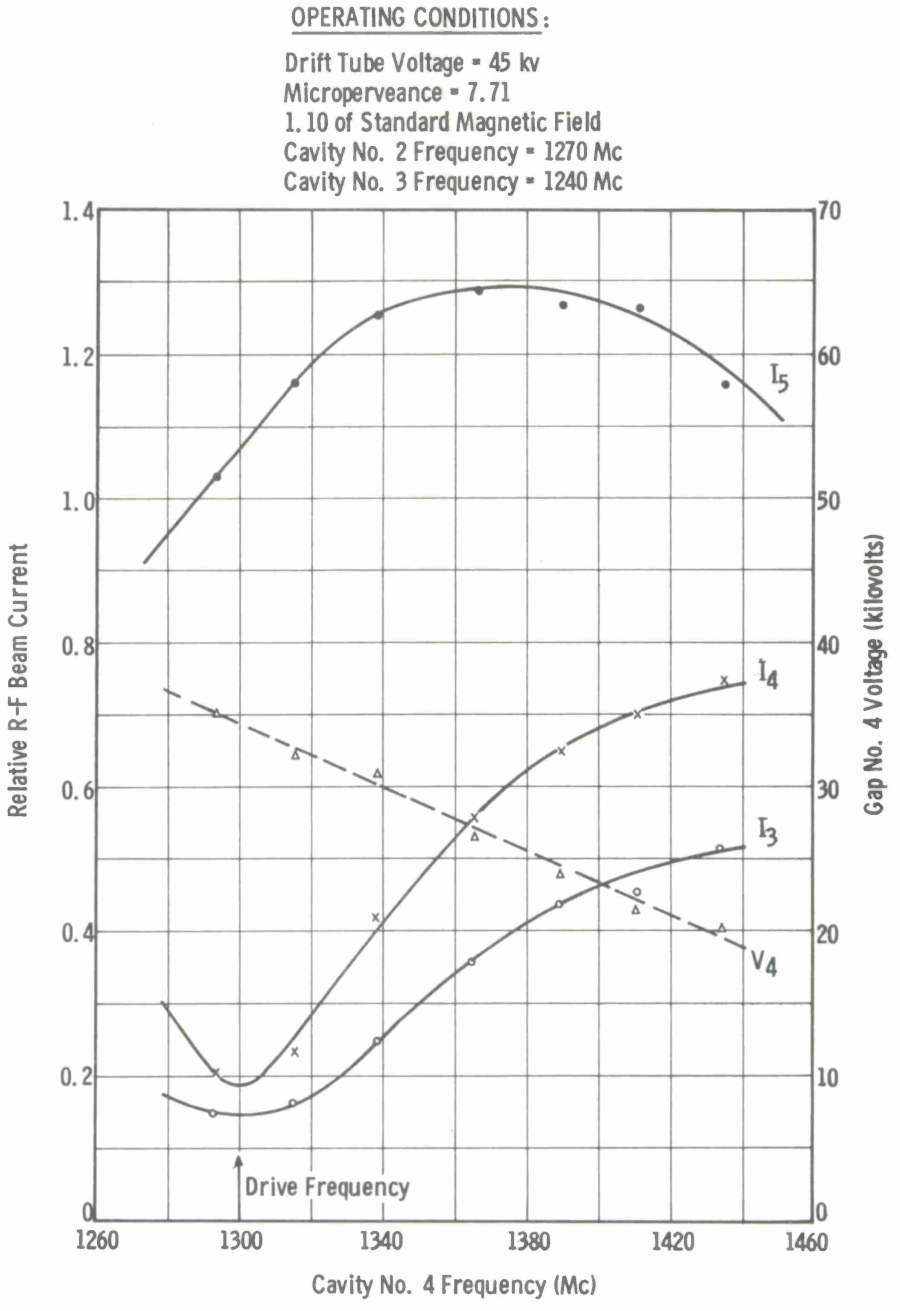

FIGURE 27
SATURATED CURRENT AT GAP NO. 5 VS TUNING OF CAVITY NO. 4 WITH CAVITIES NOS. 2 AND 3 TUNED LOW, DRIFT TUBE VOLTAGE = 45 KILOVOLTS, MICROPERVEANCE = 7.71

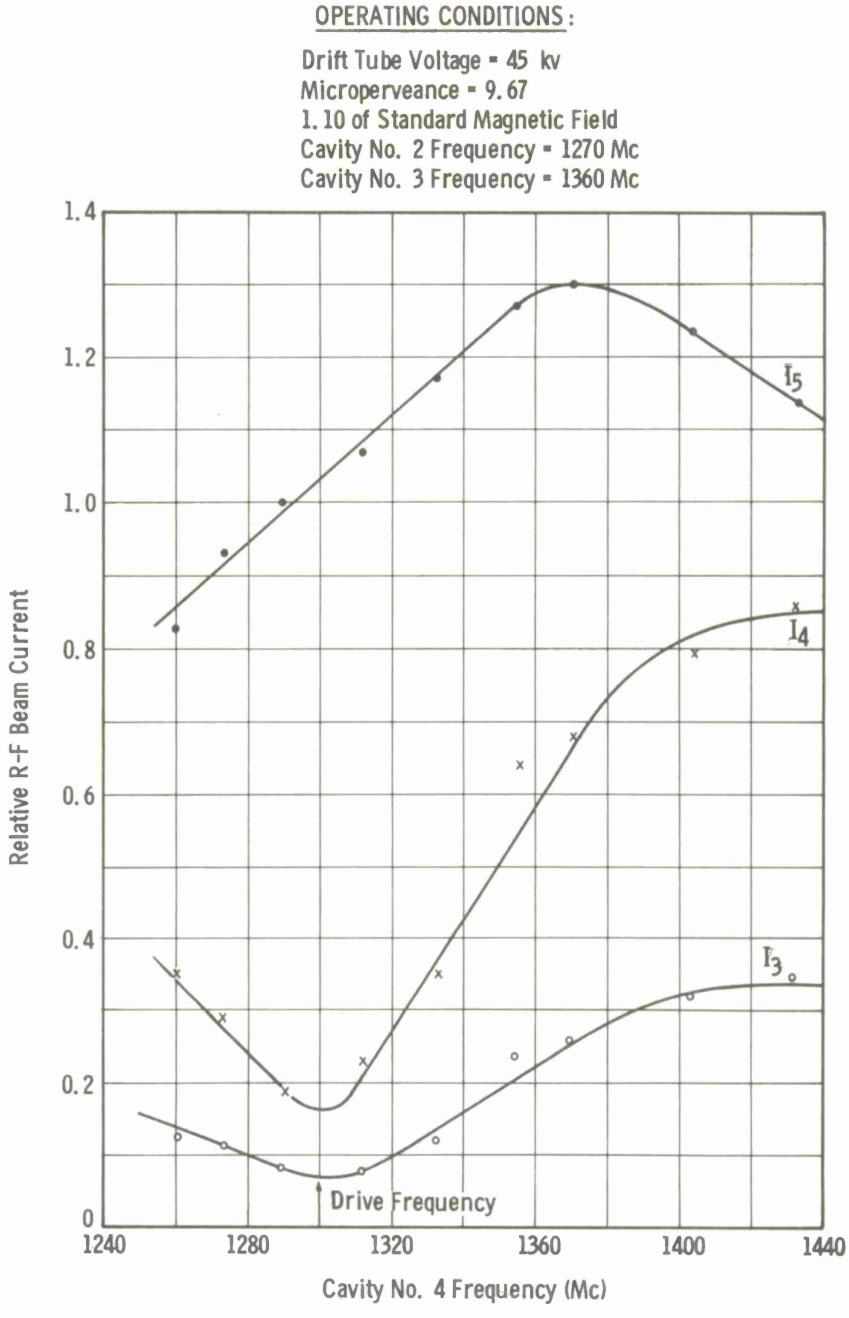

FIGURE 28
SATURATED CURRENT AT GAP NO. 5 VS TUNING OF CAVITY NO. 4 WITH CAVITY NO. 2 TUNED LOW AND CAVITY NO. 3 TUNED HIGH, DRIFT TUBE VOLTAGE = 45 KILOVOLTS, MICROPERVEANCE = 9.67

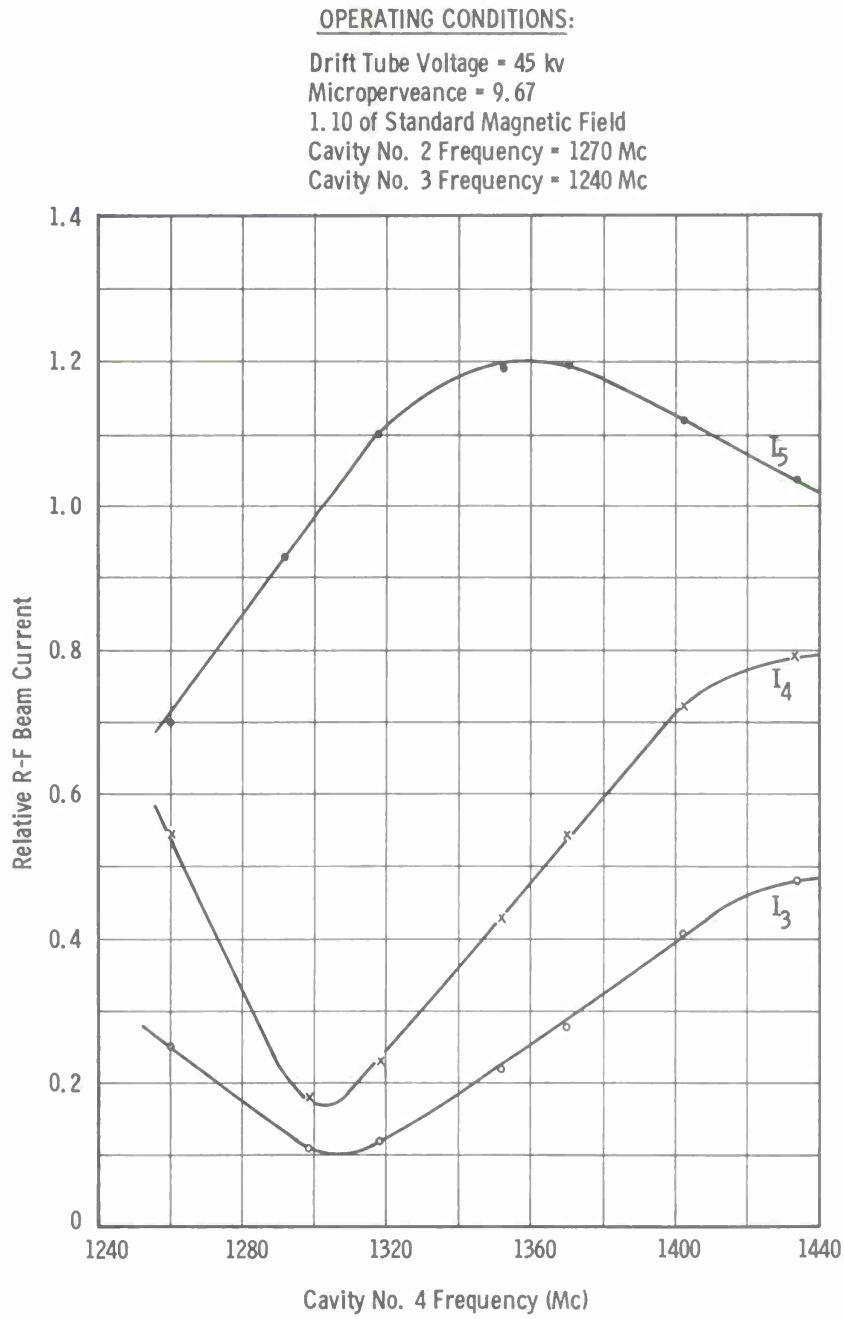

FIGURE 29
SATURATED CURRENT AT GAP NO. 5 VS TUNING OF CAVITY NO. 4 WITH CAVITY NO. 2 TUNED LOW AND CAVITY NO. 3 TUNED LOW, DRIFT TUBE VOLTAGE = 45 KILOVOLTS. MICROPERVEANCE = 9.67

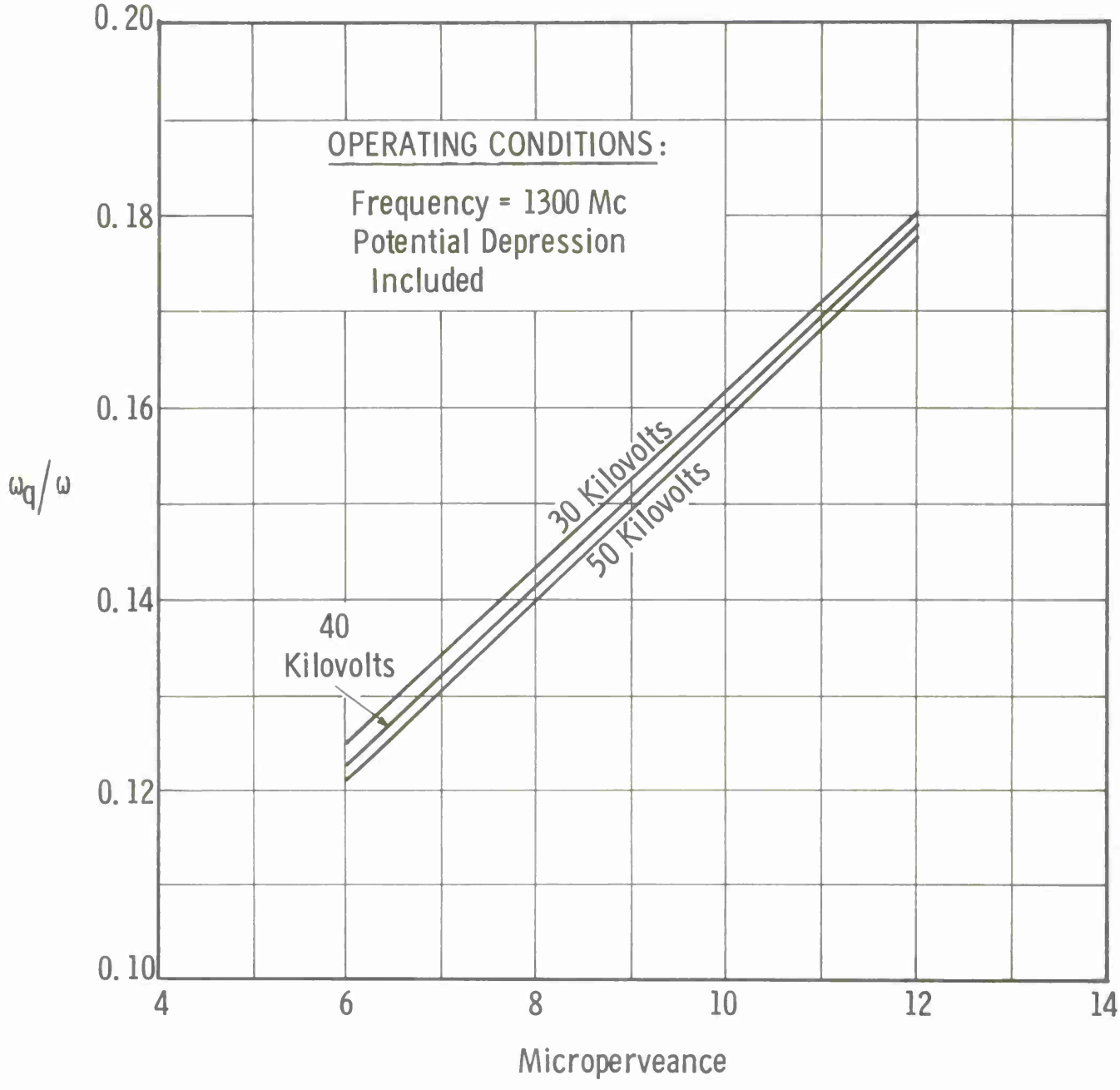

FIGURE 30
CALCULATED REDUCED PLASMA FREQUENCY VS PERVEANCE
FOR CONFINED FLOW BEAM GEOMETRY

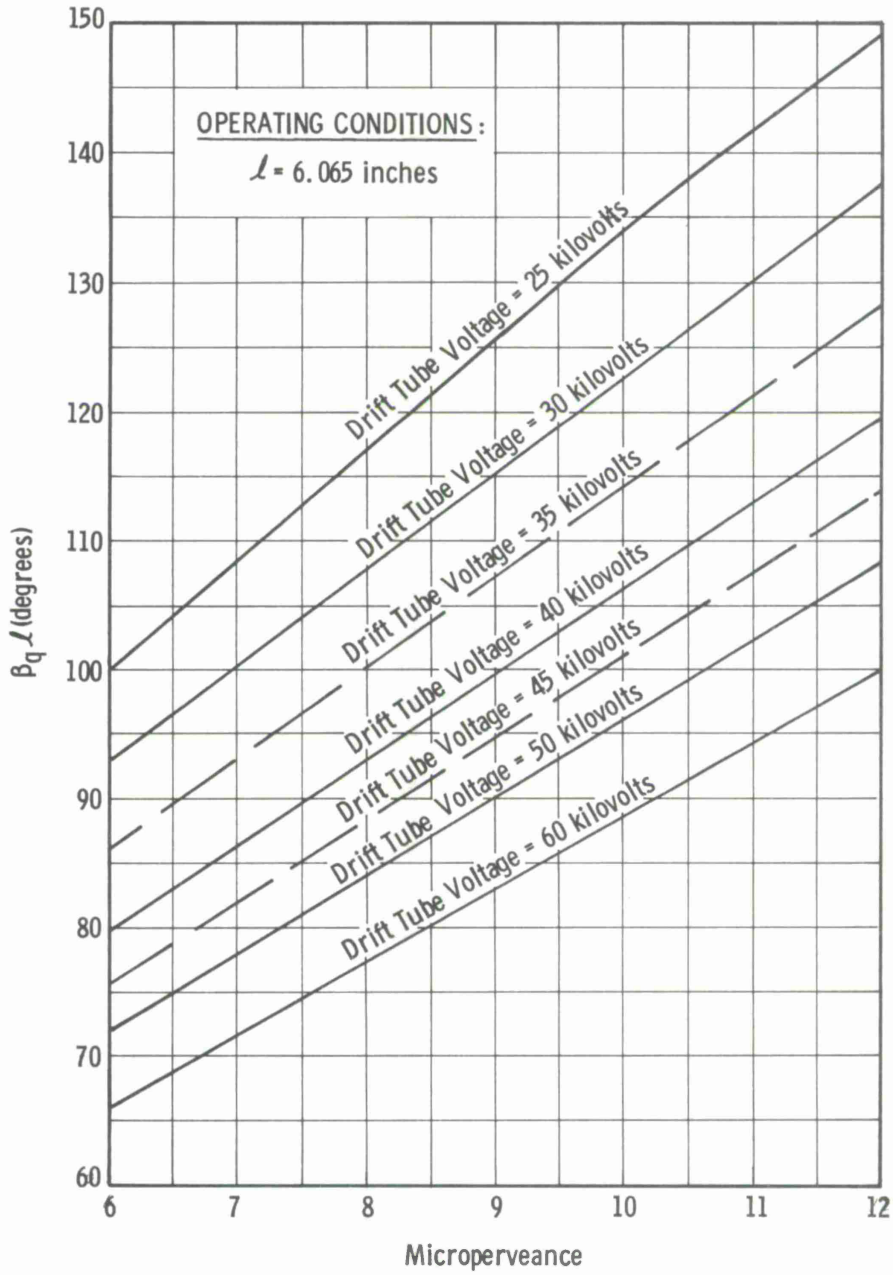

FIGURE 31
CALCULATED REDUCED PLASMA DRIFT ANGLE VS PERVEANCE

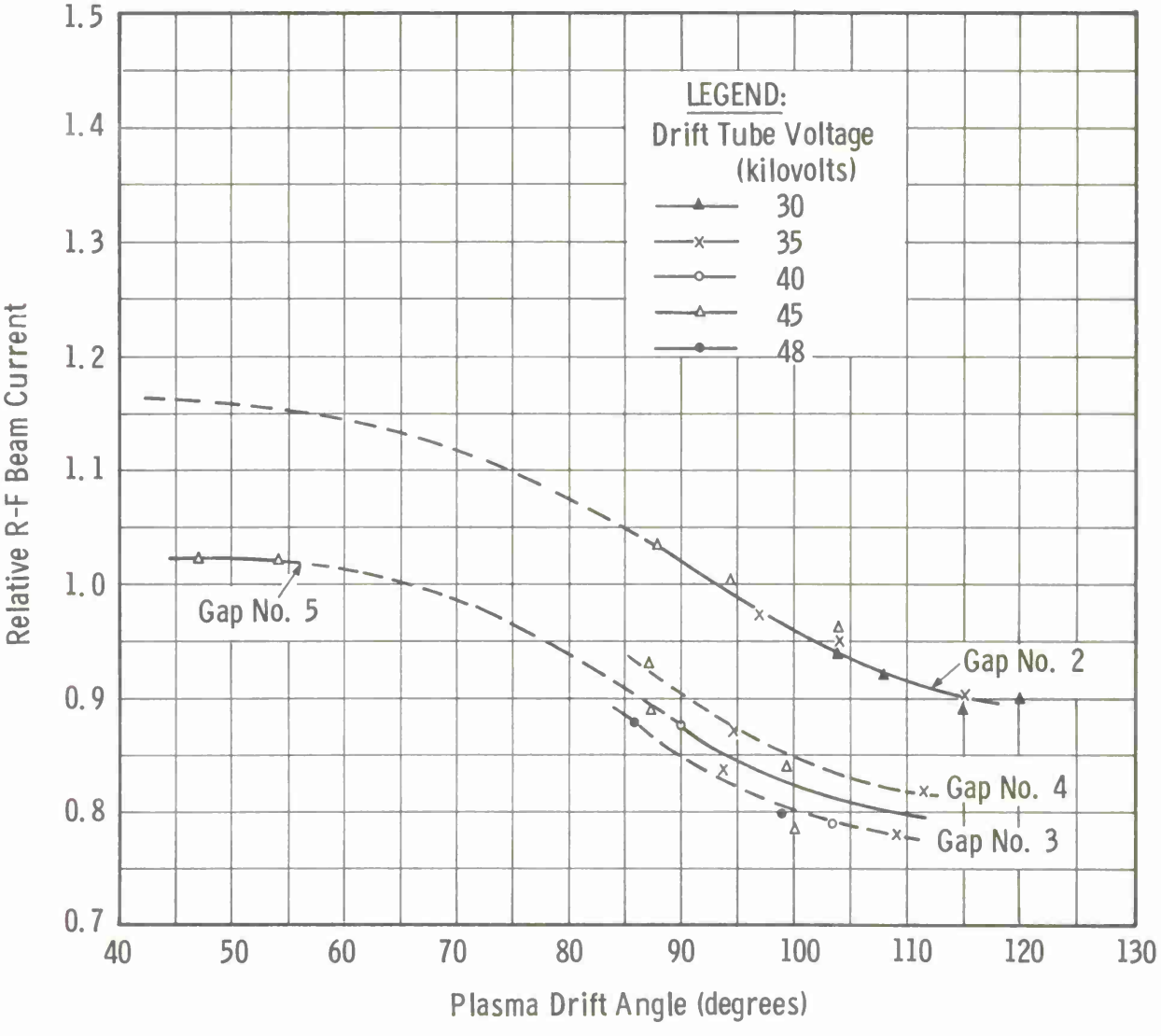

FIGURE 32
SATURATED CURRENT AT GAPS NOS. 2, 3, 4 AND 5 VS PLASMA DRIFT ANGLE FOR SYNCHRONOUSLY TUNED PENULTIMATE CAVITY

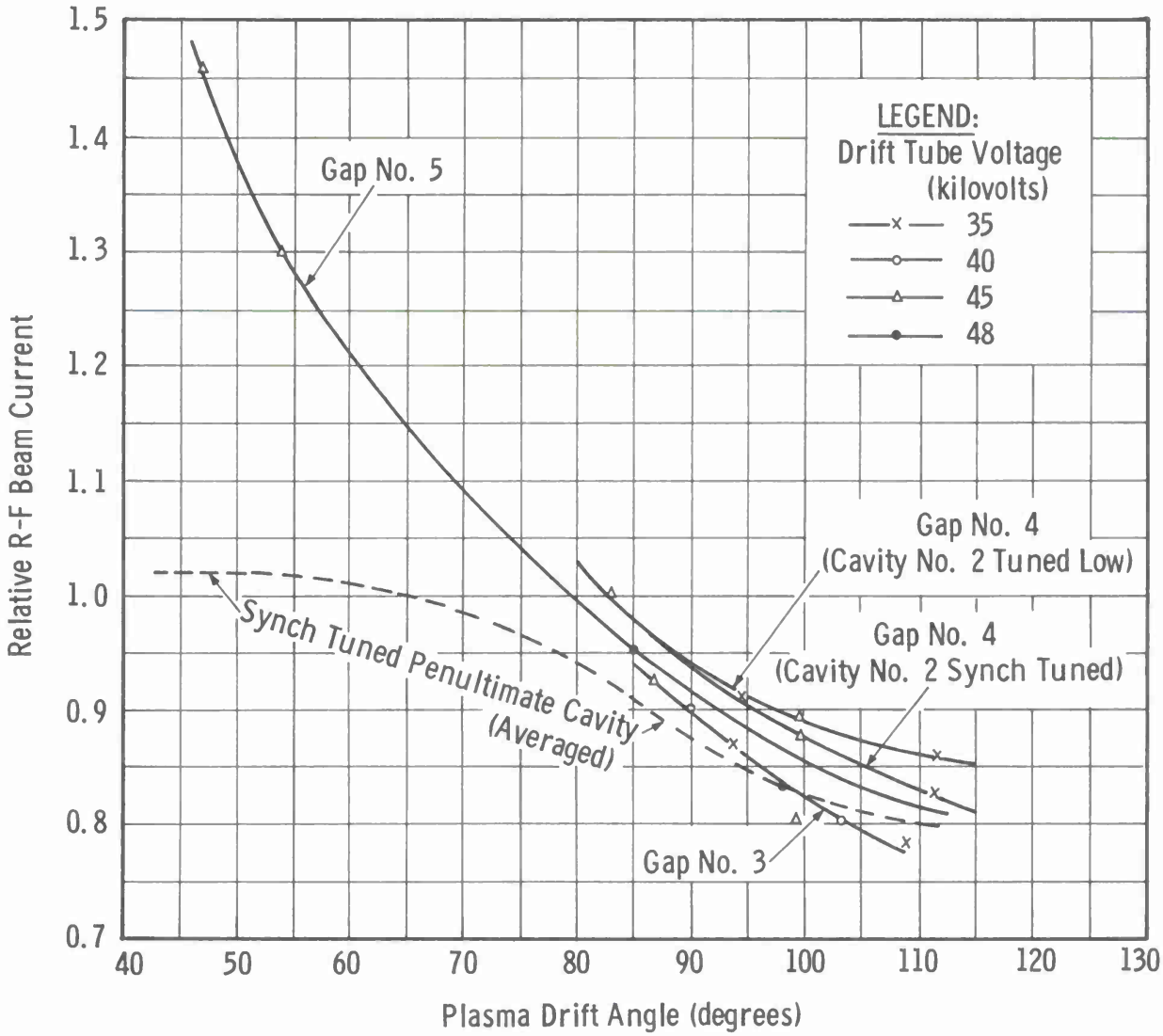

FIGURE 33
SATURATED CURRENT AT GAPS NOS. 3, 4 AND 5 VS PLASMA DRIFT ANGLE FOR OPTIMIZED TUNING OF PENULTIMATE CAVITY

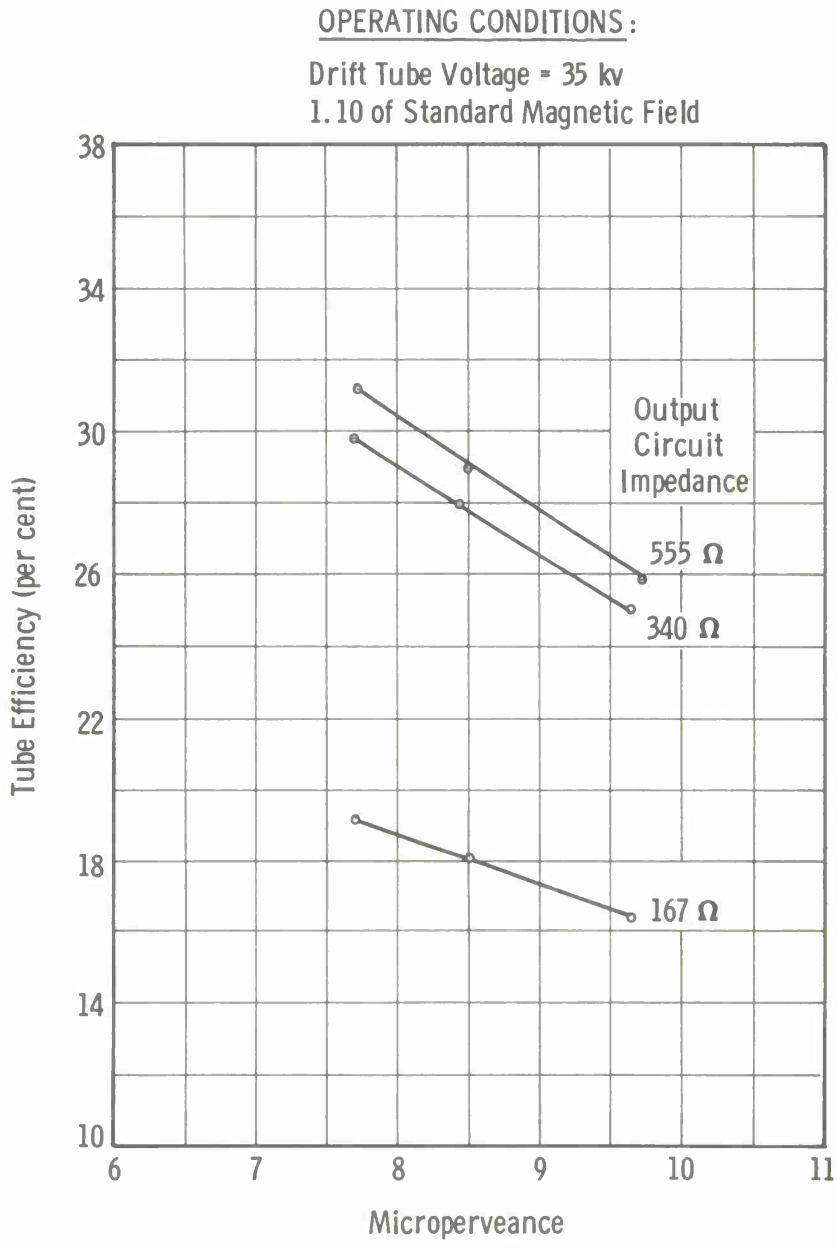

FIGURE 34
TUBE EFFICIENCY VS PERVEANCE,
DRIFT TUBE VOLTAGE = 35 KILOVOLTS

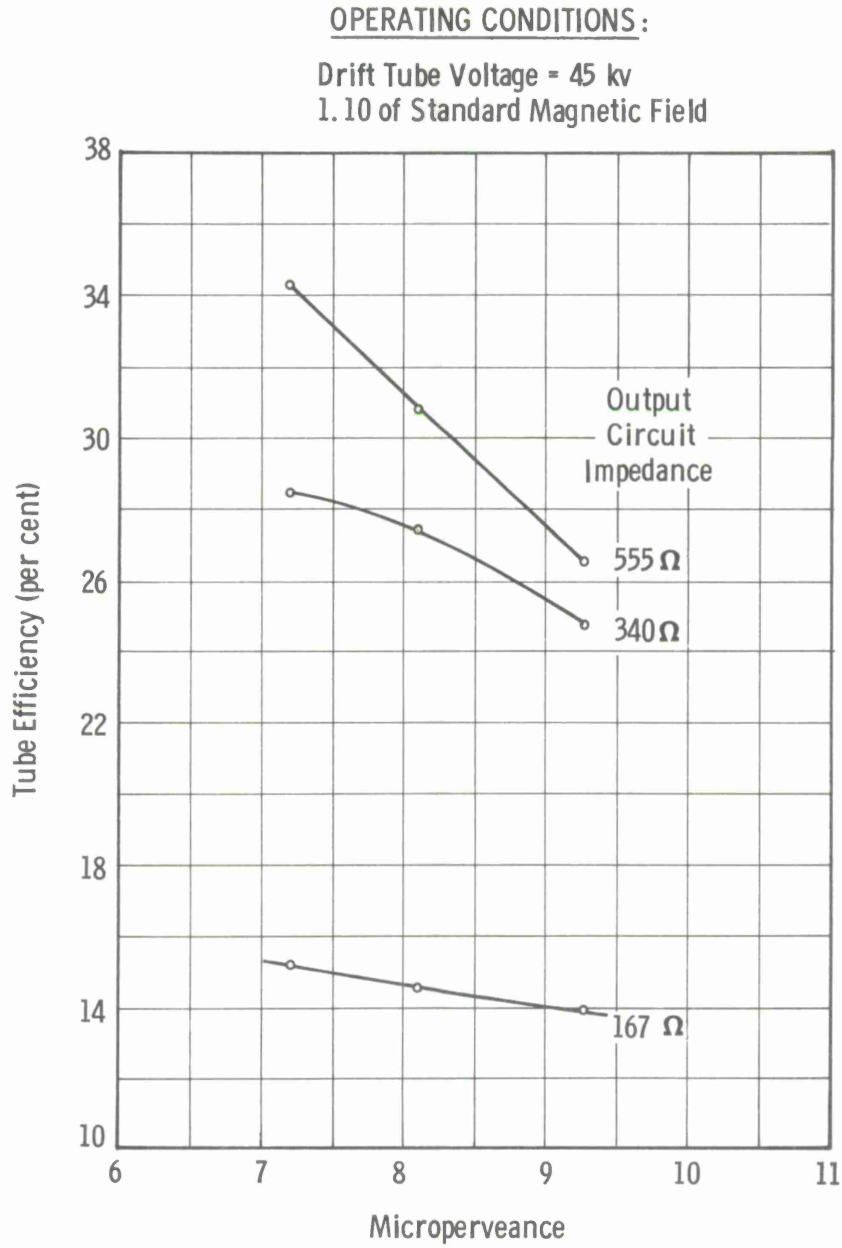

FIGURE 35
TUBE EFFICIENCY VS PERVEANCE,
DRIFT TUBE VOLTAGE = 45 KILOVOLTS

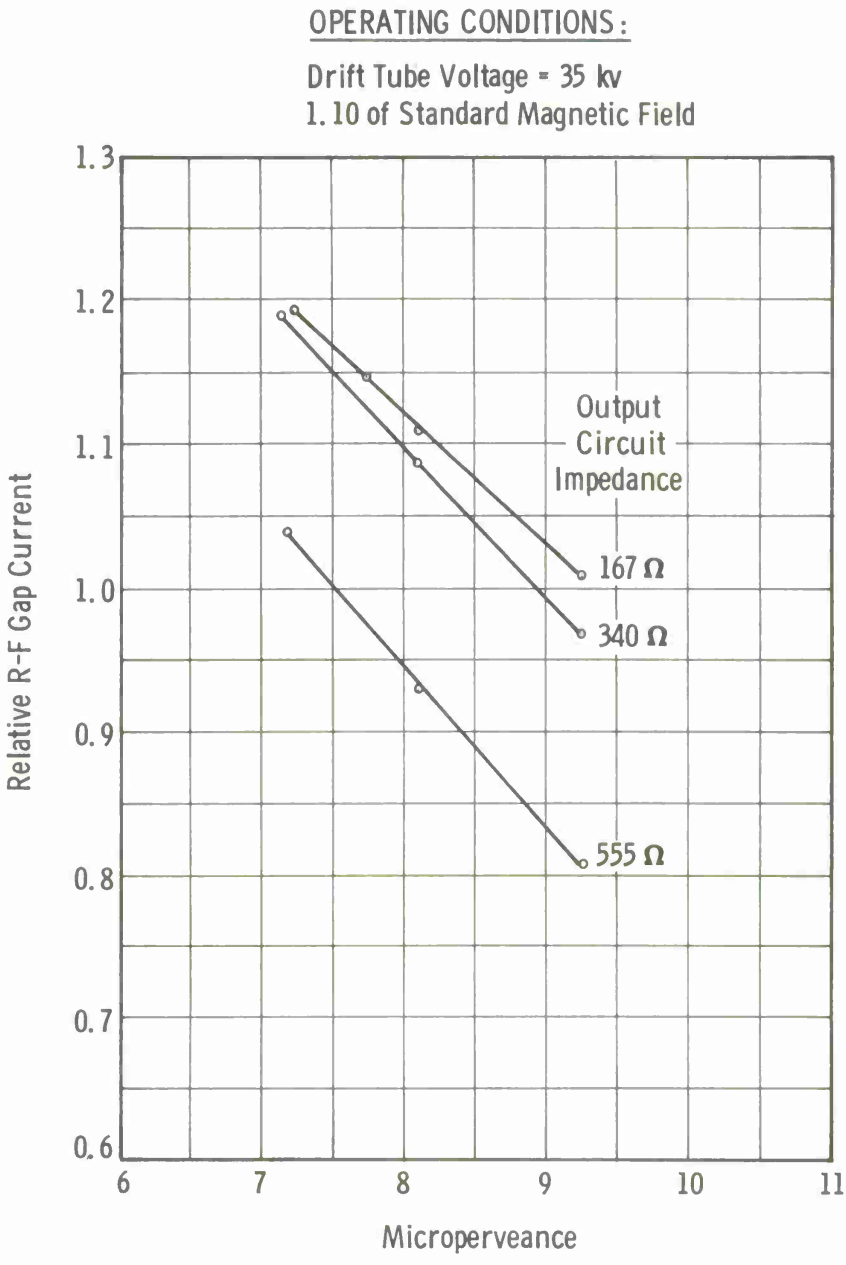

FIGURE 36
SATURATED CURRENT AT GAP NO. 6 VS PERVEANCE,
DRIFT TUBE VOLTAGE = 35 KILOVOLTS

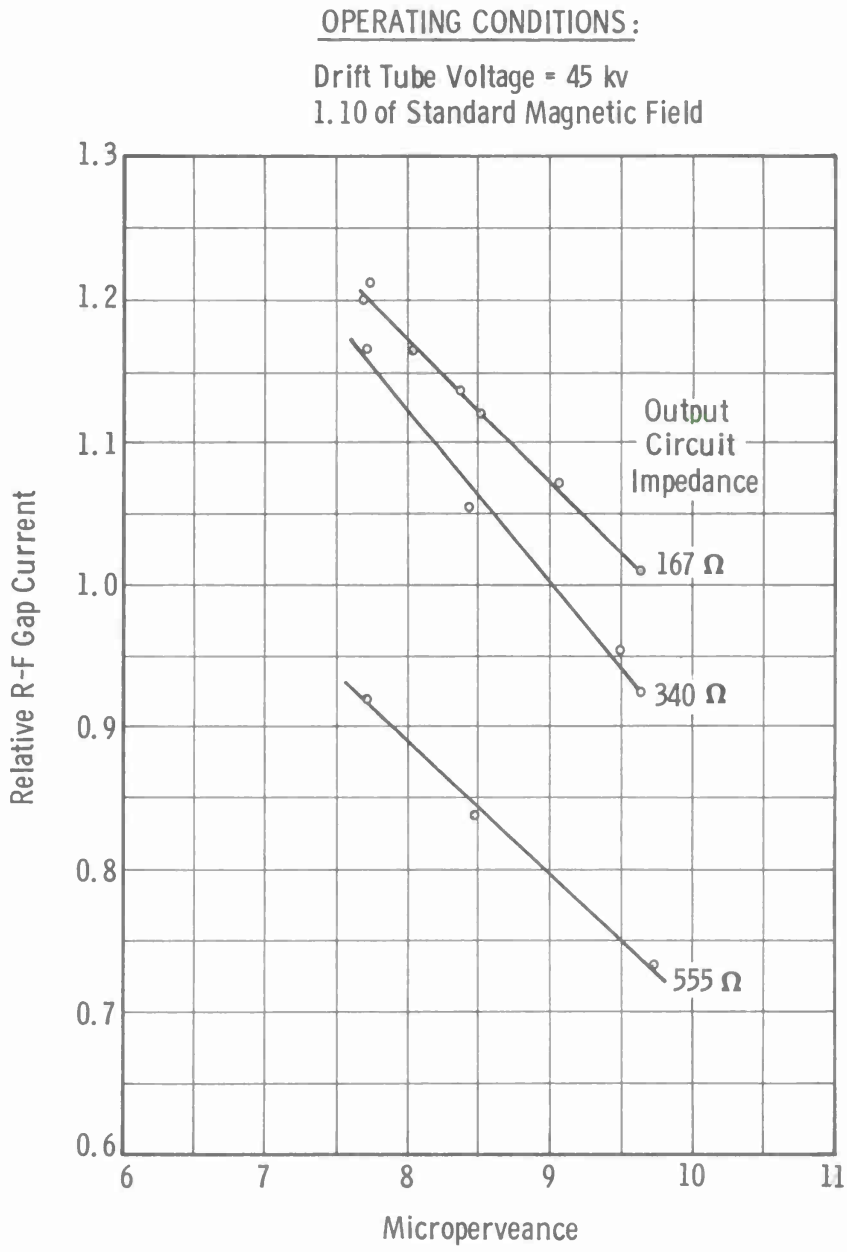

FIGURE 37
SATURATED CURRENT AT GAP NO. 6 VS PERVEANCE,
DRIFT TUBE VOLTAGE = 45 KILOVOLTS

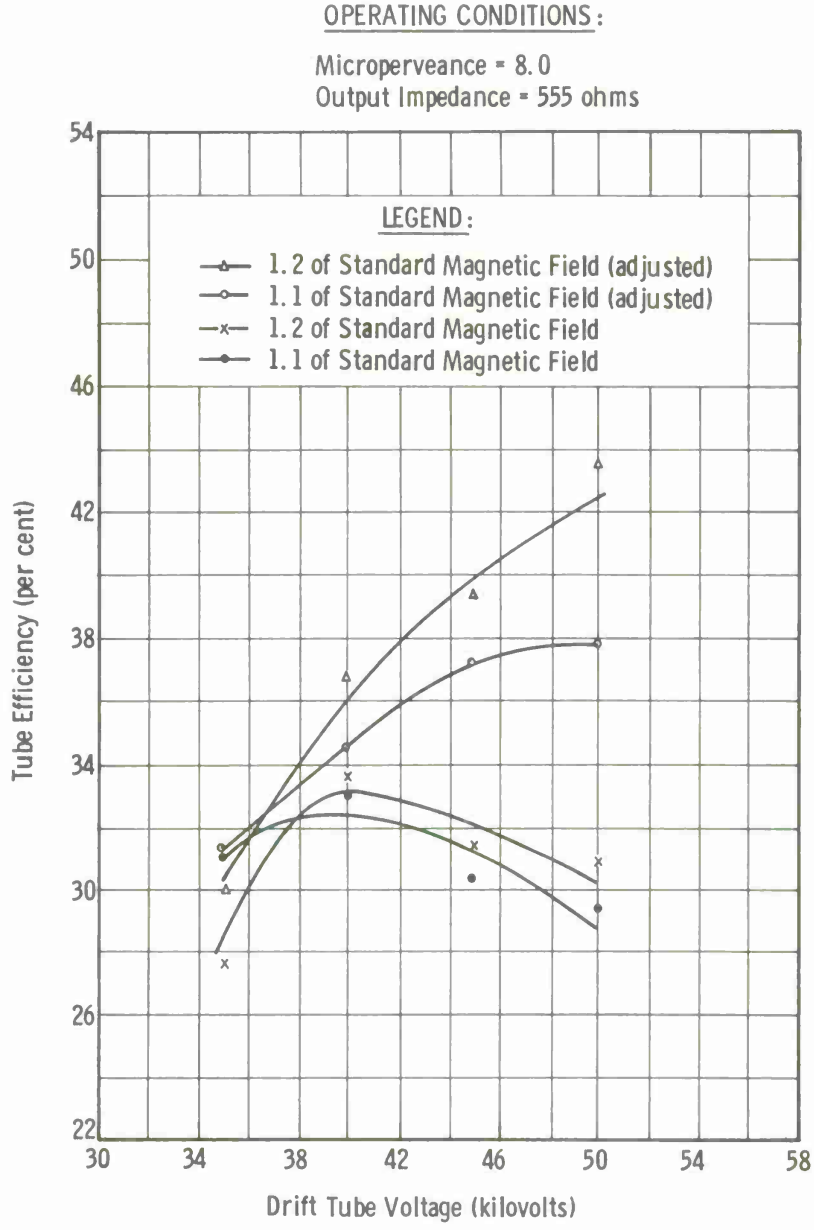

FIGURE 38
EFFICIENCY VS TUBE VOLTAGE AT A FIXED PERVEANCE AND FOR A HIGH OUTPUT IMPEDANCE

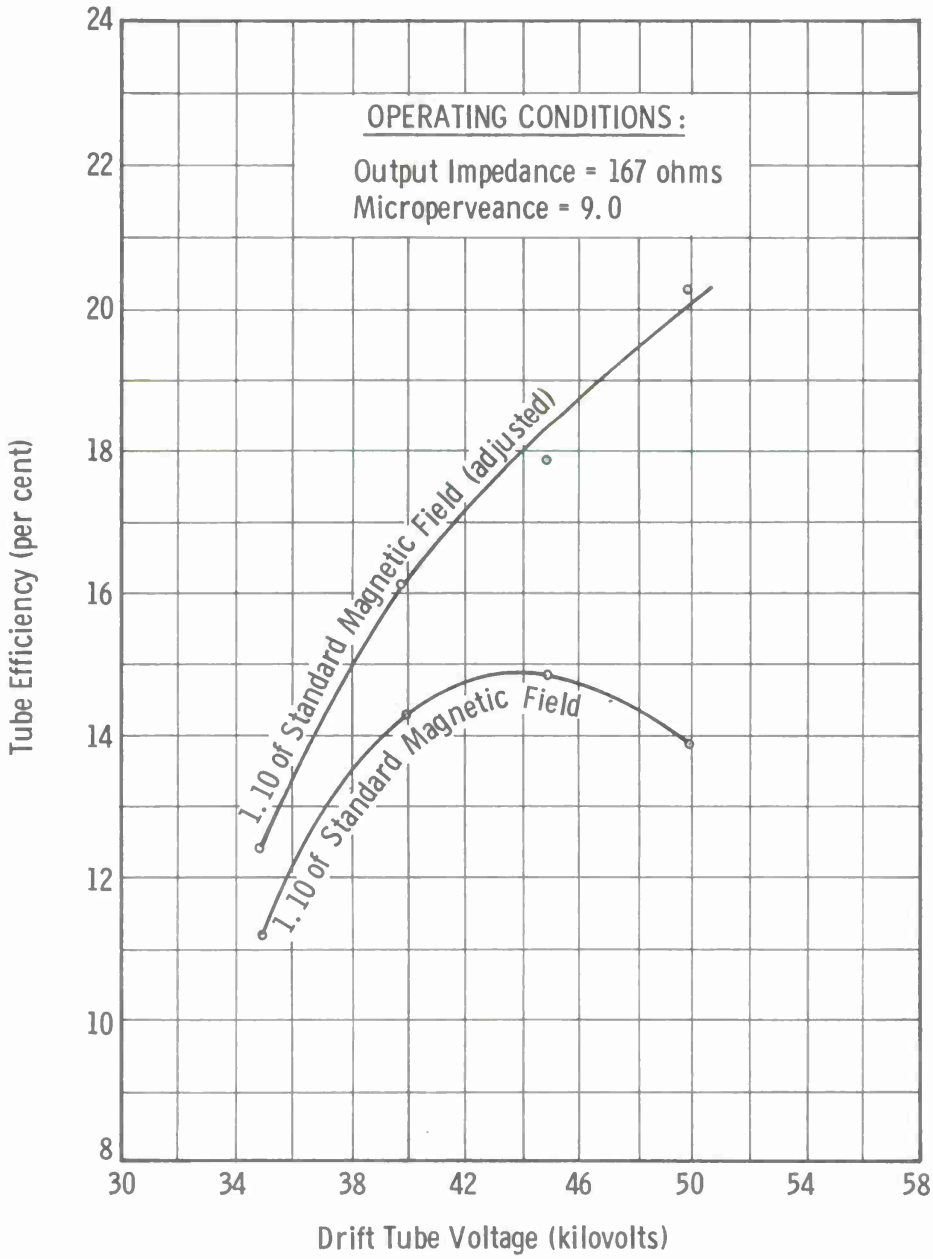

FIGURE 39
EFFICIENCY VS TUBE VOLTAGE AT A FIXED PERVEANCE
AND FOR A LOW OUTPUT IMPEDANCE

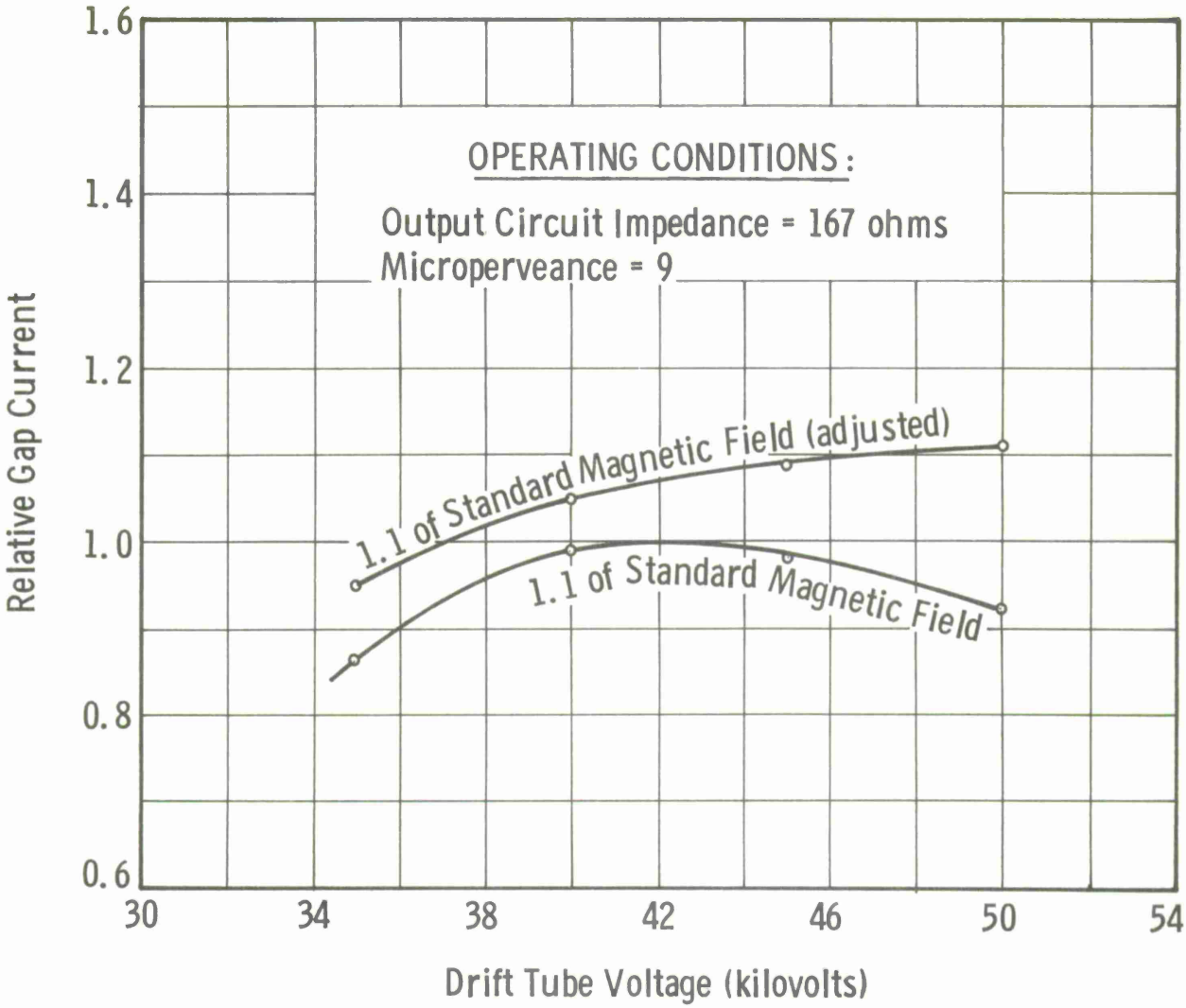

FIGURE 40
SATURATED CURRENT AT GAP NO. 6 VS DRIFT TUBE VOLTAGE
(FIXED PERVEANCE AND LOW OUTPUT IMPEDANCE)

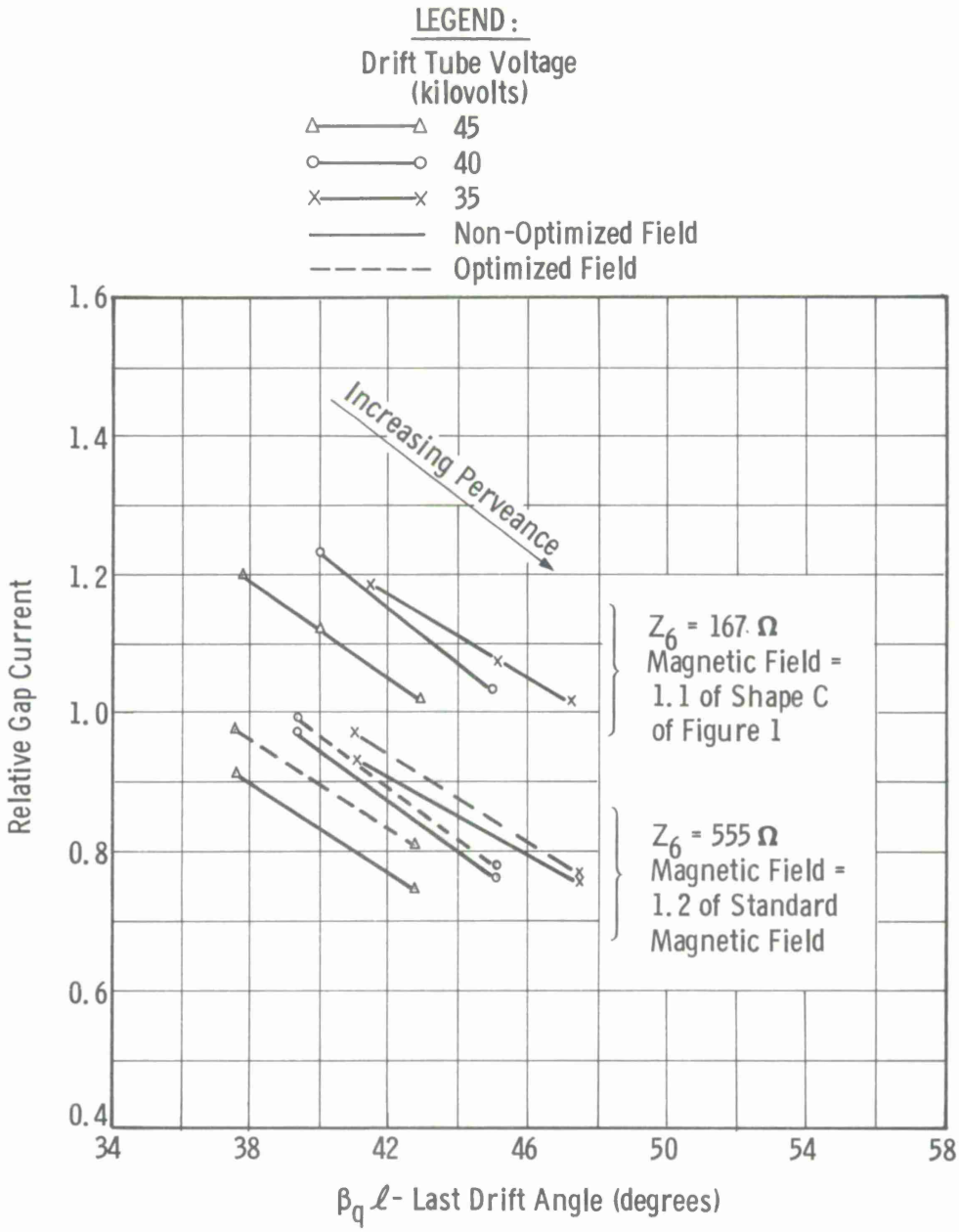

FIGURE 41
SATURATED CURRENT AT GAP NO. 6 VS PLASMA DRIFT ANGLE
FOR DIFFERENT OUTPUT IMPEDANCES AND DRIFT TUBE VOLTAGES

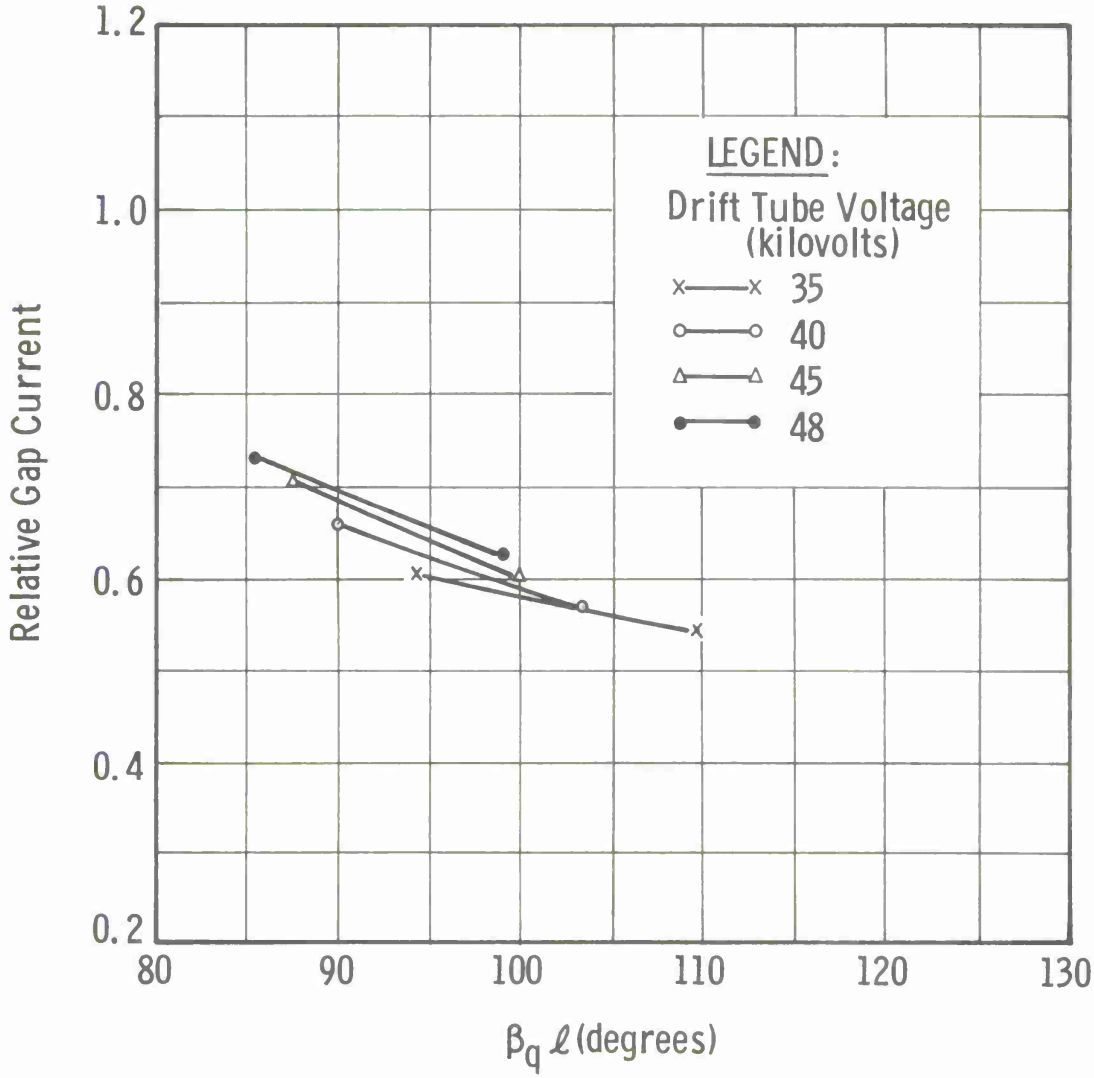

FIGURE 42
SATURATED CURRENT AT GAP NO. 3 VS PLASMA DRIFT ANGLE
FOR DIFFERENT TUBE VOLTAGES

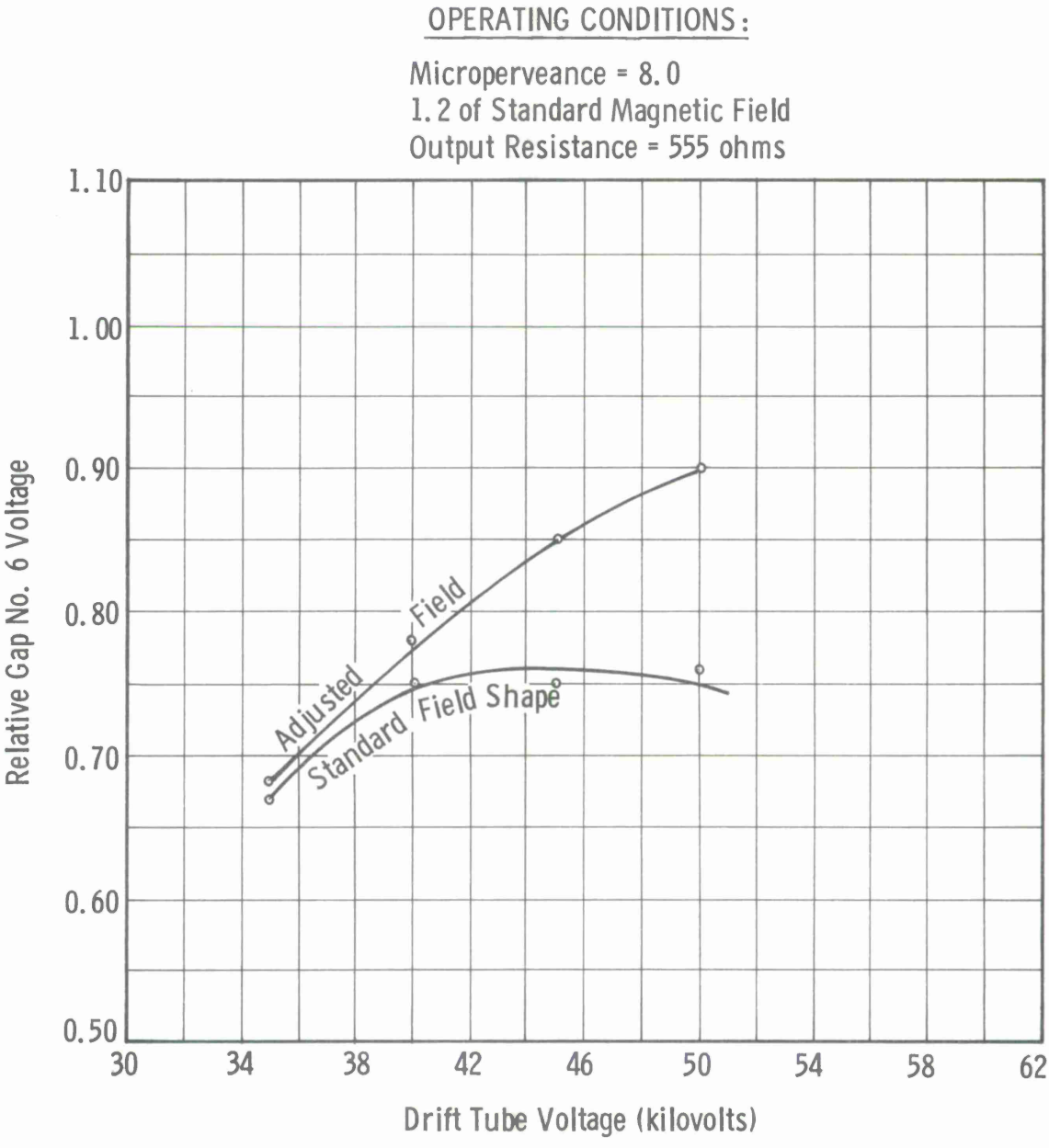

FIGURE 43
R-F VOLTAGE AT GAP NO. 6 VS BEAM VOLTAGE AT SATURATION

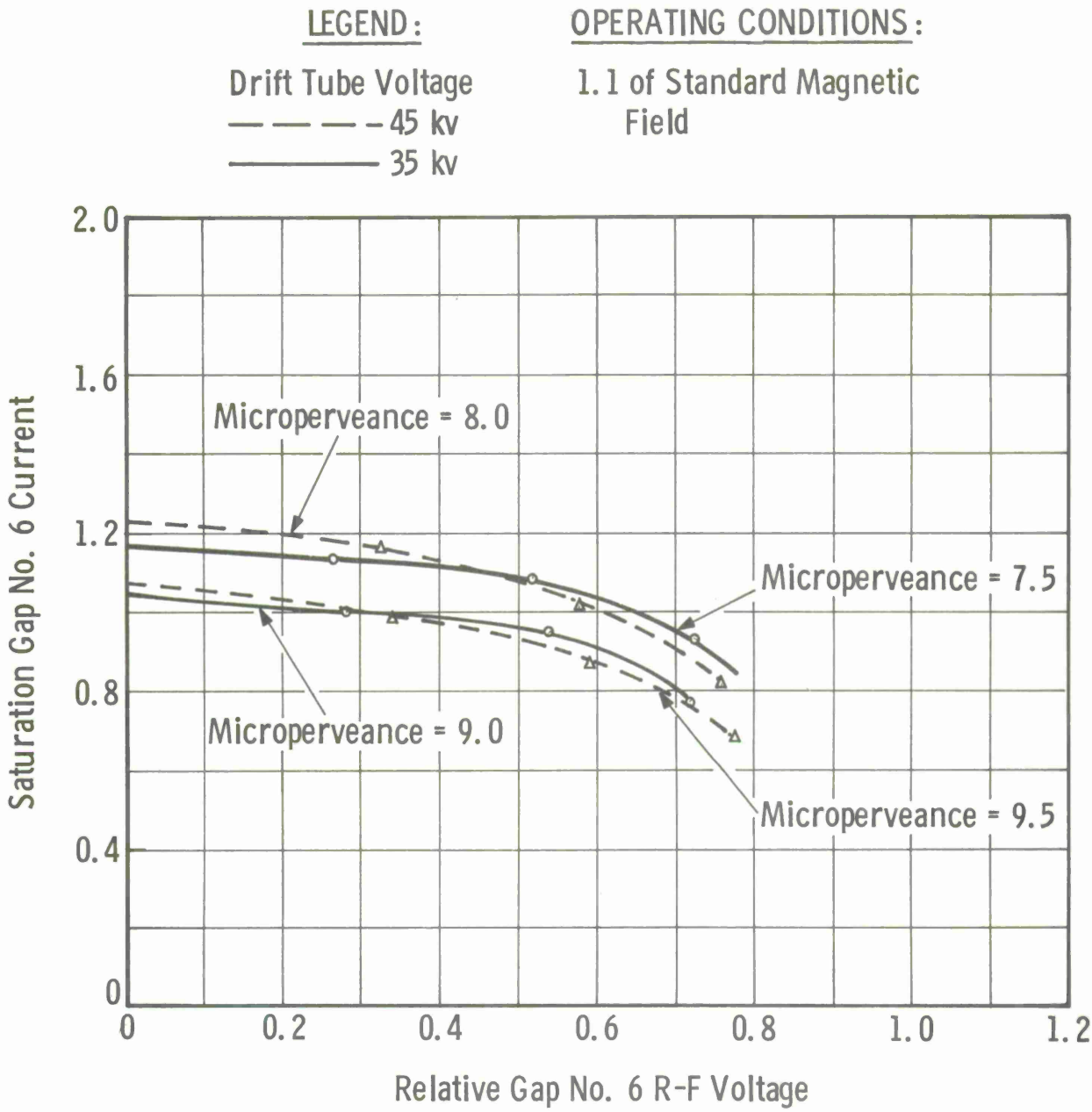

FIGURE 44
SATURATED CURRENT AT GAP NO. 6 VS GAP VOLTAGE

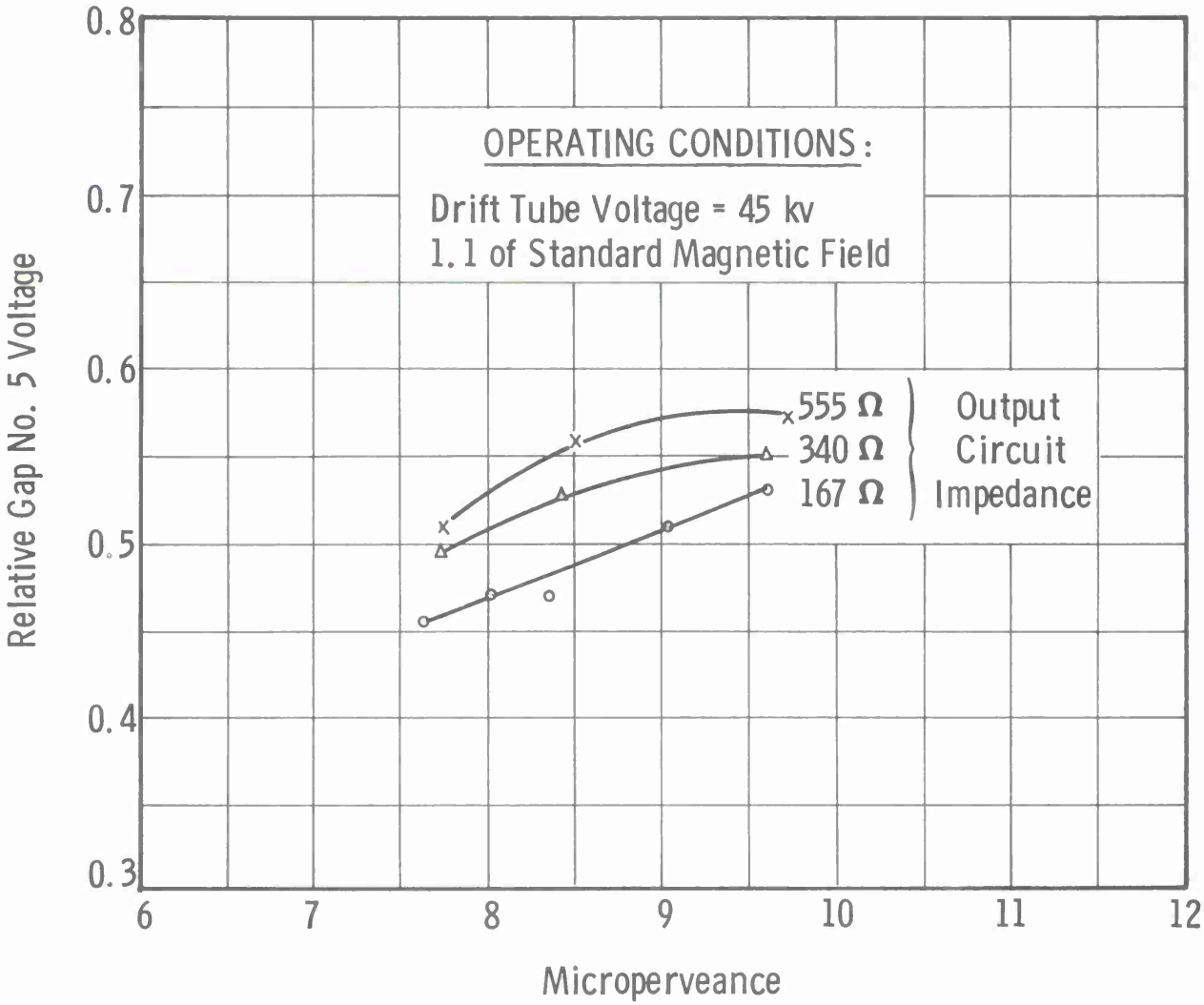

FIGURE 45
R-F VOLTAGE AT GAP NO. 5 REQUIRED TO SATURATE OUTPUT
AT GAP NO. 6 VS PERVEANCE

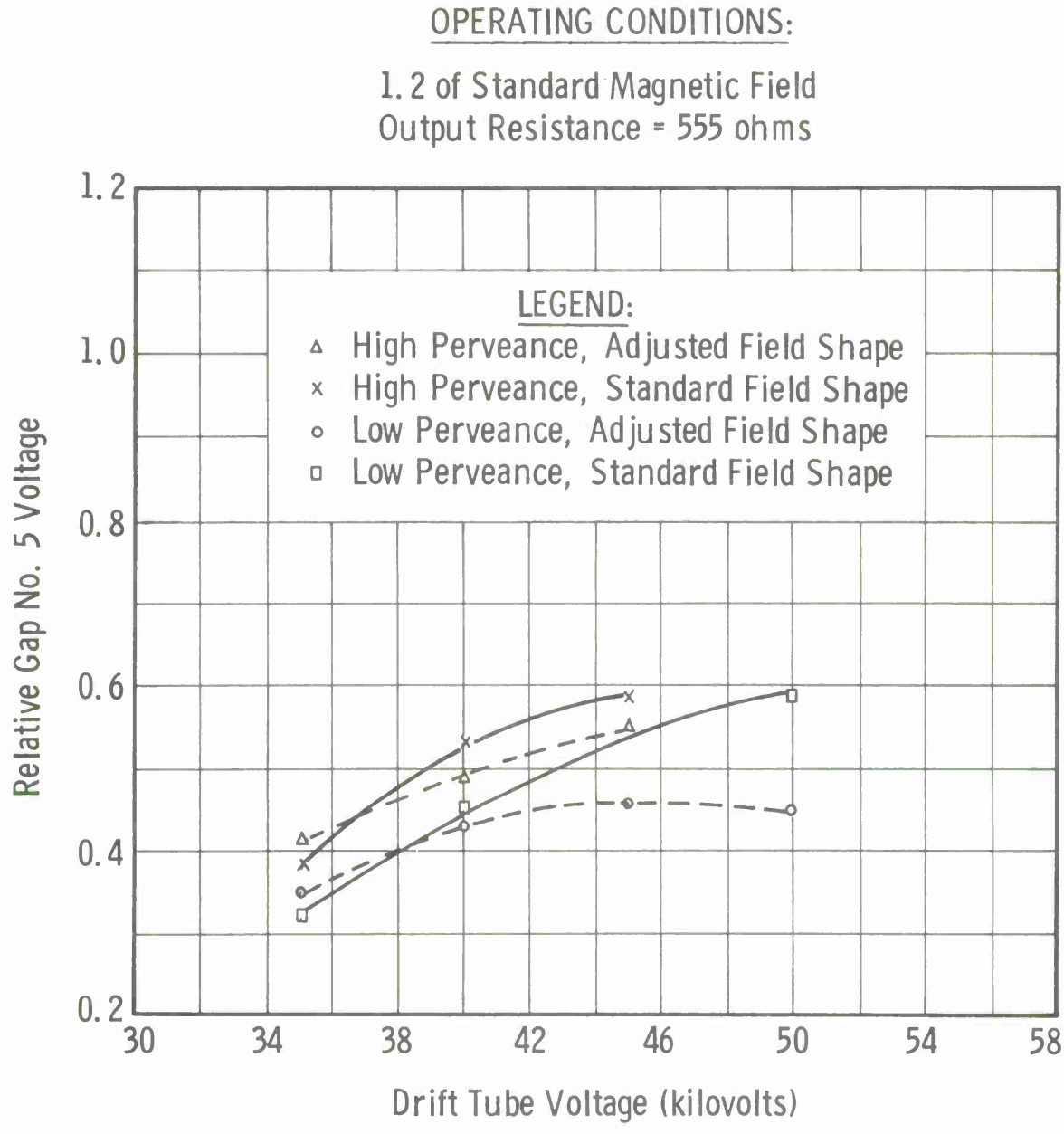

FIGURE 46
R-F VOLTAGE AT GAP NO. 5 REQUIRED TO SATURATE OUTPUT
AT GAP NO. 6 VS DRIFT TUBE VOLTAGE

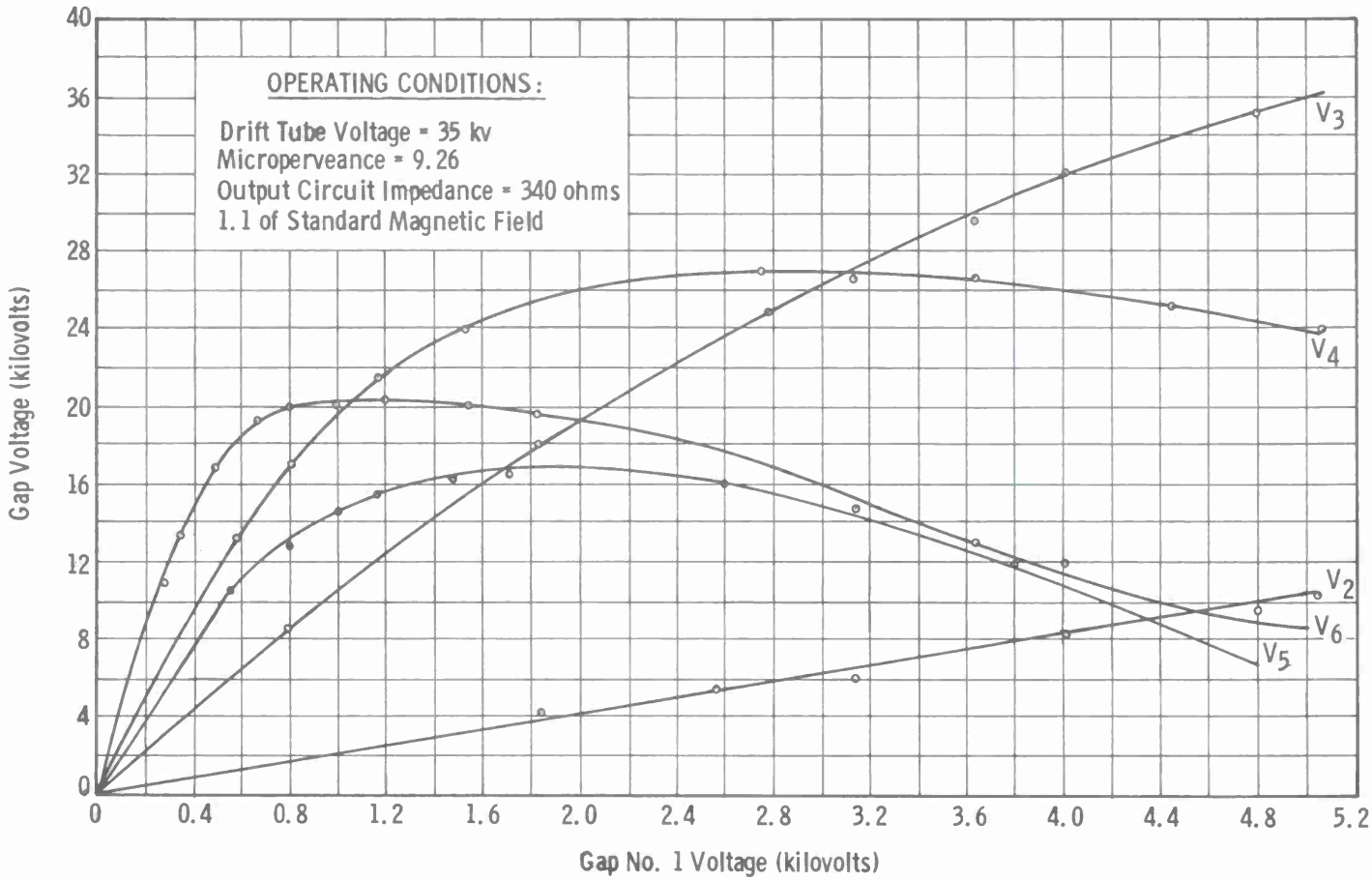

FIGURE 47
R-F VOLTAGE AT ALL GAPS VS DRIVE,
DRIFT TUBE VOLTAGE = 35 KILOVOLTS,
MICROPERVEANCE = 9.26, MEDIUM OUTPUT IMPEDANCE

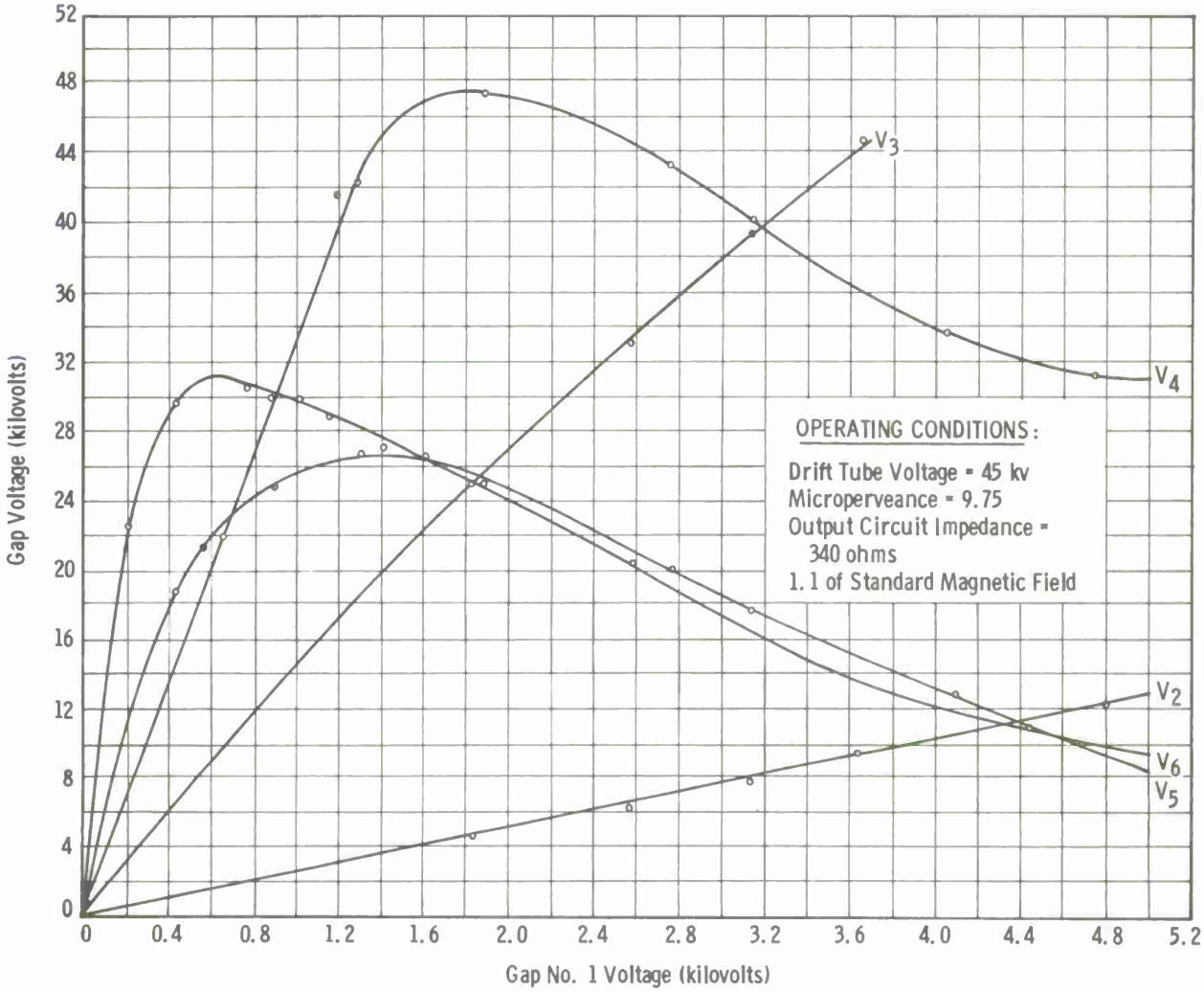

FIGURE 48
R-F VOLTAGES AT ALL GAPS VS DRIVE,
DRIFT TUBE VOLTAGE = 45 KILOVOLTS,
MICROPERVEANCE = 9.75, MEDIUM OUTPUT IMPEDANCE

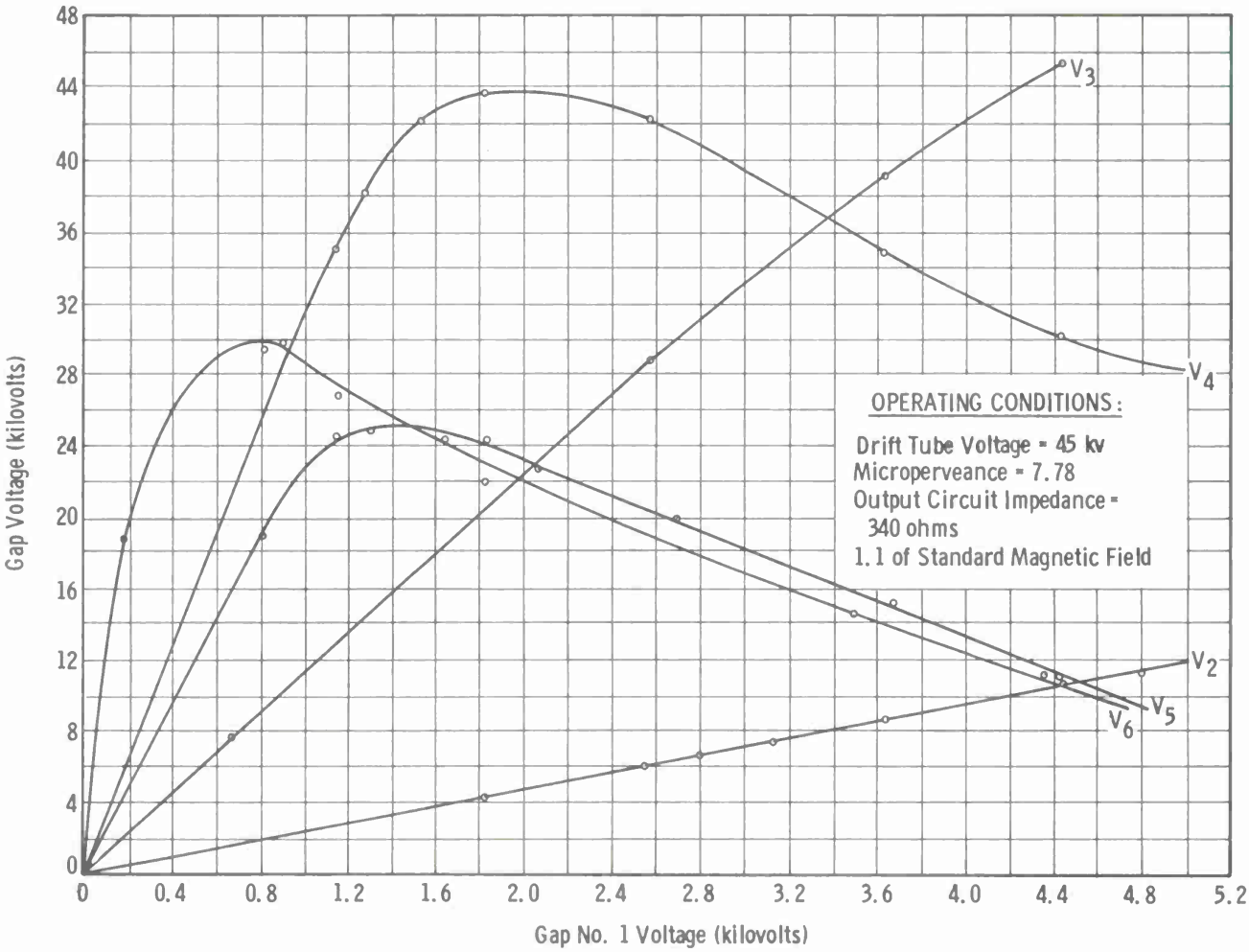

FIGURE 49
R-F VOLTAGES AT ALL GAPS VS DRIVE,
DRIFT TUBE VOLTAGE = 45 KILOVOLTS,
MICROPERVEANCE = 7.78, MEDIUM OUTPUT IMPEDANCE

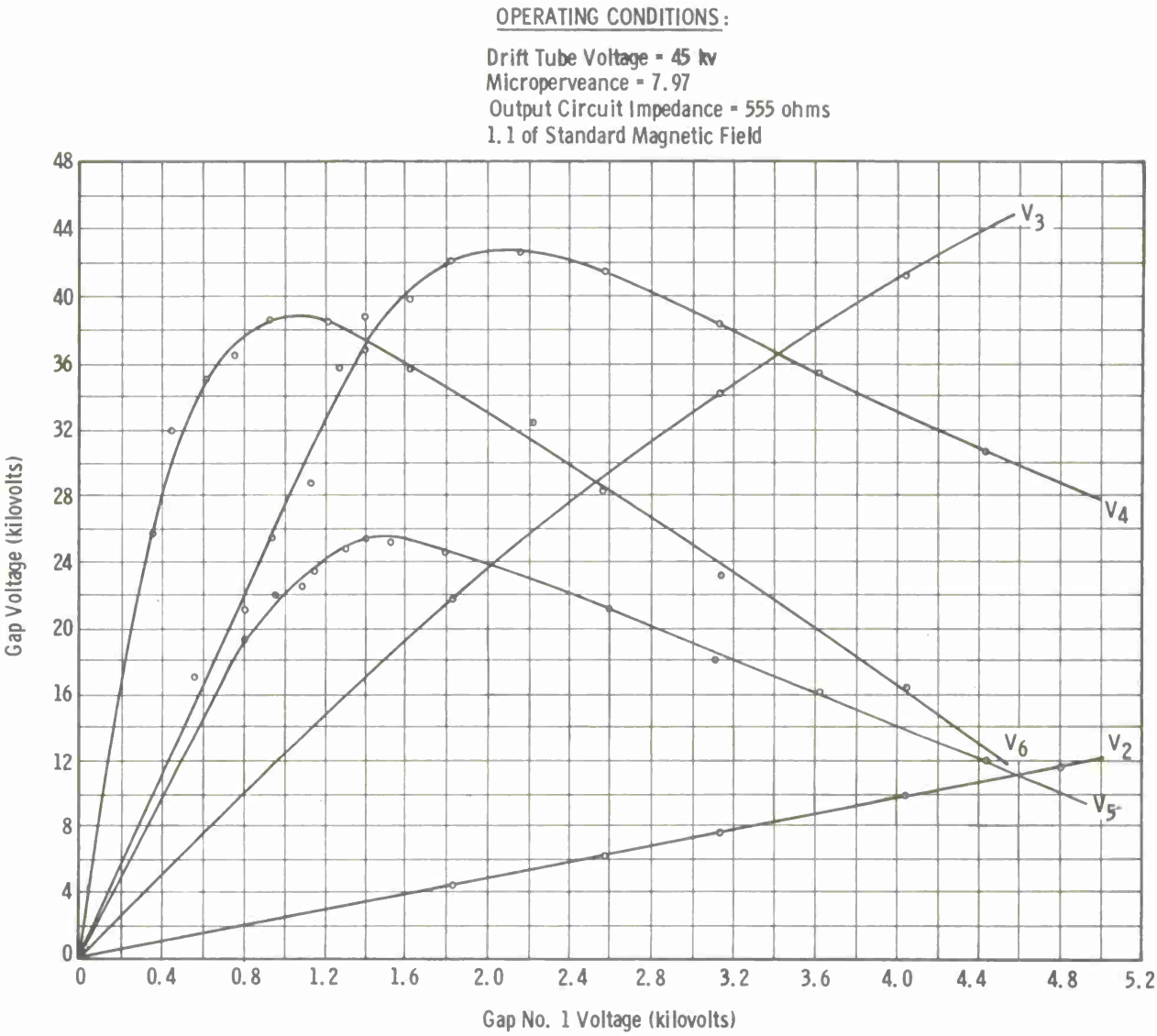

FIGURE 50
R-F VOLTAGES AT ALL GAPS VS DRIVE,
DRIFT TUBE VOLTAGE = 45 KILOVOLTS,
MICROPERVEANCE = 7.97, HIGH OUTPUT IMPEDANCE

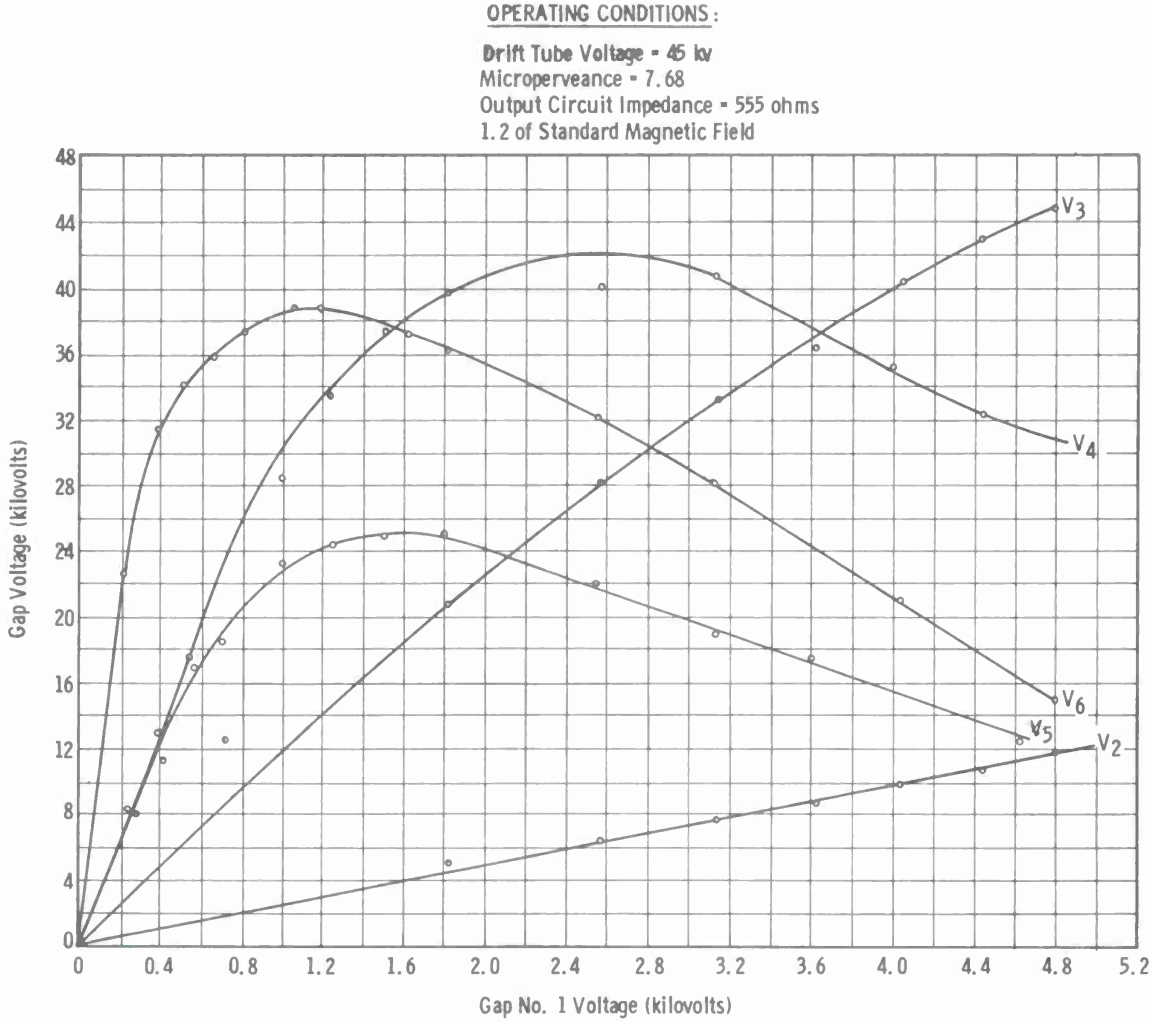

FIGURE 51
R-F VOLTAGES AT ALL GAPS VS DRIVE,
DRIFT TUBE VOLTAGE = 45 KILOVOLTS,
MICROPERVEANCE = 7.68, HIGH OUTPUT IMPEDANCE

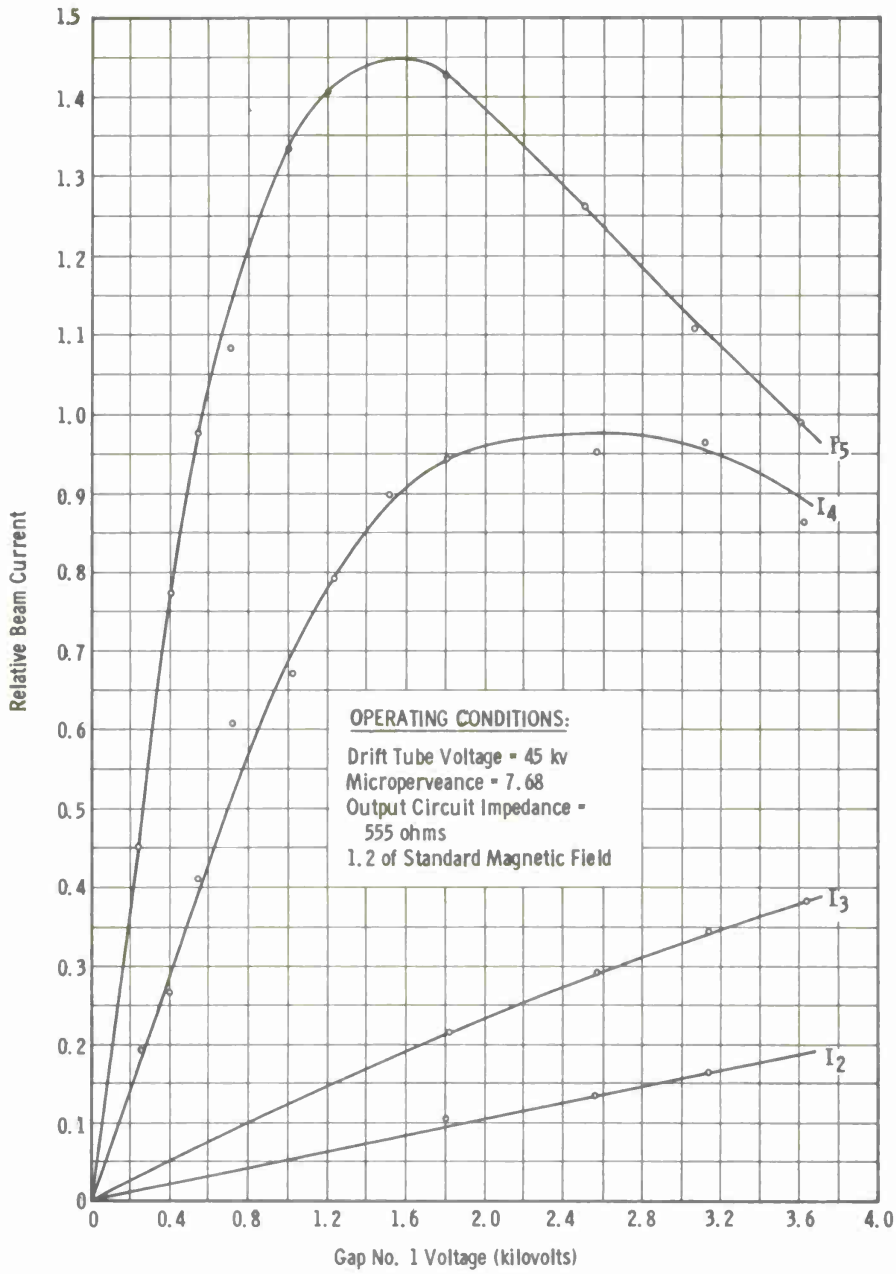

FIGURE 52
R-F CURRENTS AT ALL GAPS VS DRIVE
(CONDITIONS OF FIGURE 51)

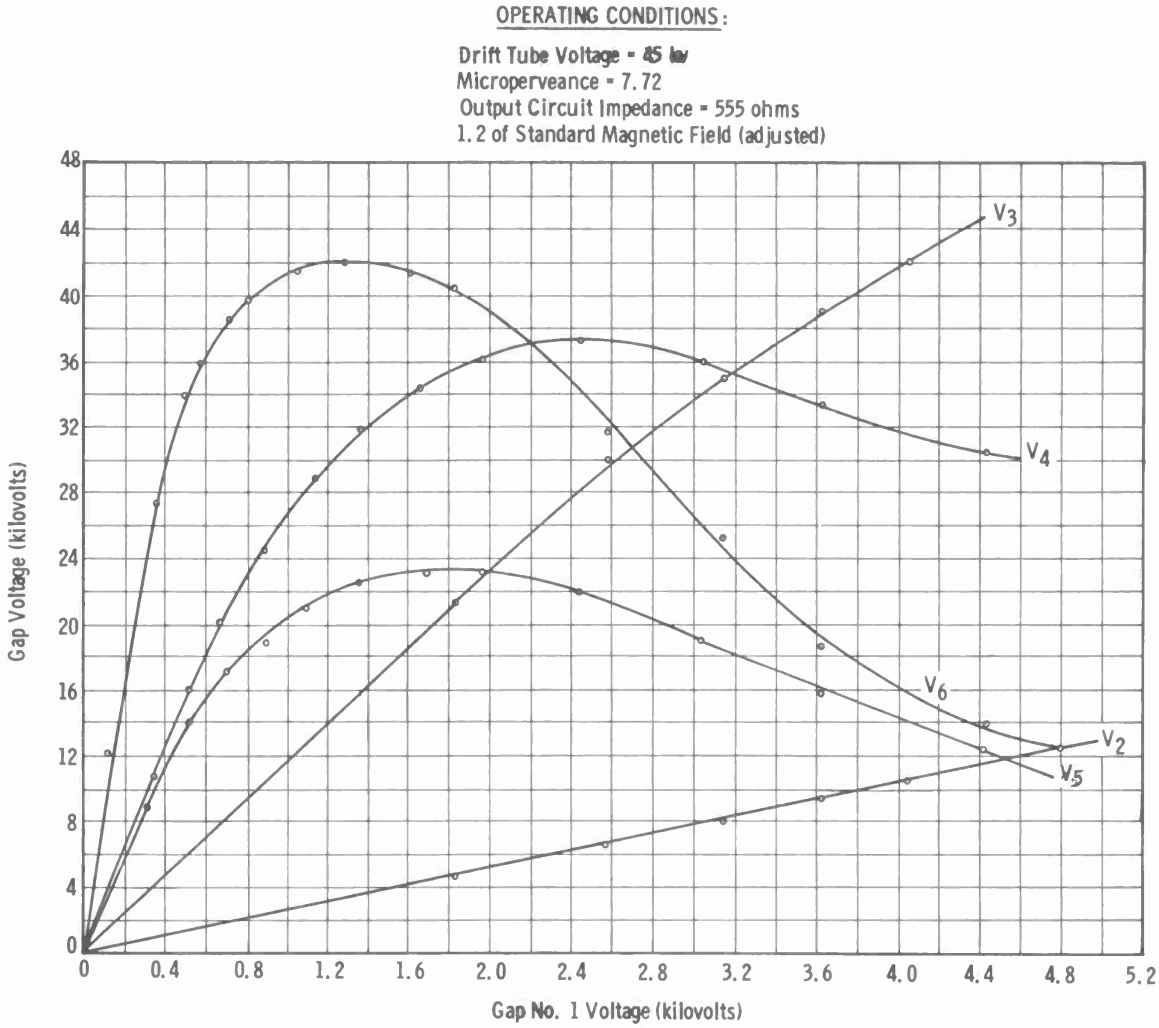

FIGURE 53
R-F VOLTAGES AT ALL GAPS VS DRIVE FOR ADJUSTED MAGNETIC FIELD, DRIFT TUBE VOLTAGE = 45 KILOVOLTS, MICROPERVEANCE = 7.72, HIGH OUTPUT IMPEDANCE

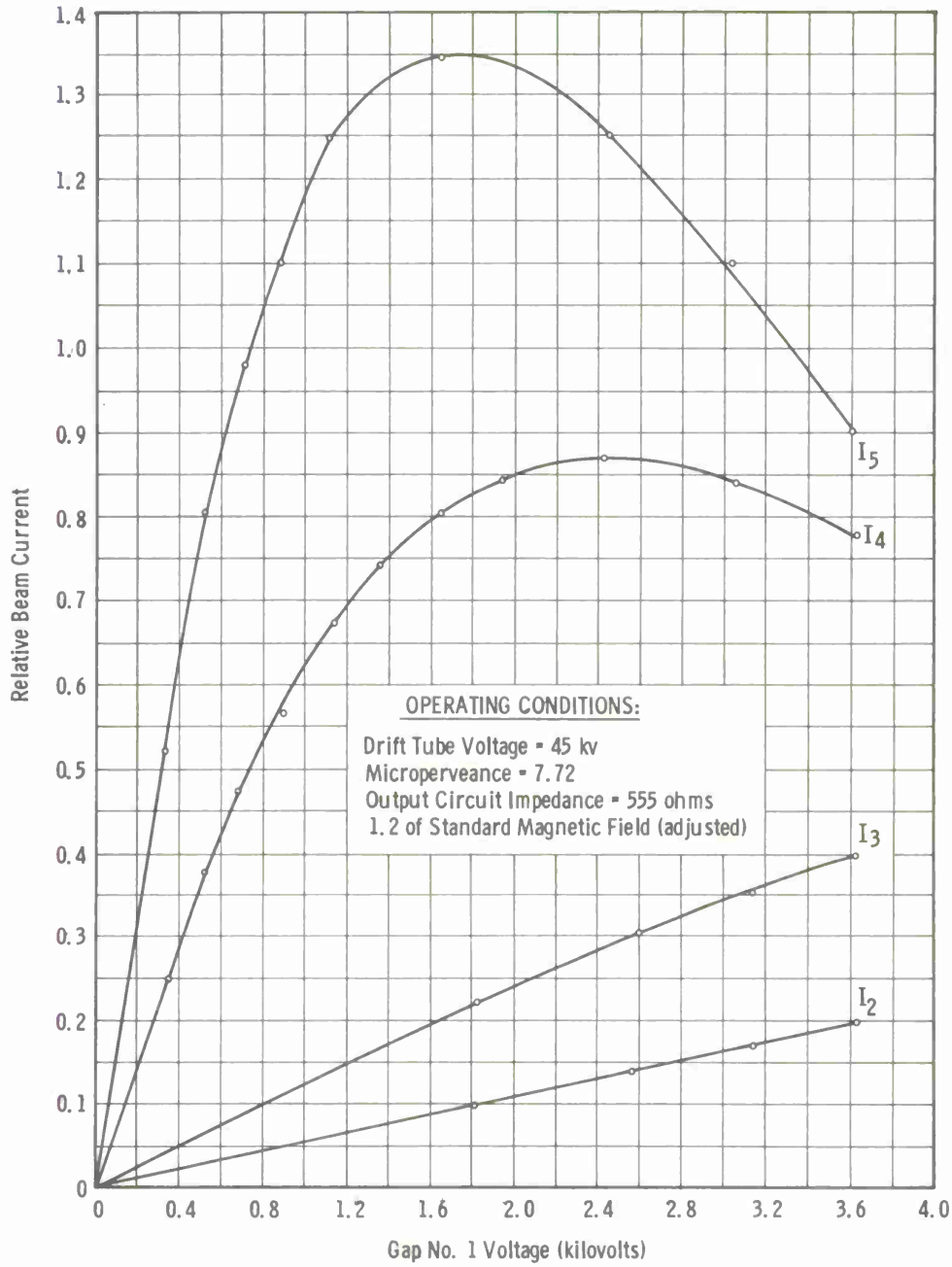

FIGURE 54
R-F CURRENTS AT ALL GAPS VS DRIVE
(CONDITIONS OF FIGURE 53)

OPERATING CONDITIONS:

Drift Tube Voltage = 45 kv
Microperveance = 7.72
Efficiency = 38 per cent
Z_{out} = 555 ohms
1.2 of Standard Magnetic Field (adjusted)

Magnet Currents	
Coil No.	Amps
1	6.95
2	6.70
3	7.90
4	6.20
5	6.50
6	7.15
7	10.30
8	1.0

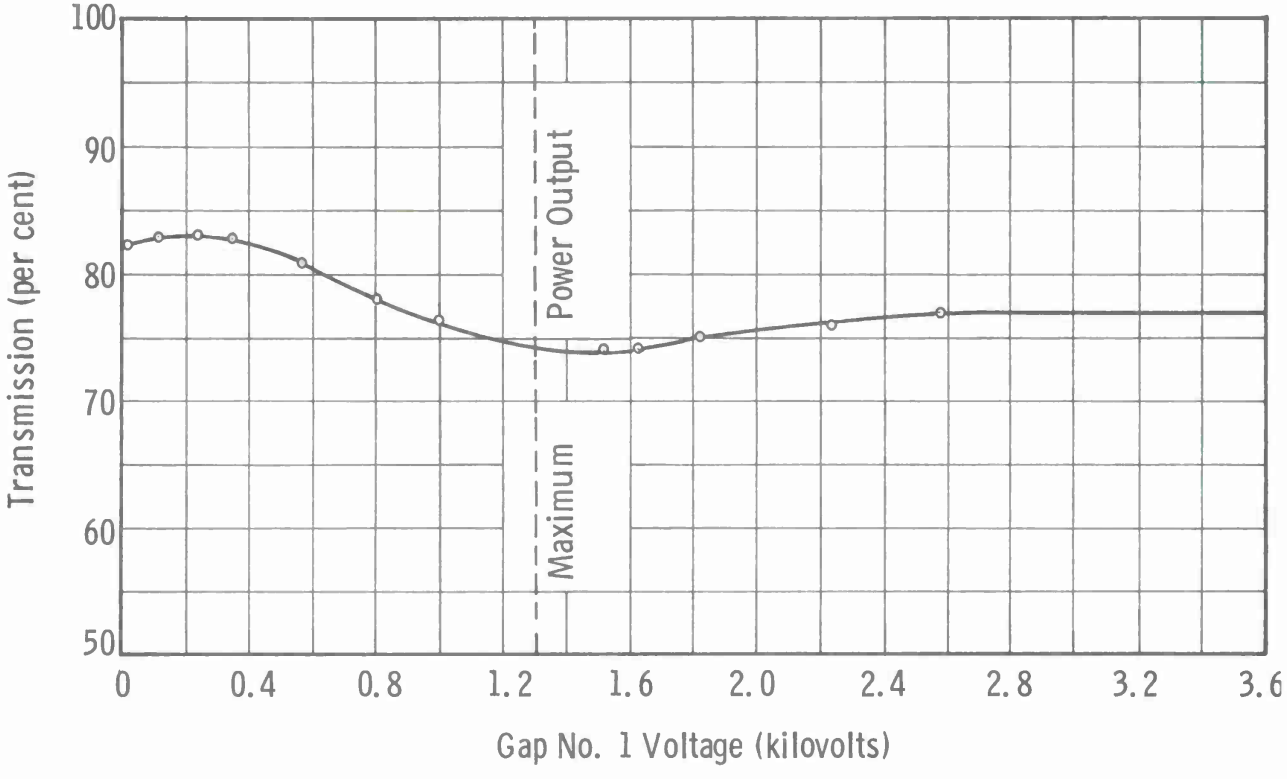

FIGURE 55
TRANSMISSION VS DRIVE (CONDITION OF FIGURE 53)

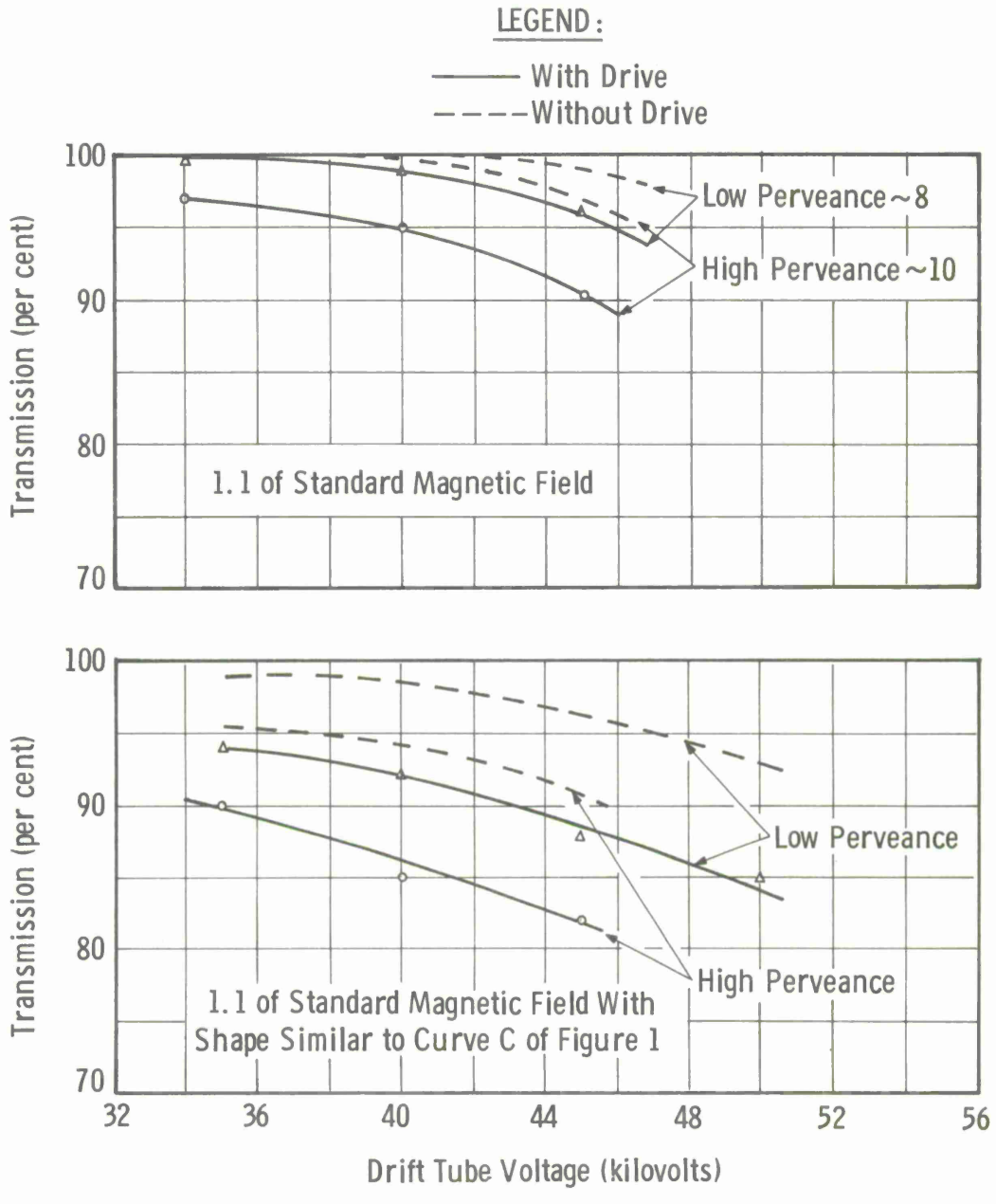

FIGURE 56
TRANSMISSION VS TUBE VOLTAGE FOR
TWO DIFFERENT MAGNETIC FIELD CONFIGURATIONS
AND LOW OUTPUT IMPEDANCE

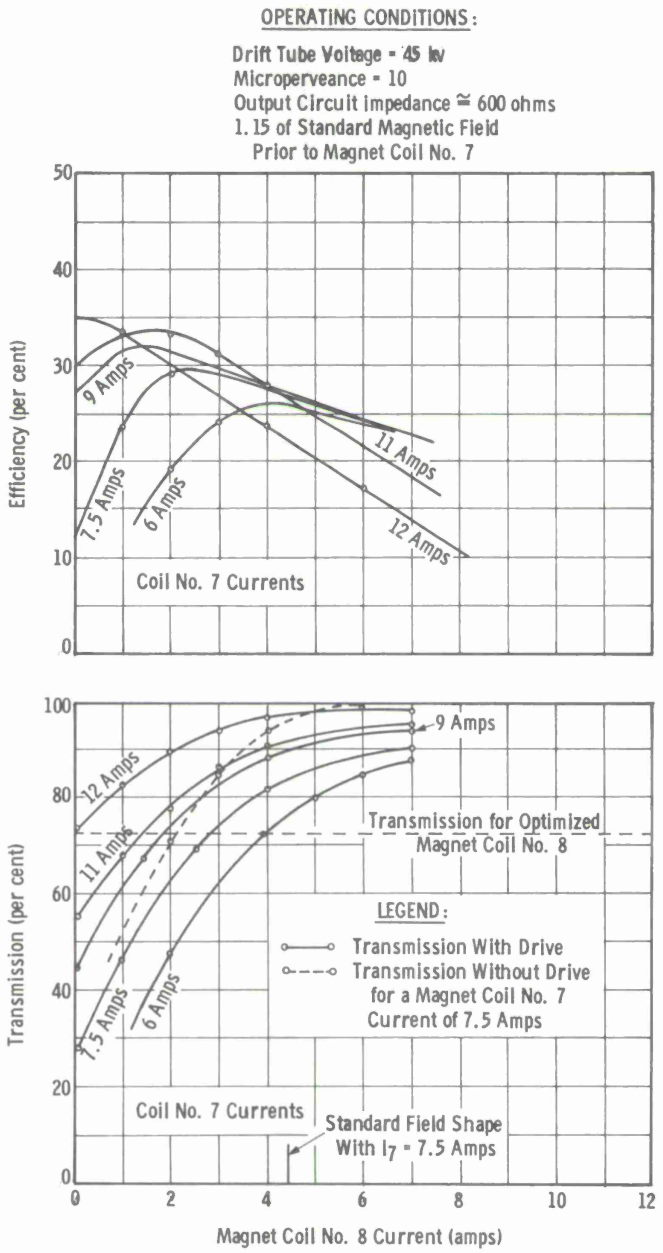

FIGURE 57
TUBE EFFICIENCY AND TRANSMISSION FOR VARIOUS MAGNETIC FIELD CONFIGURATIONS IN THE REGION OF THE LAST CAVITIES

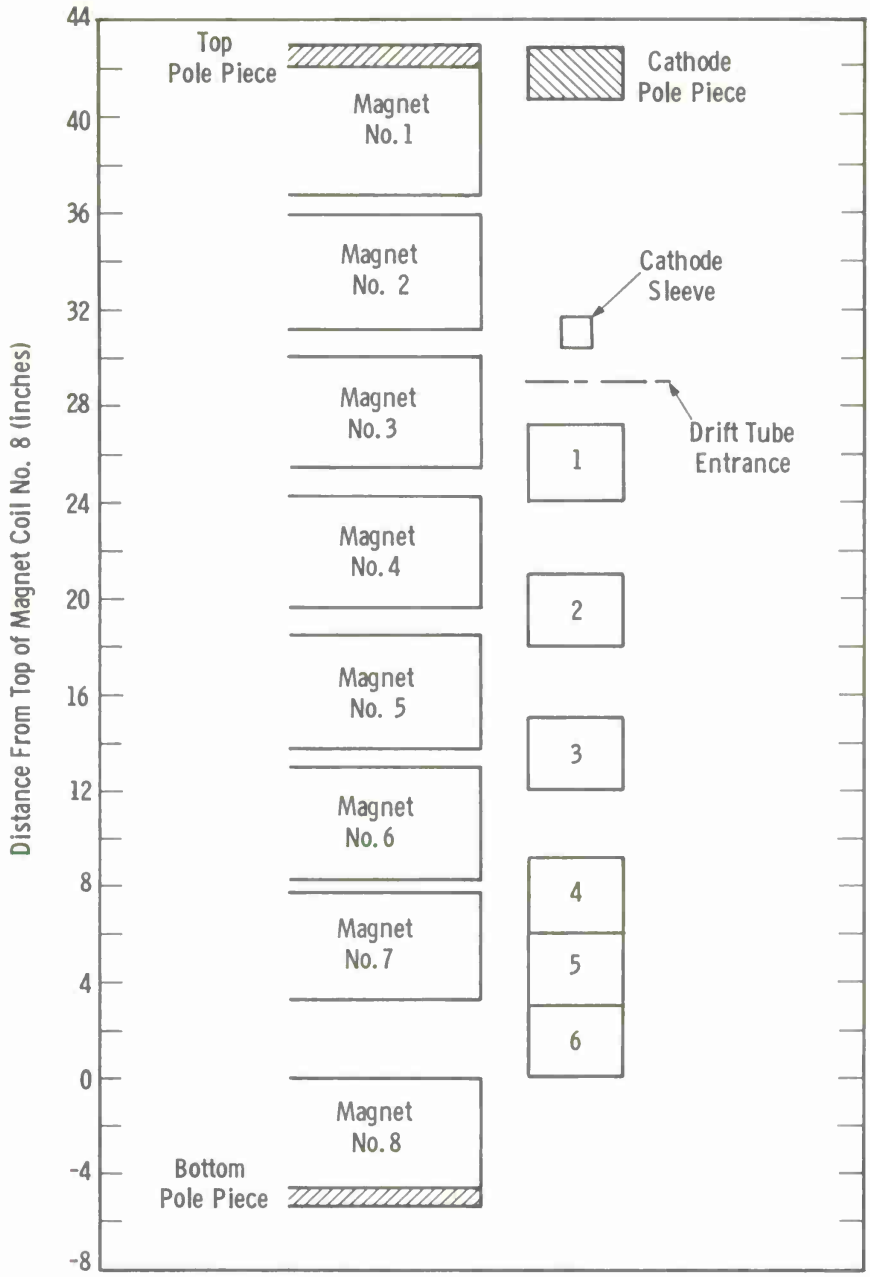

FIGURE 58
RELATIVE POSITION OF MAGNET COILS AND CAVITIES

NOTE: All dimensions are given in inches.

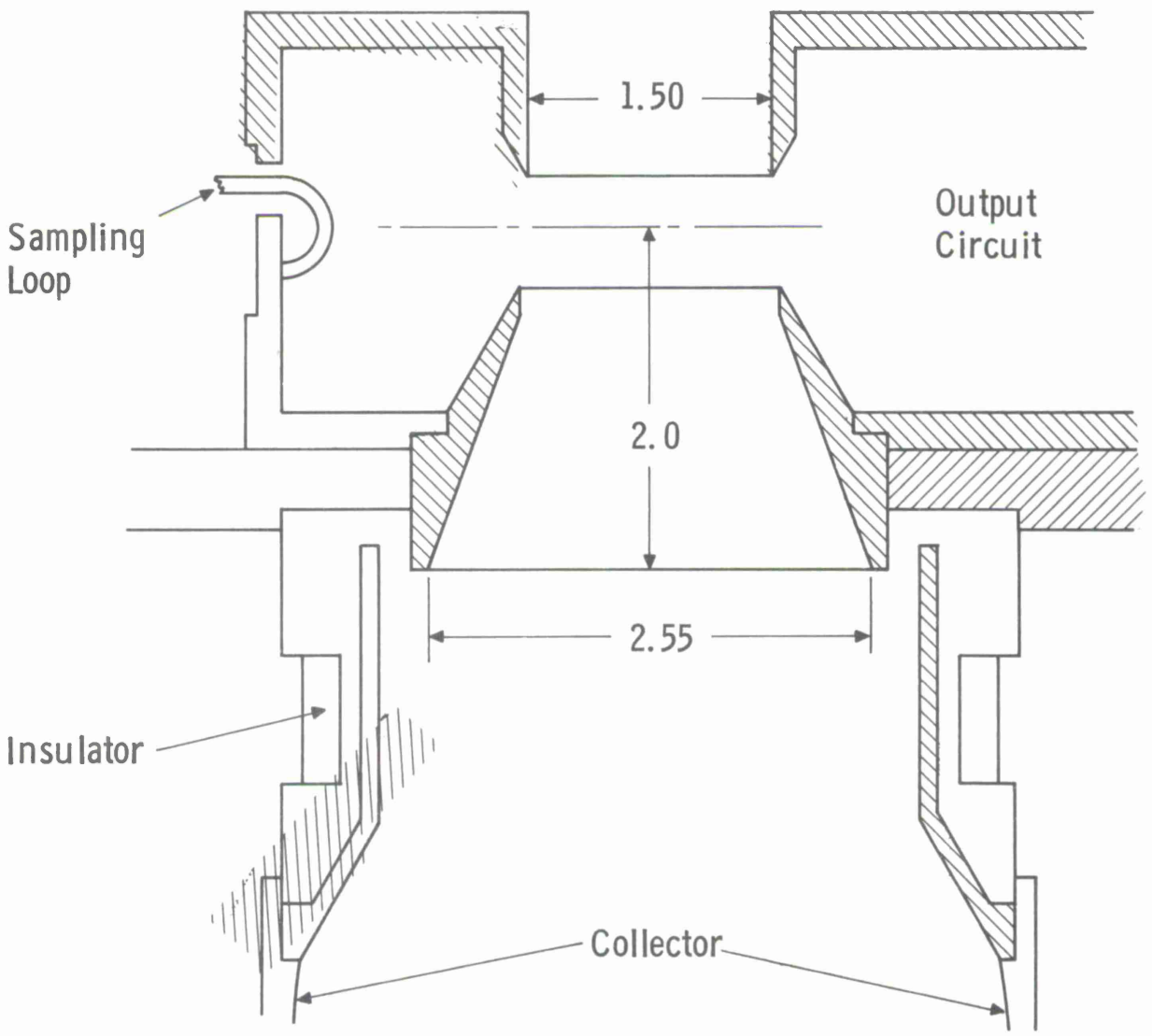

FIGURE 59
SCHEMATIC DRAWING OF OUTPUT GAP - COLLECTOR GEOMETRY

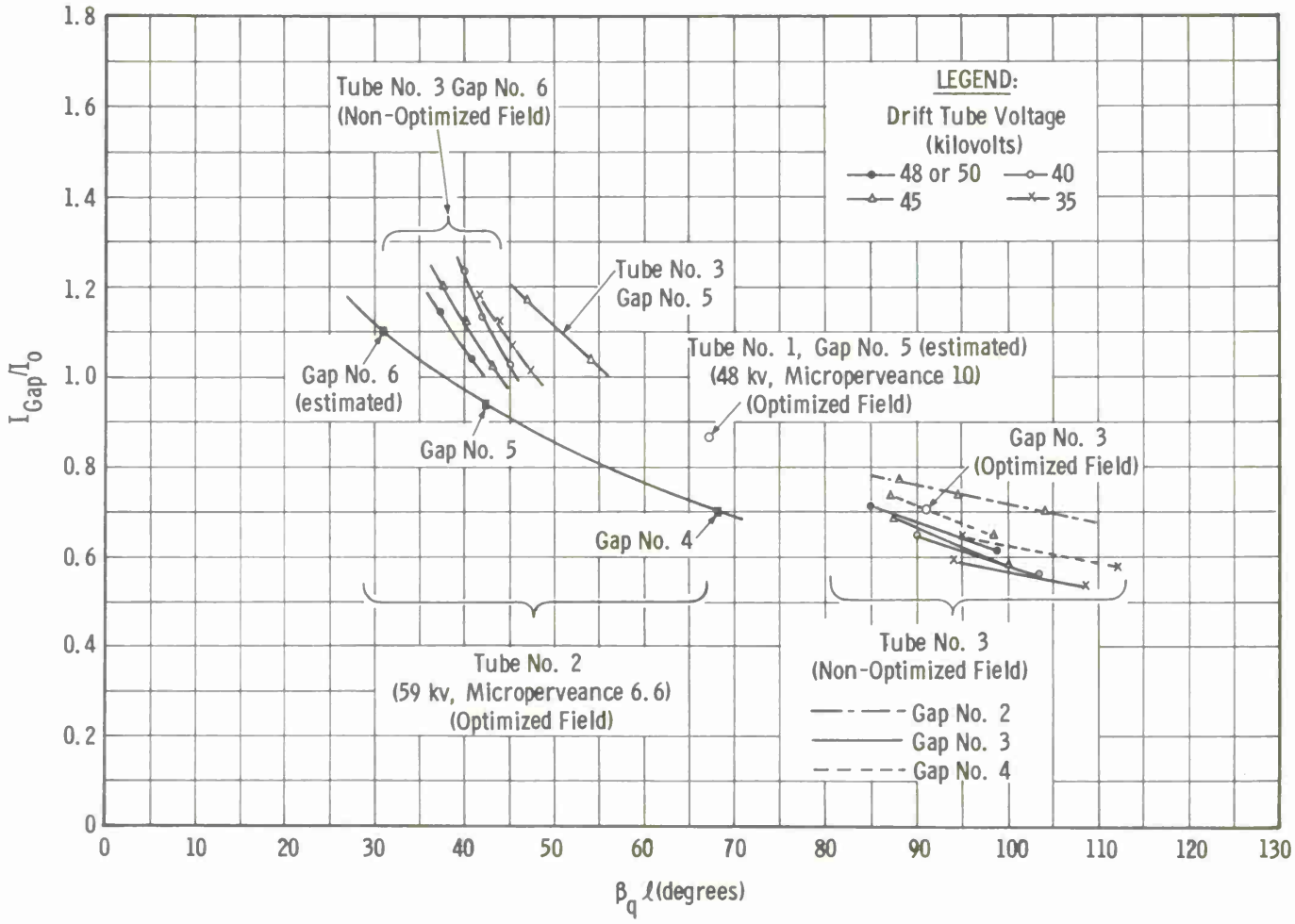

FIGURE 60
SATURATED CURRENTS VS REDUCED PLASMA DRIFT ANGLE
FOR THREE EXPERIMENTAL TUBES